UNIVERSITÉ DU QUÉBEC À TROIS-RIVIÈRES

UN EFFECTEUR DE ROUILLE AUGMENTE LA SUSCEPTIBILITÉ DES PLANTES AUX PATHOGÈNES ET INTERAGIT AVEC LA PROTÉINE DISULFURE ISOMÉRASE

A RUST EFFECTOR INCREASES PLANT SUSCEPTIBILITY AND INTERACTS WITH PROTEIN DISULFIDE ISOMERASE

THÈSE PRÉSENTÉE
COMME EXIGENCE PARTIELLE DU
DOCTORAT EN BIOLOGIE CELLULAIRE ET MOLÉCULAIRE

PAR
MOSAMMAD HUR MADINA

JANVIER 2020

UNIVERSITÉ DU QUÉBEC À TROIS-RIVIÈRES

Cette thèse a été dirigée par :

Hugo Germain, Ph. D.	Université du Québec à Trois-Rivières
Hugo Zheng, Ph. D.	Université McGill

Jury d'évaluation de la thèse :

Hugo Germain, Ph. D.	Université du Québec à Trois-Rivières
Hugo Zheng, Ph. D.	Université McGill
Tagnon Missihoun, Ph. D.	Université du Québec à Trois-Rivières
Geneviève Pépin, Ph. D.	Université du Québec à Trois-Rivières
David Joly, Ph. D.	Université de Moncton

Thèse soutenue le 27 janvier 2020.

ACKNOWLEDGEMENTS

Firstly, I would like to express my deepest gratitude to my advisor Prof. Hugo Germain for the continuous support of my Ph.D. study and related research, for his motivation, patience, and immense knowledge. His guidance helped me in all the time of research and writing of this thesis. I could not have imagined having a better advisor and mentor for my Ph.D. study. I would like to thank my co-director, Hugo Zheng for his ideas and support to my research. I am grateful for the opportunities, support and advices they have offered.

Besides my advisor, I would like to thank the rest of my thesis committee: Prof. David Joly, Prof. Genevieve Pepin, and Prof. Tagnon Missihoun, for their insightful comments and encouragement.

I would like to acknowledge Prof. Isabelle and Céline Van Themsche (Université du Québec à Trois-Rivières) for sharing instruments which helped me a lot during my experiments.

I would like to express my thanks to the Fonds de la Recherche sur la Nature et les Technologies du Québec (FRQNT) for providing me the scholarship for persuing my Ph.D. I express my gratitude to NSERC, since our laboratory was partially funded by NSERC Discovery Grants. Also, I thank my former advisors Prof. Anil Chandra Deb and Prof. Asadul Islam, University of Rajshahi, Bangladesh, for their support to get into this Ph.D. position.

I thank my fellow lab mates, Genevieve, Karen, Claire, Teura, Zainab, Ingrid, Joelle, Saif, Andrew, Bulbul, Nicolas, Tarun, Narimene, Annabelle, and Dorian for their emotional support and entertainments, stimulating discussions and for all the fun we have had in the last four years. I would like to thank Mélodie B. Plourde for assisting in

my research, valuable discussions, and proof-reading my manuscripts. Also, I thank Bruno, Catherine, and Defne for helping me out in my experiments.

Last but not the least, I would like to thank my family: my parents, Md. Saidur Rahman and Jahanara for supporting me spiritually throughout writing this thesis and my life in general. Lastly, I express my very special thanks to my dear husband Saifur Rahman, for his constant love, care, and emotional supports to overcome difficult movements in abroad.

RÉSUMÉ

Le champignon biotrophe *Melampsora larici-populina (Mlp*), l'agent causal de la rouille du peuplier, est l'un des agents pathogènes les plus dévastateurs du peuplier, et entraîne une perte de rendement importante pour la production. Au cours de l'infection, *Mlp* sécrète une série de protéines effectrices dans les cellules hôtes par le biais de son haustorium pour altérer les processus cellulaires de l'hôte. Déterminer la fonction des effecteurs à l'intérieur des cellules de la plante est essentiel pour comprendre les mécanismes de pathogénicité et améliorer notre capacité à protéger les cultures des maladies. Cependant, la fonction des effecteurs et le mécanisme spécifique par lequel ces effecteurs favorisent la virulence restent incertains et mal compris. Dans cette étude nous avons investigué Mlp124357 un effecteur candidat qui appartient à la famille des gènes CPG4890 qui comporte 10 effecteurs candidats spécifiques aux Pucciniales.

Nous avons développé une lignée d'*Arabidopsis* transgénique stable exprimant le candidat effecteur Mlp124357 fusionné avec la protéine fluorescente verte (GFP). La microscopie confocale a révélé que la protéine de fusion Mlp124357-GFP ciblait le tonoplaste, les filaments transvacuolaires et les bulbes. L'expression constitutive de l'effecteur augmente la sensibilité de la plante aux agents pathogènes bactériens et oomycètes. L'expression constitutive stable de Mlp124357 chez *A. thaliana* altère la morphologie des feuilles, leur conférant une forme plus étroite, une chlorose et un séchage des extrémités des feuilles. Un motif GxxxG prédit (x étant n'importe quel acide aminé) présent dans la séquence protéique de Mlp124357 est requis pour une localisation subcellulaire appropriée, car le remplacement des résidus glycine par des alanines (Mlp124357^{GA}) a conduit une délocalisation de Mlp124357 dans le noyau et le cytoplasme. Le motif GxxxG est également requis pour que l'effecteur augmente la suscepbilité des plantes aux pathogènes.

Nous avons utilisé l'immunoprécipitation et la spectrométrie de masse pour identifier les partenaires d'interaction Mlp124357. Nous avons sélectionné cinq protéines localisées sur le tonoplaste dans la liste d'interactants potentiels de spectrométrie de masse, croisé leurs lignes knock-out avec la ligne stable Mlp124357 et avons évalué si leur absence conduisait à une délocalisation de l'effecteur chez *Arabidopsis*. Une seule ligné knock-out a provoqué la délocalisation de l'effecteur confirmant que la protéine disulfure isomérase-11 (AtPDI-11) était nécessaire pour la localisation tonoplastique de l'effecteur, ce qui a été confirmé par un test de complémentation génétique et un essai de double hybride dans la levure et une analyse d'interaction modélisée *in silico*. Nous avons également confirmé que la protéine disulfure isomérase du peuplier (le vrai hôte) interagit avec Mlp124357. En outre, le test d'infection suggère qu'AtPDI-11 agit comme un auxiliaire pour l'effecteur Mlp124357 et non une cible, car les *pdi-11* knock-out démontre une susceptibilité normale au pathogène, donc n'ont pas de rôle de régulation positive de l'immunité. Une analyse du transcriptome complet indique également que les gènes dérégulés positivement ne contenaient pas spécifiquement de gènes impliqués dans la défense des plantes, mais que les gènes impliqués dans la

défense étaient parmi les plus réprimés, ce qui est conséquent avec le phénotype observé. Par conséquent, nos résultats ont établi qu'un effecteur de *Mlp* réside à la surface de la vacuole et module la sensibilité des plantes.

Mots-clés : Mlp124357, rouille, effecteurs, tonoplaste, brins transvacuolaires, bulbes, motif GxxxG, protéine disulfure-isomérase, sensibilité des plantes

SUMMARY

The biotrophic fungus *Melampsora larici-populina (Mlp)* is one of the most devastating pathogens responsible for the poplar leaf rust disease, it causes significant yield loss on poplar production. During the infection, *Mlp* secretes an array of effector proteins into the host cells through its haustorium to alter host cellular processes. Determining the function of effectors inside of cells is key to understanding pathogenicity mechanisms and improve our ability to protect crops from disease. However, the function of the effectors and the specific mechanism by which these effectors promote virulence remains unclear. To address this question, Mlp124357 was investigated in this study, it belongs to the CPG4890 gene family which has 10 members specific to the Pucciniales.

We developed a stable transgenic *Arabidopsis* line expressing the candidate effector Mlp124357 fused with the green fluorescent protein (GFP). The confocal microscopy revealed that Mlp124357-GFP fusion protein targeted the tonoplast, transvacuolar strands, and bulbs. Constitutive expression of the effector increases plant susceptibility to bacterial and oomycete pathogens. Stable constitutive expression of Mlp124357 in *A. thaliana* altered leaf morphology, observed through narrower leaves, chlorosis, and drying of the leave tips. A predicted GxxxG motif (x being any amino acid) present in the protein sequence of Mlp124357 is required for proper subcellular localization since replacement of the glycine residues with alanine ($Mlp124357^{GA}$) led to the delocalization of Mlp124357 into the nucleus and cytoplasm. The GxxxG motif is also required for the effector to enhance plant susceptibility.

We used immunoprecipitation and mass spectrometry to identify Mlp124357 interaction partners. We selected five proteins that localized to tonoplast from the IP interactor list, crossed their knock-out lines with Mlp124357 line, and assessed if their absence led to a re-localization of the effector in *Arabidopsis*. A single knock-out line caused delocalization of the effector confirming that protein disulfide isomerase-11 (AtPDI-11) is required for the effector tonoplastic localization, which was further confirmed by a genetic complementation test, a yeast-two hybrid assay, and molecular docking. We also confirmed that not only the *Arabidopsis* but also the host poplar protein disulfide isomerase interacts with the Mlp124357. Moreover, infection assay suggests that AtPDI-11 act as a helper for Mlp124357 effector and not as a virulence target. A full transcriptome analysis also indicates that the list of up-regulated genes did not specifically contain genes involved in plant defense, but rather genes involved in defense were among the most repressed, which is consequent with the enhanced susceptibility phenotype. Therefore, our results established that an effector of *Mlp* resides at the vacuole surface and modulates plant susceptibility.

Keywords: Mlp124357, rust, effectors, tonoplast, transvacuolar strands, bulbs, GxxxG motif, protein disulfide-isomerase, plant susceptibility

TABLE OF CONTENTS

LIST OF FIGURES

LIST OF ABBREVIATIONS AND ACRONYMS

AVR	Avirulent
BCECF	2',7'-bis-(2-carboxyethyl)-5-(and-6)-carboxyfluorescein
BIC	Biotrophic interfacial complex
Cfu	Colony forming unit
CMU	Chorismate mutase
CSEPs	Candidate secreted effector proteins
DAMP	Damage-associated molecular patterns
DDO	Double dropouts
Dpi	Days post infiltration
DTT	Dithiothreitol
eds1-1	Enhanced disease susceptibility 1-1
EHM	Extrahaustorial matrix
EM	Extrahaustorial membrane
ER	Endoplasmic reticulum
EST	Expressed sequence tag
ETI	Effector-Triggered Immunity
ETS	Effector-triggered susceptibility
FM1-43	N-(3-triethylammoniumpropyl)-4-(4-(dibutylamino)styryl) pyridinium dibromide
FM4-64	N-(3-triethylammoniumpropyl)-4-(4-diethylaminophenylhexatrienyl) pyridinium dibromide
FRAP	Fluorescence recovery after photobleaching
GFP	Green Fluorescent Protein

GO	Gene Ontology
H. a	Hyaloperonospora arabidopsidis
HR	Hypersensitive response
IH	Invasive hyphae
IP	Immunoprecipitation
IVSP	Intravacuolar spherical structures
KO	Knock out
LVs	Lytic vacuoles
MAMP	Microbes associated molecular pattern
MAMP	Microbe-associated molecular patterns
MAPK	Mitogen-Activated Protein Kinases
Mlp	*Melampsora larici-populina*
MS	Mass Spectrometry
NLS	Nuclear localization signal
NLS	Nuclear localization signal
ORF	Open reading frame
PAMP	Pathogen associated molecular pattern
PAMP	Pathogen-associated molecular patterns
PC	Phosphatidylcholine
PCD	Programmed cell death
PDI	Protein disulfide isomerase
PE	Phosphatidylethanolamine
PR	Pathogenesis related
PRR	Pattern recognition receptor
Pst	*Pseudomonas syringae* pv. tomato strain

PSVs	Protein storage vacuoles
PTI	PAMP-Triggered Immunity
QDO	Quadruple dropouts
R	Resistance
RIN4	RPM1 interacting protein 4
ROS	Reactive oxygen species
RT	Room temperature
SA	Salicylic acid
SAP11	Secreted AY-WB Protein 11
SD	Synthetic Defined
SDS-PAGE	Sodium dodecyl sulfate- polyacrylamide gel electrophoresis
SP	Signal peptide
SSPs	Small secreted protein
T3SS	ype three-secretion system
TAL	Transcription activator-like
TFs	Transcription factors
TFs	Transcription factors
TIPs	Tonoplast intrinsic proteins
TVS	Transvacuolar strand
VM	Vacuolar membrane
VPE	Vacuolar processing enzyme
Y2H	Yeast two-hybrid
YEP	Yeast extract pepton

CHAPTER I

INTRODUCTION

1.1 Plant diseases: major threats to global food security

All the living organisms on earth depends on plants and their products to survive. Unlike animals, plants are sessile and facing constant threats from various types of phytopathogenic microbes and herbivores, including insect pests. These phytopathogenic microbes, whether fungi, oomycetes, bacteria or viruses, cause diseases that have changed world history and still affect us today. One of the best examples of disease epidemics in history is the Irish potato famine. This disease devastated the potato crop in the 1840s in Ireland, it killed about a million people, and another million people were forced to emigrate from the country (Haas et al. 2009). This example illustrates how plant disease can have a profound effect on human survival and migrations. There are many such diseases, not to this scale, that are major threats to our global food securities. Old diseases, for instance, rice blast never seem to go away and new disease, for instance, kiwi bacterial canker continues to emerge globally. At the same time, with the growing demands of the world population, the food deficit is increasing day by day, and food supply and food security are currently the most urgent issues in the world (Avila-Quezada et al. 2018). Understanding the molecular basis of pathogenicity, disease resistance, and plant-pathogen interactions are indispensable to control plant pathogens and retain plants healthy for food security.

1.2 Lifestyles of plant microbes and types of interaction

The interactions between plants and pathogenic microbes can be classified in two categories: compatible interaction or incompatible interaction. In a compatible interaction, microbes are virulent and successfully infect plants (Fig. 1.1A). According to their lifestyles, virulent pathogens are generally divided into necrotrophs, biotrophs,

and hemibiotrophs (Glazebrook 2005) (Fig. 1.1B). Necrotrophs kill host cells by secreting phytotoxin or lytic enzyme and draw their nutrients and energy from dead cells of their hosts, resulting in tissue maceration, and extensive necrosis (Glazebrook 2005; Horbach et al. 2011). Biotrophic pathogens feed on living cells, develop structures to invade the cell and obtain nutrients and metabolism products. They establish a constant interaction with their hosts and deploy intricate manipulation strategies to exploit hosts while maintaining them alive. Most biotrophs are obligate parasites, which means that they cannot live outside their host. Mandatory biotrophic parasites have specialized infection structures, secrete fewer degradation enzymes and secondary metabolites, and they do not directly cause the death of the host they colonize (Kemen and Jones 2012). The hemibiotrophs meanwhile infect their hosts in two phases: first, they exhibit a biotrophic infection phase and then switch to a necrotrophic phase (Lee and Rose 2010). These pathogens typically secrete toxins at later phases of disease development to kill the host cells and then complete their life cycle on dead tissues (Horbach et al. 2011). The length of the biotrophic growth phase may vary depending on the pathogen (Goswami and Kistler 2004; Teixeira et al. 2014).

Conversely, in incompatible interactions, pathogens are avirulent and unable to establish infection (Fig. 1.1A). The attempted attack by avirulent biotrophic pathogens often results in inability to colonize the tissue or in local cell death (known as the hypersensitive response (HR) in challenged plant tissues. The spectrum of plant-associated organisms extends far beyond parasites. Many species of bacteria or fungi establish mutualist interactions with their hosts, promoting the growth of both partners with a bidirectional exchange of nutrients (Selosse 2000). For example, nitrogen can be brought to the plant by symbiotic bacteria or fungi, and in return, the host plant brings carbon resources to the symbiotic microorganism (Martin et al. 2017). In this type of mutualistic association, microorganisms generally colonize the root system of their host plants after establishing a complex molecular dialogue to activate a variety of anatomical and developmentally cues in the host and thus form exchange structures dedicated to the interaction (Martin et al. 2017).

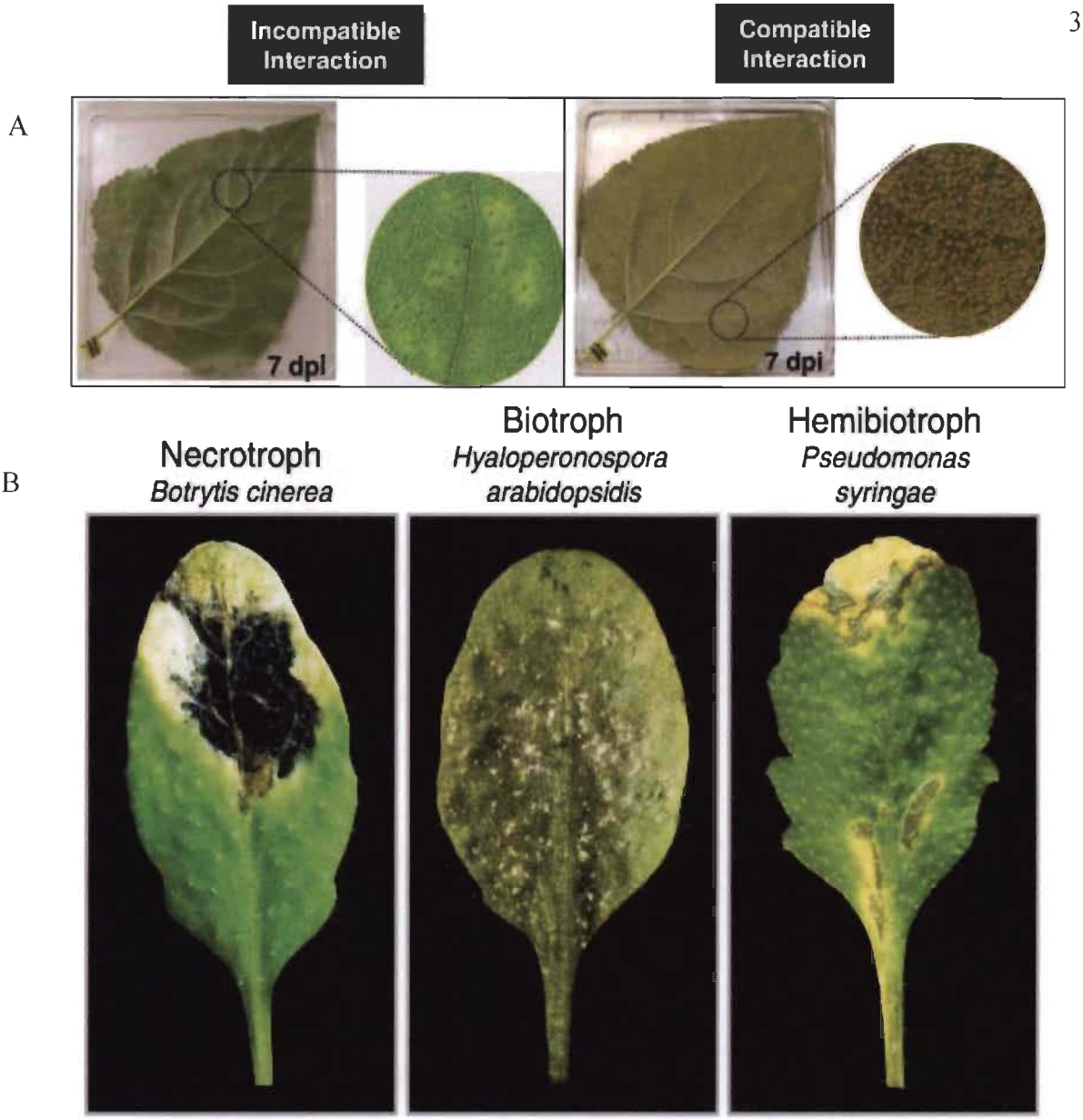

Figure 1.1 Interaction and disease symptoms of different types of plant pathogens.
A) Poplar leaves inoculated with incompatible (avirulent) and compatible (virulent) strains of *M. larici-populina* (Source: Rinaldi et al. 2007). B) Disease symptoms on *Arabidopsis* leave caused by the necrotrophic fungus *Botrytis cinerea*, the biotrophic oomycete *Hyaloperonospora arabidopsidis* and the hemibiotrophic bacterium *Pseudomonas syringae* (Source: Pieterse et al. 2009).

1.3 Molecular plant-microbe interactions: the immunity of plants

The ability of plants to resist infection, recover from disease, and prevent future infection has been reported since the early 20th century (Chester 1933). The activities of the pathogens focus on colonization within the host environment and the utilization of

their resources, while the plants adapt to detect the presence of invasive pathogens and respond with antimicrobial defenses and other stress responses. The capacity of a pathogen to confer disease in a host plant is usually the exception rather than the rule as plants have an innate ability to identify potential invading pathogens and to develop successful defenses against them. However, successful pathogens produce diseases because they evade recognition or suppress defense mechanisms of the host (Borrás-Hidalgo 2004).

In the 2000s, the Genomic revolution revealed the complexity and the diversity of genes and functions involved in the molecular mechanisms of interactions between plants and microorganisms (Dodds and Rathjen, 2010, Jones et al. 2016, Pritchard and Birch, 2014, Cui et al. 2015). In 2006, researchers Jones and Dangl proposed a model for understanding the molecular mechanisms underlying immunity in plants called the "zig-zag model" (Jones and Dangl 2006). This model is based on the fact that plant possesses a two-layer immune defense system to protect against microbial invaders; P/MAMP (Pathogen/Microbe-Associated Molecular Patterns) Triggered Immunity (PTI) and effector trigger immunity (Kunjeti et al.) (Fig. 1.2) (Jones and Dangl 2006).

1.3.1 PTI: PAMP-triggered immunity

When pathogens overcome the plant physical barrier, they are then subject to molecular recognition by specializing plant molecules (Zipfel and Felix 2005). In this first line of defense, plants use cell surface pattern recognition receptors (PRRs) which actively recognize structurally conserved components of pathogens (nonself) and host self-released molecules collectively known as pathogen/microbe-associated molecular patterns (PAMPs/MAMPs) and damage-associated molecular patterns (DAMP) (Jones and Dangl 2006; Zhou and Chai 2008) (Fig. 1.2A). Such molecules include flagellin, lipopolysaccharide and elongation factor Tu from Gram-negative bacteria; chitin, β-glucan and ergosterol from fungi; and eliciting from oomycetes (Chisholm et al. 2006; Nürnberger and Brunner 2002; Schwessinger and Zipfel 2008). Detection of these factors by pattern recognition receptors (PRRs) triggers the plant defense layer termed

PAMP-triggered immunity (PTI) (Boller and He 2009; Zipfel and Felix 2005). The PTI activation leads to intracellular responses that include mitogen-activated protein kinase (MAPK) induction, rapid calcium fluxes across the plasma membrane, nitric oxide and reactive oxygen species production, as well as the activation of stress-specific transcription factors WRKY (Nürnberger et al. 2004). These responses altogether effectively restrict the growth of non-adapted pathogens and are responsible for the general health of most plants (Jones and Dangl 2006; Ma and Guttman 2008; Schwessinger and Zipfel 2008; Zipfel et al. 2008).

1.3.2 ETS: Effector-Triggered Susceptibility

Despite the fact that PTI inhibits infection, successful pathogens have developed strategies to defeat PTI by secreting virulence factors known as effectors to lead effector-triggered susceptibility (Kawamura et al.; Kawamura et al. 2009b) and pathogen virulence (Fig. 1.2B). Extensive work on function of effectors has been done on bacterial effectors where several were found to suppress or disrupt PTI, ETI, or both (Guo et al. 2009), but remarkable advances have also been made in *Cladosporium fulvum* and oomycetes. In *C. fulvum*, the AVR2 effector inhibits at least four tomato cysteine proteases that are believed to be crucial in the basal host defense (Rooney et al. 2005), while a chitin-binding protein AVR4 protects fungi from the lytic activity of plant chitinases (Van den Burg et al. 2006). Another effector from *C. fulvum*, ECP6, is believed to be involved in the chitin fragments scavenging activity that are secreted during infection from fungal cell walls, hence preventing them from functioning as PAMP triggering molecules (Bolton et al. 2008). In oomycete species of the genus *Phytophthora*, elicitins such as INF1 triggers a range of defense responses, including programmed cell death in diverse plant species, and are thus considered as PAMPs (Kawamura et al. 2009a). Recently, the *P. infestans* AVR3a effector has been shown to interact with and stabilize host U-box E3 ligase CMPG1, which is required for the triggering of INF1-dependent cell death (Bos et al. 2010). Another oomycete effector from *Hyaloperonospora arabidopsidis*, ATR13, has been shown to suppress callose deposition, a presumed basal defense response (Sohn et al. 2007). There is ample

evidence now that one function of effectors is to suppress PTI through interaction with pattern recognition receptors (PRR) and processes downstream of PRR and mitogen-activated protein kinase (MAPK) cascades (Block et al. 2008).

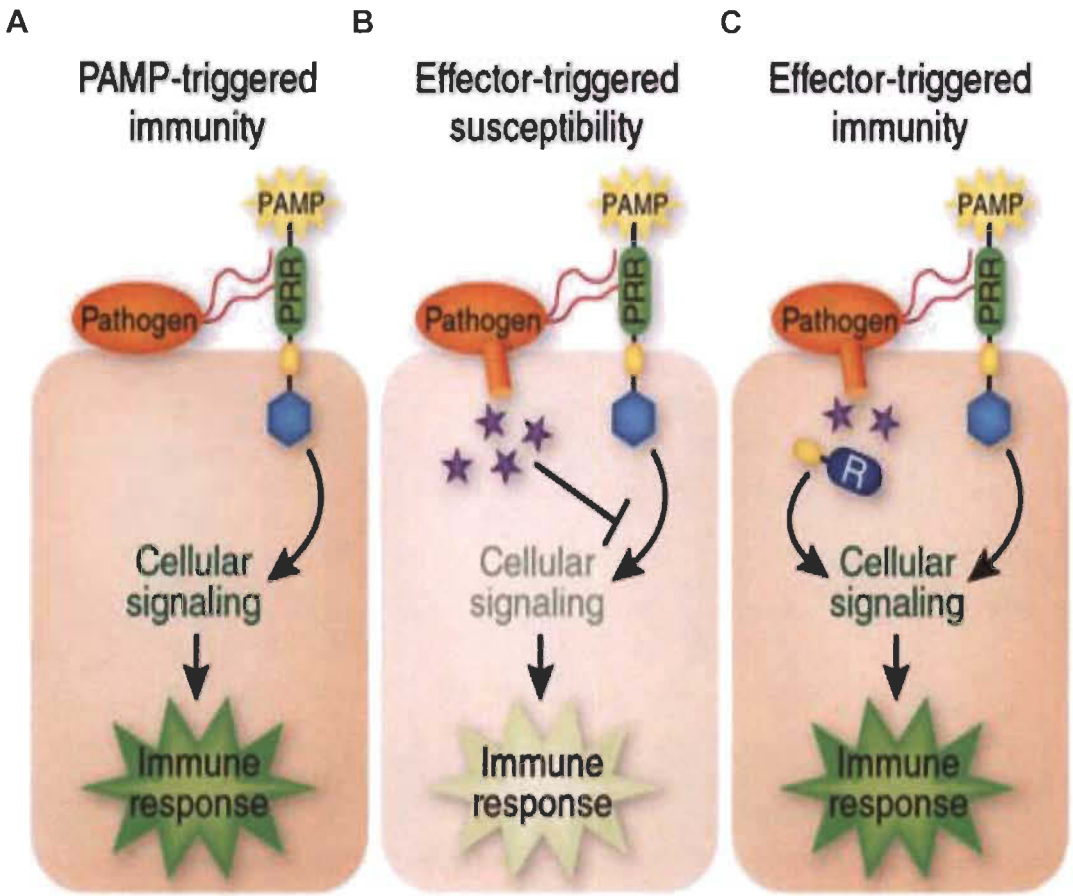

Figure 1.2 Schematic representation of the plant immune system.
Upon pathogen attack, pathogen-associated molecular patterns (PAMPs) activate pattern-recognition receptors (PRRs) in the host, resulting in a downstream signaling cascade that leads to PAMP-triggered immunity (PTI). B) Virulent pathogens have acquired effectors (purple stars) that suppress PTI, resulting in effector-triggered susceptibility (Kawamura et al. 2009). C) In turn, plants have acquired resistance (R) proteins that recognize these attacker specific effectors, resulting in a secondary immune response called effector-triggered immunity (Kunjeti et al. 2016).

1.3.3 ETI: Effector-triggered immunity

Luckily, the plant has an additional defense layer through which these effectors can be directly or indirectly be recognized by the plant defense system. This second

layer is called Effector triggered immunity, and involves mostly intracellular receptors that are the products of the classically defined resistance R proteins (Fig. 1.2C) (Flor 1971). These receptors recognize the presence of effectors of the pathogen by direct binding or indirectly by detecting their activity in the host cells, leading to a faster and stronger version defense response than PTI (Boller and He 2009). ETI is extremely specific to a race or strain of pathogen as it recognizes a virulence determinant or its effect (Mur et al. 2008). The outcome of ETI is usually the programmed cell death response called the hypersensitive response (HR) at the site of pathogen infection, which is thought to limit the spread of the pathogen from the infection site (Flor 1971). Natural selection drives pathogens to suppress ETI again, either through diversifying their effector repertoire or by acquiring new effectors. Nevertheless, natural selection also drives plants to modify their R proteins arsenal or acquire new ones, so that the pathogen effectors can be recognized and, again, the ETI can be triggered (hence the zig-zag model). Several proteins secreted in apoplast or xylem sap during colonization of tomato have been identified in *C. fulvum* or *F. oxysporum* f. sp. *lycopersici*, respectively (Huitema et al. 2004; Thomma et al. 2005), most of which are also avirulence genes that match corresponding resistance genes (Rep et al. 2004; Stergiopoulos and de Wit 2009). In the flax rust fungus *Melampsora lini*, all the identified Avr small secreted proteins are expressed in haustoria (Catanzariti et al. 2006; Dodds and Rathjen 2010), however to this date their virulence target are unknown. Similarly, avirulence genes originally isolated from oomycete pathogens encode small secreted proteins, of which transient expression in the host cytoplasm leads to R-gene-dependent cell death (Allen et al. 2004; Armstrong et al. 2005; Rehmany et al. 2005; Shan et al. 2008).

1.4 Effector biology

1.4.1 Effectors: concepts and definitions

Pathogens have developed strategies to avoid the different levels of host physical and chemical barriers to modify host structures and physiology, transforming plant tissues into a suitable niche to obtain the necessary nutrients for their development and

ensure the completion of their lifecycle (Gaulin 2017). One of the well-known strategies of pathogens is to secrete an arsenal of molecules called "Effectors" whose various functions aim to promote the success of the infection (Hogenhout et al. 2009; Win et al. 2012). Though the term "effector" is broadly used in the studies of plant-microbe interaction, its definition varies. Kamoun (2003) and Huitema et al. (2004) defined effectors as "molecules that alter the structure and function of host cells, thereby facilitating infection (virulence factors or toxins) and triggering defense response (avirulence factors or elicitors)." In another definition Birch and colleagues (2014) referred to effectors in plant-pathogen interactions as "any protein synthesized by a pathogen that is exported to a potential host, which has the effect of making the host environment beneficial to the pathogen". The widely accepted hallmarks of effectors include; small secreted proteins (SSPs) having a N-terminal signal peptide with low sequence homology across species, no conserved host-targeting signal and capable of manipulating and reprograming host metabolism and immunity (Hogenhout et al. 2009). Most of the described effectors are proteins; however, non-protein effectors have also been described such as metabolites, toxins (Amselem et al. 2011; Arias et al. 2012; Collemare and Lebrun 2011) or small interfering RNAs (Weiberg et al. 2013).

1.4.2 Different types of effectors

Effector proteins are secreted by plant-associated microbes, such as fungi, bacteria, oomycetes, and can either be apoplastic or cytoplasmic (Fig. 1.3). Apoplastic effectors are secreted, and function at the microbe-plant interface (apoplast) and most have been described as inhibitors of host proteases (De Wit 2016; Song et al. 2009). Cytoplasmic effectors are translocated in the host cytoplasm from where they be directed to various cellular compartments and modulate a broad spectrum of cellular functions such as plant immunity, physiology and metabolism in favor of microbial growth (Fig. 1.3) (Petre and Kamoun 2014; Rovenich et al. 2014).

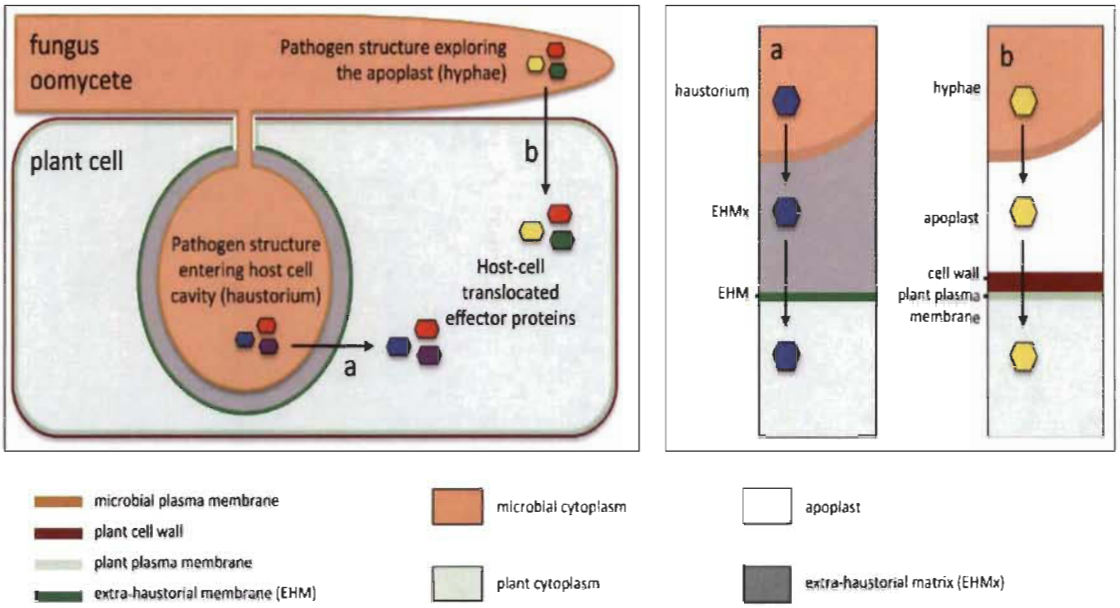

Figure 1.3 Secretory structures of the effectors of filamentous pathogens.
Left panel: Biotrophic pathogenic fungi and oomycetes have infections structures such as extracellular hyphae, invasion hyphae, and haustoria that penetrate the host cell cavity and invaginate the plasma membrane. Haustoria (A) and hyphae (B) secrete effectors that are translocated into the cytoplasm of the host cell by a mechanism still unknown. Right panel: Effectors secreted from haustoria (A) and hyphae (B) across different biological interfaces (extra-haustorial matrix [EHMx]/extra-haustorial membrane [EHM] for effector secreted by haustoria, and apoplast/plant cell wall/plasma membrane for effectors secreted by hyphae). Adapted from Petre & Kamoun, 2014.

Pathogen effectors have evolved to interfere with cellular mechanisms and physiological properties of the host cell to the benefit of the parasite (McCann and Guttman 2008). Some effectors identified especially in bacteria exhibit enzymatic activity including proteases, kinases or ubiquitinases (Deslandes and Rivas 2012). An effector of *Ustilago maydis* fungi interferes with chorismate mutase (Cmu) activity and seems to mimic the activity of certain enzymes to affect metabolic processes related to the production of secondary metabolites that would stimulate immunity (Djamei et al. 2011; Tanaka et al. 2014). Other effectors interact with target proteins to alter their function such as protease inhibitory effectors (Dong et al. 2014). Cytoplasmic effectors are often described as targeting proteins to affect their stability (for example, by promoting their accumulation or their degradation in the host cell) or their activity (for example, by inhibiting their activity enzymatic or signal transduction activity thereof (Win et al. 2012). Some effectors can also bind to DNA and modulate gene

expression, such as Transcription activator-like (TAL) effectors of *Xanthomonas spp.* (Boch et al. 2009).

1.4.3 Effector delivery systems

In order to manipulate their respective hosts, plant pathogenic bacteria, oomycete, and fungi have developed different mechanisms to deliver their effectors inside the host cells. For instance, bacteria use the specialized type III secretion system (T3SS) to secrete effector proteins into host cells (Fig. 1.4) (Zhou and Chai 2008). In the meantime, the oomycetes and the biotrophic fungi use a specialized structure called haustoria for the delivery of the effectors in the host cells. At first, it was thought that plant-membrane invaginated haustoria functioned only for nutrient uptake, but research has shown that it is also involved in effector delivery into host cells (Catanzariti et al. 2006; Dodds et al. 2004). Hemibiotrophic and necrotrophic fungi use specialized invasive hyphae (IH) for effector delivery inside host cells. For instance, the hemibiotrophic rice pathogen *M. oryzae* accumulates effectors into a lobed structure at the hyphal tip known as a biotrophic interfacial complex (BIC) before its subsequent delivery into the host cytosol (Khang et al. 2010). To date, nothing is known about the effector's release mechanism into the host cells used by mutualistic fungi, including mycorrhiza. However, it has been assumed that mutualistic fungi might utilize similar structures as pathogenic fungi like haustoria or IH to deliver effector protein inside of the plant cells. For example, mycorrhizal fungi use arbuscules as the site of nutrient and signal exchange between the plant and the fungus, which may also be involved in the secretion of effector into the plant cells.

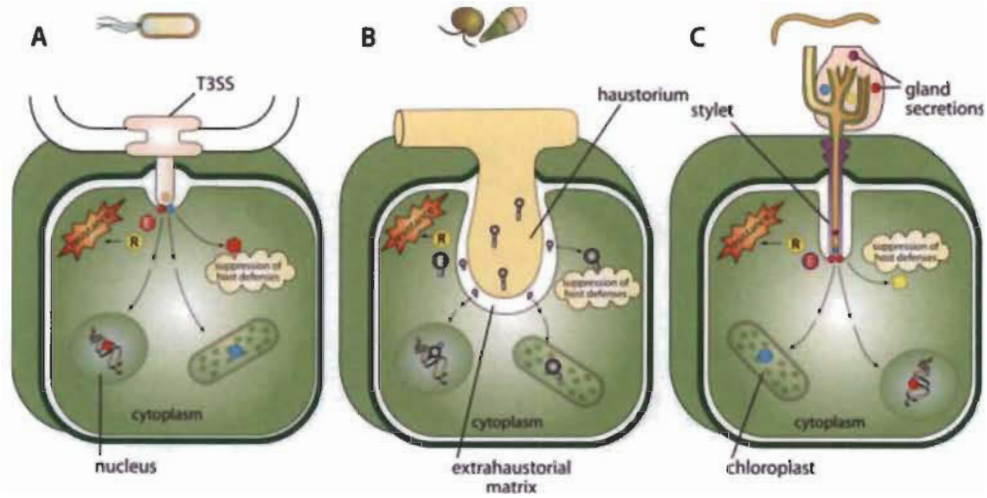

Figure 1.4 Effector delivery structures of Gram-negative bacterium, oomycete, fungus, and nematode in a plant cell.
A) Type III secretion system in Gram-negative bacterium injects effectors into the host cell. B) The haustorium in biotrophic and hemibiotrophic filamentous pathogens is believed to be the site of effector release into the host cell. C) Gland secretions, which include effectors, are injected into the plant cell via the stylet of the nematode. Effectors (E) thus delivered, can either suppress host defenses or trigger host cell defenses, which include programmed cell death (PCD) upon recognition by resistance (R) proteins. Recognition of effectors by R proteins may occur directly (observed with some fungal effectors) or indirectly as a result of the interaction of the effectors with other host protein(s) (observed with several bacterial effectors). Potential subcellular locations of effectors such as the nucleus and chloroplasts are also shown.

1.4.4 Host-protein targets of effectors

It is now well established that the pathogen effectors directly target host proteins and manipulate host targets for their benefit (Rovenich et al. 2014; Win et al. 2012). The first host-targets of plant-pathogen effector proteins to be identified were of bacterial type III effector (T3Es), many of which target positive regulators of immunity in order to inhibit their activity (Deslandes and Rivas 2012). One particularly notable example of a host target is the *A. thaliana* RPM1-interacting protein RIN4 (Win et al. 2012). Some bacterial effectors are enzymes, such as some of T3SS delivered effectors which biochemically alter host molecules, such as HopZ1a which has been reported to physically interact with GmHID1 (2-hydroxyisoflavone). The interaction of HopZ1a and GmHID1 leads to degradation of GmHID1 and thereby leads to enhanced bacterial multiplication (Cunnac et al. 2009; Deslandes and Rivas 2012). Few effectors do not convey enzymatic activity; however, they bind to host proteins to alter host cellular

functions. In addition to this, many such effectors prevent plant enzymes activity (kinases, glucanases, peroxidases, and proteases) (Song et al. 2009; Tian et al. 2004; Tian et al. 2007). Other groups of bacterial effectors bind nucleic acids and regulate gene expression, for example, *Xanthomonas* Transcription Activator-Like (TAL) effectors directly bind to promoter motifs of host genes to modify host transcription (Boch et al. 2009; Gu et al. 2005; Yang et al. 2006). SWEET sugar transporters are one of the host susceptibility genes which are induced by TAL effectors (Li et al. 2013).

Identification of the effector targets in the host cell remains challenging because of a large number of uncharacterized or unidentified effectors from the diverse group of pathogens, microbes and symbionts. For the same reason, the biochemical mechanisms of how effectors manipulate their host target are also poorly understood. Regardless of the specific target of effectors, now it has been reported that a single effector can target multiple plant proteins or can disturb diverse cellular processes in the host (Fig. 1.4) (Win et al. 2012). For example, the *P. syringae* type-III effectors AvrPto and AvrPtoB in tomato and *Arabidopsis,* directly bind to several immune receptor kinases to abrogate their function and impede PTI signaling pathways (Abramovitch et al. 2006; Gimenez-Ibanez et al. 2009; Shan et al. 2008; Xiang et al. 2008; Zheng et al. 2012). The HopM1 effector, degrades several plant proteins, including AtMin7 (Nomura et al. 2006). Similarly, secreted AY-WB Protein 11 (SAP11), a phytoplasma effector, binds to both class I and II of Teosinte branched 1/Cycloidea/Proliferating (TCP) transcription factors (TF), but subverts the class II type TCP TF (Sugio et al. 2011); hence one of the main function of effectors is the suppression of immunity.

1.4.5 Host-protein helpers of effectors

Regardless of the proteins used as effectors target, some plant proteins act as a co-factor for effector function or post-translationally modify effectors in the cytoplasm and are required for the maturation or trafficking of effector protein to their final subcellular destination within the host cell (Win et al. 2012). Therefore, host proteins that facilitate effectors maturation or activity, are known as effectors helper proteins

(Fig. 1.5A-B) (Win et al. 2012). Several host effector helpers have been identified. Classic examples of helper protein are the cyclophilin (a chaperone) CYP1. AvrRpt2, a cysteine protease is secreted as an inactive form by *P. syringae*, but as soon as it is inside the host cell, it interacts with cyclophilin. The association of AvrRpt2-cyclophilin accelerates folding of the effector and cyclophilin activates self-processing of AvrRpt2, aggravating the breakdown of RPM1 Interacting Protein 4 (RIN4), the target protein of AvrRpt2 (Coaker et al. 2005). Another *P. syringe* type-III effector, HopZ1a, is activated by cellular phytic acid from the host to become a functional acetyltransferase that acetylates tubulin, a plant target of HopZ1a (Lee et al. 2012). Other type-III effectors require host-mediated biochemical modifications, like myristoylation and phosphorylation, to become functional. Myristoyl transferase is an example which myristoylates the AvrPto T3SS secreted effector of *Pseudomonas syringae*. Myristoylation of AvrPto and AvrRpm1 is necessary for their avirulence and virulence activities, suggesting that plant N-myristoyl transferase act as a host-cell helper to the effector (Anderson et al. 2006; Nimchuk et al. 2000). The plant protein importin-α is an another well-studied helper protein that mediates nuclear trafficking and is exploited by several pathogen effectors, including SAP11, TAL and Crinklers (Bai et al. 2009; Schornack et al. 2010; Szurek et al. 2001). TAL effector AvrBs3 interacts with importin which enables its accumulation in the host-cell nucleus where it directly binds to plant DNA harboring a conserved promoter element, which is its "real" target, to activate plant gene expression (Kay et al. 2007; Szurek et al. 2001). Therefore, host proteins can act either as an effector helper or target that are taken or manipulated by the pathogen to enable their effector proteins to function and ultimately, establish a state of effector-triggered host susceptibility. Therefore, conceptually the host proteins used as target or helper for the effectors are host susceptibility factors (Win et al. 2012).

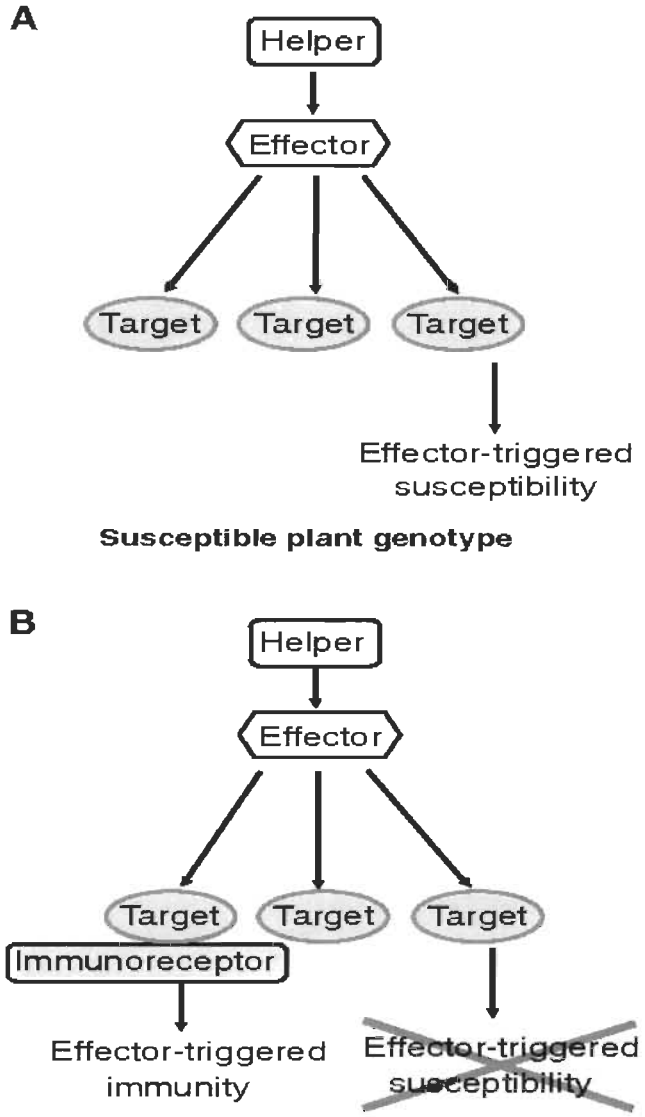

Figure 1.5 Effectors and their host-cell helpers and targets.
This genetic model describes the position of pathogen effectors and their respective host-cell helpers and targets in the signaling pathways leading to susceptibility (A) and resistance (B). Effector targets and effector helpers are distinct plant susceptibility factors. Pathogen effectors recruit host helper proteins and interact with them for proper function. Activated effectors bind cognate targets, manipulate them, and form active effector-target complexes. In a susceptible interaction, the effector-target complex is not recognized and results in an altered cellular state of effector-triggered susceptibility. In a resistant interaction, this complex trigger host recognition by cognate immune receptors leading to effector-triggered immunity (Source: Win et al 2012).

1.5 Poplar-*Melampsora larici-populina* interaction

Poplars, the common name for the trees of genus *Populus*, are an endemic species and ecologically and economically important in Canada (Cooke and Rood 2007). Poplar is mainly grown for wood production. Poplar was the first tree whose genome was sequenced, it is also one of the easiest trees to manipulate in the laboratory, making it a model species of reference in tree biology (Tuskan et al. 2006). The *Populus* genus includes poplars and aspens and belongs to the family Salicaceae. The genus *Populus* contains 29 species of poplars to which must be added natural hybrids resulting from naturally or artificially occurring crosses. Poplars are fast-growing dioecious trees with deciduous, single-leafed foliage. They grow on moist soil, typically in riparian forests of Europe, North America, and Asia. In general, inter-American hybrids (*Populus thricocarpa* x *Populus deltoides*) or Euramericans (*P. deltoides* x *Populus nigra*) are grown in poplar plantations. Wood is harvested at 15-20 years of age for the production of food packaging, fire wood and timber. In Canada, the main limitation to popular culture comes from epidemics of the poplar leaf rust caused by the fungi of the genus *Melampsora*.

Melampsora larici-populina (Mlp), one of the most devastating pathogens, cause rust disease on poplar (Basidiomycete, Pucciniomycete) and belongs to the order Pucciniales which represents the largest group of phytopathogenic fungi, with more than 8000 described species (Aime et al. 2014). Pucciniales are obligate biotrophs which need their hosts to achieve their life cycle. The *Melampsora* alone has more than 50 species, of which 17 are pathogenic of poplars (genus *Populus*, (Vialle et al. 2011)). Like other rust fungi, one of the remarkable features of *Mlp* is heteroecism; it infects two completely unrelated host plants to complete their life cycle; poplar *(Populus sp.,* a dicot, telial host) for asexual reproduction and larch (*Larix sp.,* conifer, aecial host*)* for sexual reproduction. To do so, they exhibit a macrocyclic lifestyle which involves producing five different spore forms; teliospores, basidiospores, pycniosopores, aeciospores, and urediniospores (Fig. 1.6). Diploid teliospores (2n) of *Mlp* hibernates on dead leaves of poplar over the winter. Once spring starts, telieospores go through karyogamy and meiosis and yield wind born haploid basidiospores (n) which infect larch

needles. Henceforth, within few days, pycniospores (n) are produced on needles of larch and plasmogamic fusion of opposite mating type pycniospore generate aeciospores (n+n). At the end of the spring, aeciospores infect poplar leaves and produce another yellow-orange pustule-like sporulation (uredinium) on the abaxial side of mature leaves. Uredinium release uredinospores (n+p.) (asexual phase) and can spread over large distances, and function as inoculum for further infection for poplar epidemics. Numerous infectious vegetative cycles emerged throughout summer and autumn. However, at the end of summer/autumn, telia (black pustule) forms on poplar leaves which again produce teliospores (overwintering spores) and complete the life cycle of *Mlp* (Fig. 1.6A) (Hacquard et al. 2011). As most pathogenic observations materialize during the asexual developmental phase of the vegetative cycle (uredinospore formation and spreading) of *Mlp* (Fig. 1.6B), this phase drew the attention of molecular pathologists concentrating on functional characterization of poplar-*M. larici-populina* interactions (Hacquard et al. 2011).

The symptoms caused by *Mlp* on these two hosts are very different. The infection of larch needles by *Mlp* is marked by limited symptoms over time without impacting the development or growth of the host and usually leads to minor damage. On the contrary, poplar infection by *Mlp* has considerable consequences, and causes epidemics in poplar plantations for many years. Repeated attacks can lead to growth losses of up to 60%, a general weakening of trees, decreased photosynthesis efficiency, early defoliation, and increased susceptibility possibly cause their death (Pinon and Frey 2005). Most poplar cultivars share *P. deltoides* as one of their parents, a species that has not evolved in the presence of European parasites (Pinon and Frey 1997) and has been a source of disease resistance genes (Jorge et al. 2005). After several years of cultivation of completely resistant cultivars, *Mlp* broke down several complete resistance genes, and new virulent genotypes produced through recombination were amplified by an intense selective pressure (Frey et al. 2005). The recently published comprehensive resistance genes were quickly overcome after each new commercial use, prompting the search for durable resistance (Dowkiw et al. 2003; Pinon and Frey 2005). Even varietal mixtures of poplar clones were unable to reduce disease severity (Miot et al. 1999).

A

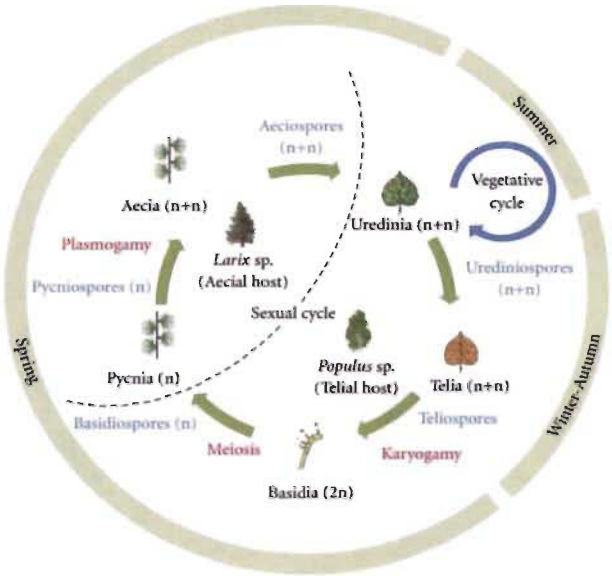

B

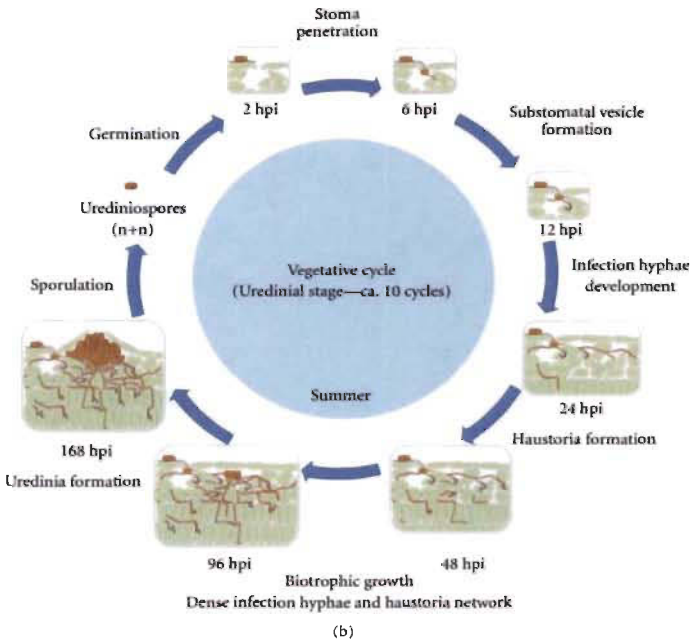

Figure 1.6 The Life cycle cycle of *Melampsora larici-populina*.
A) The biological macrocyclic heteroecious cycle of *M. larici-populina*. B) Vegetative cycle occurring on poplar leaves and used as a model for molecular investigations of the poplar-poplar rust interaction (Source: Hacquard et al. 2011).

1.6 Poplar and poplar rust: a model system

The poplar-poplar rust pathosystem was the first pathosystems involving a tree in which both the host and pathogen genomes are available. Progress made through the study of the genomes and transcriptomes of poplar and *Mlp*, place this pathosystem as an

advanced model for studying the molecular interactions between trees and pathogen (Duplessis et al. 2011a; Duplessis et al. 2011b; Hacquard et al. 2013; Hacquard et al. 2010; Hacquard et al. 2012; Joly et al. 2010; Pernaci et al. 2014; Persoons et al. 2017; Petre and Kamoun 2014; Tuskan et al. 2006). It is also an excellent and exclusive model for studying rusts in general. *Mlp* has a large diploid genome of 101 Mb which is enriched in repetitive and transposable elements (TE), a common characteristic of rust genomes. There are an estimated 16,399 genes in the poplar rust genome (Duplessis et al. 2014). Since 2011, the annotations and *in silico* predictions of the secretome of *Mlp* helped to identify a broad repertoire of genes encoding small secreted proteins (SP). *Mlp* has more than a thousand SP genes with unknown functions that could correspond to effectors (Duplessis et al. 2011a; Hacquard et al. 2012). To date, the molecular mechanisms underlying the colonization of foliar poplar cells by *Mlp* remain to be elucidated, including an understanding of the potential role of updated candidate effectors.

1.7 CSEPs from *Melampsora larici-populina* (*Mlp*)

1.7.1 Identification and selection

The Candidate Secreted Effector Proteins (CSEPs) of *Mlp* were initially identified when the *Mlp* genome was published (Duplessis et al. 2011a). Recently a distinctive pipeline (Lorrain et al. 2015) for CSEPs prioritization in *Mlp* has been outlined based on the findings of two independent groups (Hacquard et al. 2012; Saunders et al. 2012), which is represented in Fig. 1.7. The analysis of the *Mlp* genome revealed 1,184 small secreted proteins with an N-terminal signal peptide, no homology to proteins outside of the Pucciniales, and no predicted transmembrane domains (Duplessis et al. 2011a). In agreement with this, expression analysis found that 79% of these genes were preferentially expressed in haustoria. A more comprehensive analysis, integrating genomic, transcriptomic, and proteomic techniques have also been used to identify the candidate effectors. However, Petre and collaborators gave stronger weight to some of the criteria used by the two studies reported earlier (Hacquard et al. 2012; Saunders et al.

2012). Redundant family members were removed to emphasize on orphan and lineage-specific CSEPs, given that pathogenicity mechanisms indicate highly specific functions. This criterion directed to a subset of 24 priority CSEPs from initially identified 1,184 SSPs of *Mlp* (Petre et al. 2015). All 24 prioritized CSEPs were used for further functional characterization to unravel the molecular interaction between *Mlp* and plant.

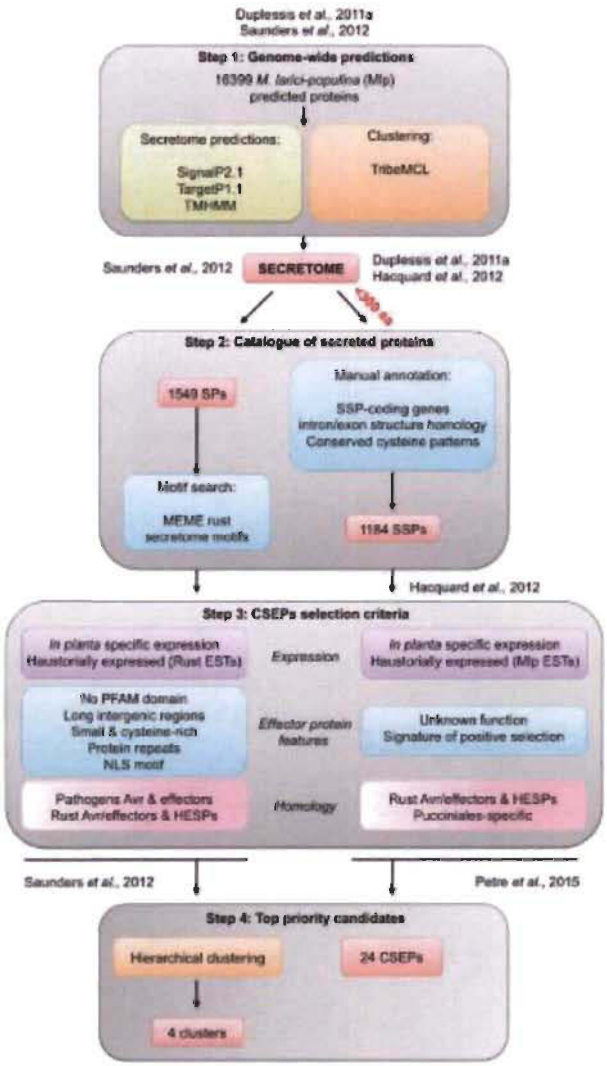

Figure 1.7 Pipelines of effector mining of *Mlp* for prioritizing CSEPs.
Mlp effector mining pipeline comprises four major steps: step 1: Genome-wide predictions identify the secretome of *Mlp* using prediction tools (green) and clustering of gene families with TribeMC (orange); step 2: Catalog of secreted proteins identifies a set of secreted proteins; step 3: CSEPs selection criteria identifies CSEPs by different characteristics; and step 4: Top priority candidates prioritize CSEPs for further functional studies. Avr = avirulence protein; EST = expressed sequence tag; SP = secreted protein; SSP = small secreted protein; HESP = haustorial expressed secreted protein (Adapted from Lorrain et al. 2015).

1.7.2 Subcellular localization of *M. larici-populina* effectors

To better understand the molecular mechanism of the pathogenicity of *Mlp*, it is crucial to understand the subcellular accumulation of *Mlp* effectors in the host cell (Petre et al. 2015). Twenty candidate effectors of the poplar rust fungus were studied in *N. benthamiana* to identify their cellular localization and potential host proteins (Petre et al. 2015). Eight candidates showed either a specific localization when transiently expressed without their signal peptide in fusion with GFP or a specific interaction with plant proteins by co-IP/MS. A candidate effector, Mlp124017, has been shown to interact with the poplar TOPLESS-related proteins 4 by co-IP when co-expressed in *N. benthamiana* (Petre et al. 2015). A study by the same author also shows a candidate effector targeting chloroplasts (chloroplast-targeted protein 1; MlpCTP1). A transit peptide is necessary and sufficient as well for the MlpCTP1 effector to accumulate in the chloroplasts (Petre et al. 2016).

Recently our laboratory used stable transgenic *A. thaliana* lines to show the subcellular localization of sixteen other candidate *Mlp* effectors (in fusion with GFP) (Germain et al. 2018). Out of sixteen, three candidates showed accumulation in chloroplasts, plasmodesmata and cytoplasmic bodies respectively, while the rest of the thirteen effectors showed a non-informative distribution in the nucleus and the cytosol, like the free GFP (Fig. 1.8). Three candidates promoted both oomycete and bacterial growth as well and were considered as *bona fide* virulence factors (Germain et al. 2018). Two more effectors studied from our lab, among them the Mlp124202 accumulated in the membrane and cytoplasm while the Mlp124478 accumulated in the nucleus and nucleolus of plant cell to promote the growth of the oomycete pathogen (Gaouar et al 2016; Ahmed et al. 2018). Virulence effect of *Mlp* in host plants depends on the cumulative functional effects of its diverse effectors, including their interaction with host proteins or how they manipulate host subcellular programs. Therefore, it is certainly important to uncover the subcellular accumulation of diverse effector proteins.

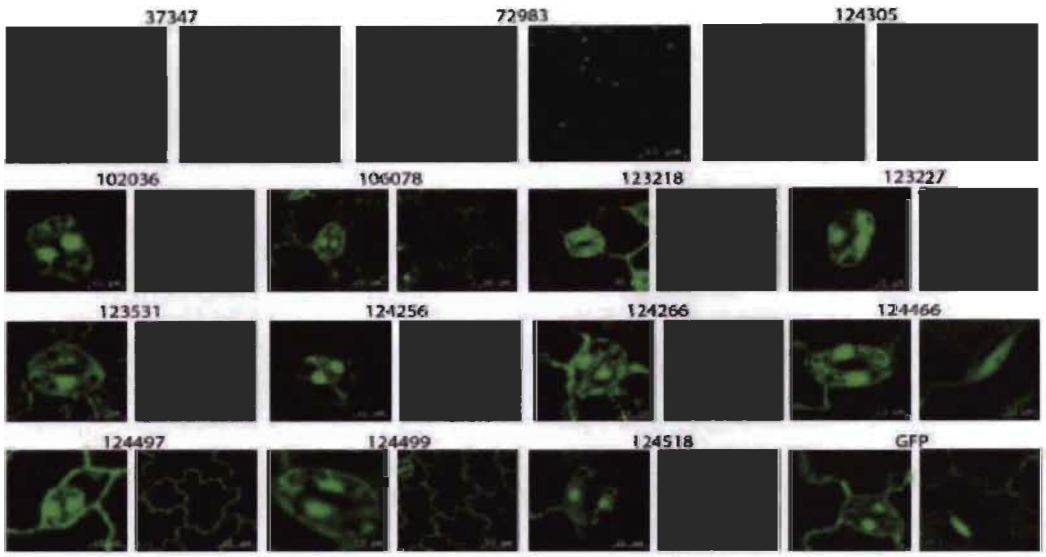

Figure 1.8 Subcellular localization of candidate effectors of *M. larici-populina*.
Confocal images were taken from leaf epidermal cells of 7-day-old *Arabidopsis* transgenic plantlets expressing candidate effectors fused to a green fluorescent protein (GFP) (SSP-GFP) in the Col-0 genetic background. The top three effectors are those displaying informative localization, whereas the bottom three rows display the effectors showing nucleocytoplasmic localization (Source: Germain et al. 2018).

1.7.3 Heterologous system to study effectors

For the functional characterization of effectors, several time-effective and cost-effective assays exist. These assays often depend on the heterologous expressions of tagged effector without their signal peptide directly inside leaf cells of model plant species such as *A. thaliana* or *N. benthamiana*. The heterologous system comprises the expression of the gene in a host organism other than the source, which is simpler than the natural source (Yesilirmak and Sayers 2009). *Arabidopsis thaliana* appeared as a model organism over three decades ago (Meyerowitz 1989; Meyerowitz 2001; Ossowski et al. 2008; Rédei 1975) and its role in genetics resulted as a powerful model system in molecular biology (Koornneef and Meinke 2010) and in molecular plant-microbe interactions. The fact that *Arabidopsis* is a host for many pathogens including insects, bacteria, fungi and nematodes facilitates and speeds the understanding of the plant-pathogen interaction. Furthermore, the fast and simple generation of mutation and transgenic plant enable forward gene function studies. *Nicotiana benthamiana* is another notorious heterologous model plant which is susceptible to various plant pathogens such

as virus, bacteria, oomycete, and fungi. Simplified and efficient transfection method enabled *N. benthamiana* for transient expression of proteins which attracted plant biologist rapidly (Chapman et al. 1992; Escobar et al. 2003; Goodin et al. 2005; Goodin et al. 2007; Goodin et al. 2002; Goodin et al. 2008). Lately, several groups have reported on the use of heterologous systems to investigate the localization, function or interaction partners of effectors from biotrophic pathogens (Caillaud et al. 2012a; Caillaud et al. 2012b; Du et al. 2015 ; Gaouar et al. 2016; Germain et al. 2018; Ahmed et al. 2018; Kunjeti et al. 2016; Petre et al. 2016; Petre et al. 2015).

1.8 Research objectives

A sustainable level of resistance is crucial to reduce the damage by rust pathogen for improving crop production. To develop targeted defense strategies and produce more resistant crops, it is essential to better understand plant-microbe interactions. Plant-microbe interactions are influenced by numerous factors, among which are effector proteins which suppress the plant innate immune system to induce susceptibility of the host plant. Even though increasing knowledge has been gained on the function of bacterial effectors, the contributions of effectors from filamentous pathogens to virulence remain a blurred picture. This is especially true for effectors of poplar rust fungi. However, recent successful applications of new technologies that have led to the identification of effector molecules of *Mlp* provided a model for using a set of pre-determined criteria in selecting candidate gene families (Catanzariti et al. 2006; Vleeshouwers and Oliver 2014). With increasing numbers of poplar rust effectors being identified, the next important step is to unravel their molecular function and understand their role in the interaction of *Mlp*-host pathosystems.

For this thesis research, we selected an effector from *Mlp* pathogen; Mlp124357 and wanted to solve the following questions:

1) Where does the Mlp124357 accumulate in plant cells?
2) Does it manipulate plant defense?
3) If yes, then how does it occur?

To address the questions stated above, we have separated the work in three chapters, two of which are already accepted in scientific peer-reviewed journal while the third will be submitted shortly.

Very early in this project it became obvious that the tonoplast would take a huge importance in this work given that the effector under study localizes to the tonoplast. We observed that there was very limited literature on tonoplast, although it is the largest membrane system delimiting the largest plant organelle, the literature with regards to its role in immunity was scarce. For this reason, we wrote a review on the tonoplast, this review was accepted recently in Plant Molecular Biology and is presented as **Chapter II**, it can be seen as a continuation of the introduction with a focus on the tonoplast and the vacuole.

When we realized that Mlp124357 was targeting the tonoplast it also became obvious that it behaves differently than some well-known tonoplast marker and for this reason it became a useful tool to investigate the tonoplast and the tonoplast sub-cellular compartment, the bulbs and the transvacuolar strands. This investigating is the subject of **Chapter III**.

Finally, to core of the work of this project was to investigate if the effector affected the plant susceptibility and if yes how did it achieve it role in virulence. To answer these questions we perform pathogenicity assays, use immunoprecipitation to find and interaction partner, confirmed the interaction using yeast-two hybrid, obtained a further genetic confirmation, created a mutant of the effector, performed a full-transcriptome analysis and use *in silico* modeling and docking. These results are presented in **Chapter IV** and will be submitted shortly.

A discussion is presented in **Chapter V**.

Chapter II discusses about the dynamics of vacuolar membrane structures and different types of marker for study them. It also highlights their roles in plant-pathogen interactions.

CHAPTER II

VACUOLAR MEMBRANE STRUCTURES AND THEIR ROLES IN PLANT-PATHOGEN INTERACTIONS

Mst Hur Madina, Md Saifur Rahman, Huanquan Zheng, and Hugo Germain

Published on 16th of October 2019 in *Plant Molecular Biology*.

2.1 Author contributions

Madina, Germain, and Zheng designed the study. Madina and Saifur prepared the literatures. Zheng and Germain reviewed the figures and edited the manuscript.

2.2 Résumé de l'article

Les plantes n'ont pas de cellules immunitaires spécialisées, chaque cellule doit donc se défendre elle-même contre les agents pathogènes envahissants. Une stratégie typique de défense des plantes est la réponse hypersensible entraînant la mort des cellules hôtes au site de l'infection, un processus largement médié par la vacuole. Dans les cellules végétales, la vacuole est un organite vital qui joue un rôle central dans de nombreux processus fondamentaux, tels que le développement, la reproduction et les réponses cellulaires aux stimuli biotiques et abiotiques. Sa membrane est constituée de structures membraneuses diverses en constante transformation. Les progrès techniques récents en visualisation et en imagerie de cellules vivantes ont considérablement modifié notre vision des structures vacuolaires et de leur dynamique. Comprendre la nature active des structures vacuolaires et les mécanismes des réponses de défense impliquant les vacuoles est d'une grande importance pour la compréhension des interactions plante-pathogène. Dans cet article de revue, nous présentons un aperçu des connaissances

actuelles sur la vacuole et ses structures internes, ainsi que leur rôle dans les interactions plante-microbe. Jusqu'à présent, les informations sur la modulation des structures vacuolaires par les agents pathogènes sont limitées, mais des recherches récentes ont identifié la vacuole comme cible possible des interférences microbiennes.

Mots-clés : tonoplaste, vacuole, bulbe, filament transvacuolaire, défense des plantes.

2.3 Full article in English: Vacuolar membrane structures and their roles in plant-pathogen interactions

Abstract

Plants lack specialized immune cells, therefore each plant cell must defend itself against invading pathogens. A typical plant defense strategy is the hypersensitive response that results in host cell death at the site of infection, a process largely regulated by the vacuole. In plant cells, the vacuole is a vital organelle that plays a central role in numerous fundamental processes, such as development, reproduction, and cellular responses to biotic and abiotic stimuli. It shows divergent membranous structures that are continuously transforming. Recent technical advances in visualization and live-cell imaging have significantly altered our view of the vacuolar structures and their dynamics. Understanding the active nature of the vacuolar structures and the mechanisms of vacuole-mediated defense responses is of great importance in understanding plant-pathogen interactions. In this review, we present an overview of the current knowledge about the vacuole and its internal structures, as well as their role in plant-microbe interactions. There is so far limited information on the modulation of the vacuolar structures by pathogens, but recent research has identified the vacuole as a possible target of microbial interference.

Keywords: tonoplast, vacuole, bulb, transvacuolar strand, plant defense

Introduction

The plant vacuole and its function in the cell

Unlike cells from other organisms, plant cells have a uniquely large and prominent organelle called the vacuole, occupying 90-95% of the cell's volume (Owens and Poole 1979). The vacuole has important physiological functions, one of the main being the preservation of turgor pressure against the cell wall, thus supporting the structural stability of the cell and of the surrounding tissue (Marty 1999). It also serves as a storage

tank holding many different materials needed by the cells, including but not limited to: sugars, metabolites, carbohydrates, lipids, amino acids, enzymes, proteins, and anthocyanins (Marty 1999; Paris et al. 1996). In addition, the vacuole stores toxic ions and many other compounds that play a role in the defense against bacterial pathogens and herbivores (Martinoia et al. 2012; Van der Hoorn and Jones 2004).

Depending on tissue and cell types, vacuoles are diverse in their morphologies and functions (Swanson et al. 1998). Two main types are found in plants, the protein storage vacuoles (PSV) and the lytic vacuoles (LV) and they are functionally distinct (Hoh et al. 1995; Paris et al. 1996; Robinson et al. 1995). The typical storage compartment PSVs are most abundant in seeds (Epimashko et al. 2004; Hoh et al. 1995; Otegui et al. 2005; Paris et al. 1996; Swanson et al. 1998) and are formed during seed development and maturation. They accumulate large amounts of storage proteins, which are synthesized in the endoplasmic reticulum (ER) and delivered into vacuoles via the prevacuolar complex (Sansebastian et al. 2017), where they remain stored until they are mobilized during germination and seedling growth (Bewley and Black, 1994). PSVs also store defense proteins for the response against microbial pathogens and herbivores. After seed imbibition, PSVs are converted into lytic vacuoles (Bewley et al. 1994; Wang et al. 2007), which are the predominant compartments occurring in vegetative cells and are also called vegetative vacuoles. The identity of each vacuole is determined by its pH and by the presence of specific proteins known to be localized to PSVs or LVs, such as tonoplast intrinsic proteins (TIPs), which are integral membrane proteins found in specific vacuolar membranes (Jauh et al. 1999; Johnson et al. 1989). For example, the PSVs have a neutral pH and are defined by the presence of α- and δ-tonoplast intrinsic protein (TIP), whereas the LVs have an acidic pH and are marked by γ-TIP (Jiang et al., 2000; Jauh et al. 1999).

Vacuoles are increasingly recognized for their role in cellular signaling during growth (Zhang et al. 2014), the immune responses (Hatsugai and Hara-Nishimura 2010), and the regulation of cell death (CD) (Hara-Nishimura and Hatsugai 2011; Koyano et al. 2014). However, little is known about vacuolar structures and their roles in the defense

response against pathogens. Several reviews have summarized the interactions between the plant vacuole and pathogenic microbes (Hara-Nishimura and Hatsugai 2011; Hatsugai et al. 2006). Here, the first section of this review focuses on the most up-to-date insights about the plant vacuolar structures and dynamics and vacuolar markers. The last section briefly focuses on the role of the vacuole and vacuolar structures in plant-pathogen interactions.

Vacuolar structures

Recent advances in the visualization of the vacuole together with developments in image analysis has revealed the highly organized and complex morphology of the vacuole as well as its dynamics. The plant vacuole is surrounded by a membrane barrier known as the tonoplast, which separates the vacuolar content from the cytoplasm (Fig. 1). The semi-permeable tonoplast maintains a balance of nutrients and ions inside and outside of the vacuole, thus keeping a suitable turgor pressure in the plant cell.

The tonoplast not only surrounds the typical large vacuole but also other transient and mobile structures such as transvacuolar strands (TVS) and bulbs, represented in Fig. 1 (Ruthardt et al. 2005; Uemura et al. 2002). TVSs are dynamic thin tubular structures that traverse the central vacuole, containing cytoplasm and even small organelles (Uemura et al. 2002). Moreover, TVSs provide a direct connection between the perinuclear cytoplasm and the cortical cytoplasm of the cell and as such they act as an important transport route for the distribution of the cytoplasmic content, including the smaller organelles (Grolig and Pierson 2000; Nebenführ et al. 1999). Indeed, it was observed that Golgi bodies (Nebenführ et al. 1999), mitochondria (Van Gestel et al. 2002), endosomes (Ovečka et al. 2005; Ruthardt et al. 2005), and amyloplasts (Saito et al. 2005) dynamically move through the TVSs. Additionally, they play a role in the positioning of the nucleus (Katsuta et al. 1990; Kumagai and Hasezawa 2001; Williamson 1993). The dynamics of the TVS depends on the actin cytoskeleton; consequently, the disruption of the actin filaments leads to the loss of the transvacuolar

strands and inhibition of their movement (Kovar et al. 2000; Kutsuna et al. 2003; Tominaga et al. 2000).

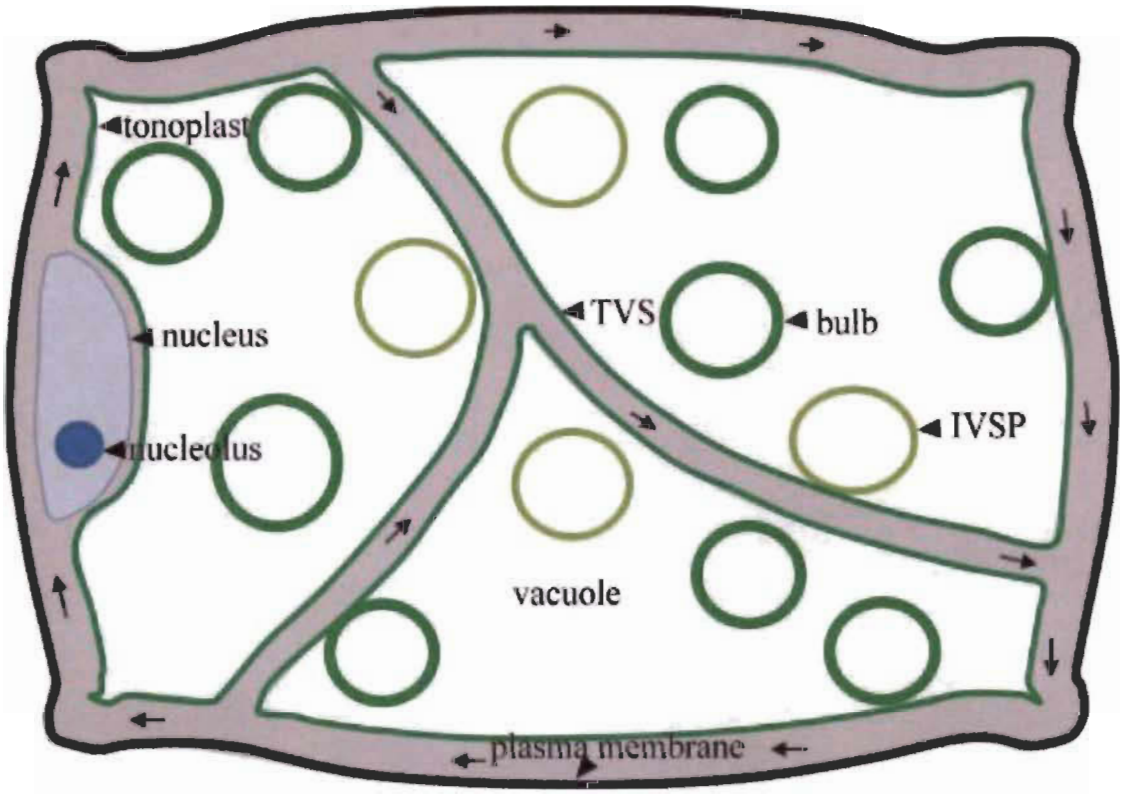

Fig. 1 Schematic diagram presents the vacuole and vacuolar structures in plant cells. The vacuole structures tonoplast, TVS, bulb, IVSP, nucleus, nucleolus, and plasma membrane are shown with arrowheads and the cytosolic flow with arrows. TVS = transvacuolar structures, IVSP = intravacuolar spherical structures.

On the other hand, the bulbs are small highly dynamic spherical structures between 1 and 22 μm of diameter located in the vacuolar lumen (Madina et al. 2018; Saito et al. 2002). 3-D reconstruction of electronic microscopic images indicates that the bulbs are formed of a double membrane and cytoplasmic material is detected between the two lipid bilayers (Saito et al. 2002). This double membrane of the bulbs is responsible for their brighter fluorescence signal compared to that of the tonoplast membrane (Saito et al. 2002). Similar to the dynamics of the TVSs, the movement of the bulbs is dependent on actin (Beebo et al. 2009; Uemura et al. 2002). However, whether bulbs are naturally occurring structures has recently been questioned by Segami et al. (2014), as they propose that some bulbs are artifacts due to the dimerization of the

GFP moiety of tagged tonoplastic proteins, while intravacuolar spherical structures (IVSP) form naturally. The IVSPs are different from bulbs in florescence intensity (2 folds the fluorescence intensity of the tonoplast vs 3 or more folds for the bulbs) and thickness of the double membranes (Segami et al. 2014). These structures are also less abundant in cells and are believed to temporarily store membrane components, however, whether IVSPs are independent structures remains to be resolved (Segami et al. 2014). This model also needs to be further explored as GFP dimerization alone cannot explain the accumulation of bulbs in the YFP-2xFYVE *A. thaliana* line, as this marker binds to the membrane via a protein-lipid interaction and not a transmembrane domain (Saito et al. 2011a). Two functions have been proposed for bulbs; first they may be involved in tonoplastic proteins degradation inside of the vacuole (Maîtrejean et al. 2011; Saito et al. 2002). On the other hand, they may be useful for rapid cell expansion by serving as membrane reservoirs (Saito et al. 2002). Recently, Han et al. (2015) even proposed that bulbs may not have specific functions other than the transient accumulation of tonoplast and cytoskeletal proteins until the bulb membrane is reabsorbed back into the tonoplast. Thus, the definitive function and biogenesis mechanism of bulbs still need to be fully elucidated.

Markers to study the vacuolar structures

The large central vacuole can be easily detected as a large transparent region in the plant cell as seen in light microscopy (Marty 1999), whereas the fine structure of the tonoplast and the intravacuolar compartments had mostly been studied by electron microscopy (Gaffal et al. 2007; Gao et al. 2015; Morita et al. 2002; Saito et al. 2002). The development of chemicals and fluorescent protein markers made possible the use of live-cell imaging to study the vacuole in a more detailed manner, which allows a greater understanding of its structure and dynamics under different growth conditions and various stress types (Reisen et al. 2005). Two different approaches for visualizing the plant vacuolar structures are presented here in below: chemical and protein markers. For selecting a particular technique, it is important to be aware of its advantage and limitations.

Chemical markers

To date, a number of fluorescent/chemical dyes have been identified for staining the tonoplast and vacuolar membranous structures (presented in Table 1). For example, the well-known amphiphilic styryl dyes, FM1-43 (N-(3-triethylammoniumpropyl)-4-(4-(dibutylamino)styryl) pyridinium dibromide) and FM4-64 (N-(3-triethylammoniumpropyl)-4-(4-diethylaminophenylhexatrienyl) pyridinium dibromide), are valuable and frequently used chemical dyes for vital staining of the tonoplast ie staining in live cells (Kim et al. 2001; Kutsuna and Hasezawa 2002; Kutsuna et al. 2003; Leshem et al. 2006; Okubo-Kurihara et al. 2008; Parton et al. 2001; Silady et al. 2008; Tanaka et al. 2007). The FM4-64 has also been reported for staining transvacuolar strands (Kutsuna and Hasezawa 2002; Kutsuna et al. 2003; Silady et al. 2008; Tanaka et al. 2007) and bulbs (Kim et al. 2001; Silady et al. 2008; Tanaka et al. 2007). The FM dyes initially stain the plasma membrane, then small cytoplasmic compartments, and finally reach the tonoplast in a process that is time, temperature, and energy-dependent. In general, to label the tonoplast with FM dyes, the cells are pulsed labeled for several minutes and then chased for several hours in fresh medium. The optimal duration of the chase period depends on the trafficking activity of the cells. In the initial stage of the chase period, the dyes simultaneously label the tonoplast and the other endomembrane components, including the endosomal organelles and developing cell plates (Higaki et al. 2008; Kutsuna and Hasezawa 2002; Ovečka et al. 2005; Parton et al. 2001; Tanaka et al. 2007; Ueda et al. 2001; Vermeer et al. 2006), whereas a longer chase period is required to visualize only the tonoplast (Emans et al. 2002; Kutsuna and Hasezawa 2002; Ueda et al. 2001). In addition to the FM dyes, BCECF (2',7'-bis-(2-carboxyethyl)-5-(and-6)-carboxyfluorescein) fluorescently labels the vacuolar lumen, the tonoplast, the transvacuolar strands, and the bulbs (Higaki et al. 2007; Kutsuna and Hasezawa 2002; Mitsuhashi et al. 2000; Swanson et al. 1998; Toyooka et al. 2006). Vital staining using dyes is rapid, simple to perform, and compatible with the concomitant visualization of fluorescently tagged protein markers. However, this method has several limitations, in either sensitivity or specificity, and vital dyes themselves can sometimes introduce artifacts that must be taken care of during sample preparation or live cells imaging (Melan 1999; Schnell et al. 2012).

Table 1. Chemical and protein markers for labeling tonoplast, TVS, and bulbs

Protein markers				
Name of proteins	Tonoplast	TVS	Bulbs	References
Nitrate transporter (chloride channel a; CLCa)	✓	X	X	(De Angeli et al. 2006)
gamma-TIPs	✓	X	X	(Okubo-Kurihara et al. 2008; Opalski et al. 2005)
	✓	X	✓	(Gattolin et al. 2009; Hunter et al. 2007)
	✓	✓	✓	(Beebo et al. 2009; Boursiac et al. 2005; Hawes et al. 2001; Hicks et al. 2004; Hunter et al. 2007; Saito 2003)
δ-TIP	✓	✓	✓	(Sheahan et al. 2007)
δ-TIP2;1	✓	X	X	(Boursiac et al. 2005; Jaquinod et al. 2007)
Small G protein (AtRab75c)	✓	✓	X	(Saito et al. 2002)
BobTIP26-1-GFP	✓	✓	✓	(Reisen et al. 2005)
Carbohydrate transporter	✓	X	X	(Endler et al. 2006; Jaquinod et al. 2007; Wormit et al. 2006)
Phosphate transporter homolog GFP	✓	X	✓	(Escobar et al. 2003)
Metal transporter	✓	X	X	(Jaquinod et al. 2007; Thomine et al. 2003)
Syntaxin (Vam3 or SYP22)	✓	X	✓	(Bottanelli et al. 2011; Foresti et al. 2006; Kusumi et al. 2005)
	✓	✓	✓	(Uemura et al. 2002)
lipocalin	✓	X	X	(Jaquinod et al. 2007)
CCD1	✓	X	X	(Jaquinod et al. 2007)
Ca^{2+} transporter	✓	X	X	(Kamiya et al. 2006; Peiter et al. 2005)
Zn^{2+} transporter	✓	X	X	(Kobae et al. 2004)
Malate transporter	✓	X	X	(Kovermann et al. 2007)
Organic cation transporter	✓	X	X	(Küfner and Koch 2008)
Phospholipase-like protein	✓	X	X	(Morita et al. 2002)
AtIREG2	✓	X	X	(Schaaf et al. 2006)
K^+ transporter	✓	X	✓	(Voelker et al. 2006)
Cytochrome P450	✓	X		(Xu et al. 2006)

Protein markers				
Name of proteins	Tonoplast	TVS	Bulbs	References
Phosphatidylinositol 3-phosphate probe (2xFYVE)	✓	X	✓	(Vermeer et al. 2006)
GFP: EBD	✓	X	✓	(Kim et al. 2001)
YFP-AtRabG3c	✓	X	✓	(Bozkurt et al. 2015)
Tonoplast potassium channel 1 (TPK1)-GFP (AtTPK1-GFP)	✓	X	✓	(Maîtrejean et al. 2011)
DUF679 Membrane Protein 1 (DMP1)-enhanced GFP (DMP1-eGFP)	✓	✓	✓	(Kasaras et al. 2012)
Vacuolar H^+-pyrophosphatase (VHP1)-GFP	✓	✓	✓	(Segami et al. 2014)
Mutation of some genes				
Vacuole defective gene (*vcl1*)	✓	✓	✓	(Hicks et al. 2004)
rbb1	✓	✓	✓	(Han et al. 2015)
Pathogen's protein marker				
Mlp124357	✓	✓	✓	(Madina et al. 2018)
HpaRxLR	✓	✓	✓	(Caillaud et al. 2012; Inada and Ueda 2014)
Chemical Markers				
FM1-43	✓	X	X	(Kim et al. 2001; Kutsuna and Hasezawa 2002; Kutsuna et al. 2003; Leshem et al. 2006; Okubo-Kurihara et al. 2008; Parton et al. 2001; Silady et al. 2008; Tanaka et al. 2007)
FM4-64	✓	✓	✓	(Higaki et al. 2006; Kim et al. 2001; Kusumi et al. 2005; Kutsuna and Hasezawa 2002; Kutsuna et al. 2003; Leshem et al. 2006; Okubo-Kurihara et al. 2008; Parton et al. 2001; Silady et al. 2008; Tanaka et al. 2007)
BCECF (2',7'-bis-(2-carboxyethyl)-5-(and-6)-carboxyfluorescein)	✓	✓	✓	(Higaki et al. 2007; Kutsuna and Hasezawa 2002; Mitsuhashi et al. 2000; Swanson et al. 1998; Toyooka et al. 2006)

✓= label; x = not label

Protein markers

In addition to chemical markers, many marker proteins tagged with fluorescent proteins are used to label the tonoplast and the vacuolar structures in living cells (Table 1). Most of those markers are integral membrane proteins, with the exception of YFP-2xFYVE which lacks a transmembrane domain and binds to phosphatidylinositol 3-phosphate (Saito et al. 2011a). As YFP-2xFYVE labels bulbs more intensely than the tonoplast, it suggests that PI3P is more concentrated in the bulbs (Vermeer *et al.*, 2006; Saito et al. 2011a). However, not all tonoplast markers can also label bulbs, showing that bulb membranes are qualitatively different than tonoplast membranes (Saito et al. 2002). For example, γ-TIP-GFP was found to be concentrated in tonoplast and bulbs, whereas GFP-AtRAB7c, another tonoplast marker, did not give any fluorescent signal in bulbs form transgenic plants, although the presence of bulbs in these lines was confirmed by transmission electron microscopy (Saito et al. 2002). Some aquaporin isoforms also specifically label tonoplast or bulbs, for example TIP2;1-GFP exclusively localizes in the tonoplast but does not label the bulbs in salt-treated root cells, whereas TIP1;1 relocalized into intracellular spherical structures hypothesized to be tonoplast compartmentalization domains specialized for degradation of this isoform (Boursiac et al. 2005). In addition, two candidate effectors of pathogens have been observed to target the tonoplast and tonoplast-derived structures (TVSs and bulbs): HaRxLR17 from the oomycete *Hyaloperonospora arabidopsidis* (*Hpa*) (Bozkurt et al. 2015; Caillaud et al. 2012) and Mlp124357 from the fungus *Melampsora larici-populina* (*Mlp*) (Madina et al. 2018), and they can be used to study those organelles. The GFP-tagged marker proteins allow the visualization of the vacuole and vacuolar structures without further experimental manipulations once the transgenic lines are constructed. Although this is a powerful technique, it is laborious, time-consuming, and often not practical for many laboratories (Melan 1999; Schnell et al. 2012).

Protein distribution and motility in tonoplast and bulbs

Protein distribution

The complexity and dynamic changes in vacuolar lumen content raise the question of how cells regulate the movement of these materials between the cytosol and the vacuole. A controlled transport across the tonoplast is essential for appropriate plant responses to environmental conditions and for adequate intracellular signaling. The tonoplast contains numerous proteins that facilitate the transport of water, ions and metabolic products across the membrane (Martinoia et al. 2012; Zhang et al. 2014). In response to variation in the cytoplasmic environments, the activity of tonoplast enzymes, transporters, and channels is changed and thus they regulate the material exchange between the cytoplasm and the vacuolar lumen, maintaining cellular homeostasis. For example, H+-ATPase (V-ATPase), H+-pyrophosphatase (V-PPase), and water channels (aquaporins) have been characterized and their roles in the regulation of transport across the membrane have been discussed (Hedrich 2012; Martinoia et al. 2012; Neuhaus and Trentmann 2014).

On the other hand, the lipids of the tonoplast provide an essential molecular environment for the activity of the membrane proteins and serve as a barrier between the cytoplasm and the vacuolar lumen. Interestingly, lipids and proteins in the tonoplast are not always uniformly distributed and tend to be enriched in particular regions, termed membrane micro-domains, that depend on sphingolipids and sterols (Kusumi et al. 2005; Lillemeier et al. 2006; Minami et al. 2009). For example, the tonoplast of *Arabidopsis* suspension cultured cells contains micro-domains with higher ratios of the saturated phospholipids phosphatidylcholine (PC) and phosphatidylethanolamine (PE) in which the vacuolar-type proton ATPase (V-ATPase) was more abundant in detergent-resistant microdomains and appeared to be unevenly distributed in the tonoplast, whereas the vacuolar-type proton pyrophosphatase (V-PPase) was distributed evenly (Yoshida et al. 2013). Another study showed a similar non-uniform distribution of the V-ATPase in the tonoplast of isolated maize root cells (Kluge et al. 2004) and detergent-resistant micro-domains containing a high percentage of sphingolipids, free sterols and saturated fatty

acids were described in the tonoplast of sugar-beet roots (Ozolina et al. 2011). The causes of this precise distribution of lipids and proteins in the tonoplast membrane are not fully elucidated yet; however, the environmental conditions seem to act as important regulators. For example, under phosphate deficiency the *Arabidopsis* phospholipase D PLDζ2 adopts an uneven distribution in which the higher concentrations of PLDζ2 were preferentially positioned close to mitochondria and chloroplasts and thus facilitated transfer between them and the tonoplast (Yamaryo et al. 2008).

Recently, it was observed that an overexpression in *Arabidopsis* of tonoplast intrinsic protein 1;1 fused with GFP (AtTIP1;1-GFP) labels both the tonoplast and the bulbs of the central vacuole but that the distribution of the GFP fusion protein was uneven along the tonoplast (Beebo et al. 2009). We also observed an uneven distribution of a fluorescently tagged protein on the bulb membrane (Video S1; https://doi.org/10.1007/s11103-019-00921-y). Our recent report showed that the candidate effector protein Mlp124357-eGFP localized in the tonoplast, the TVS, and the bulbs of the vacuolar lumen in *Arabidopsis* (Madina et al. 2018). With the help of high-resolution 3-D imaging, we observed two different distribution patterns on the bulb membranes for both Mlp124357-eGFP and the well-known tonoplast marker γ-TIP-YFP. This suggests the existence of two distinct bulb types in these cells, some with a regular marker protein distribution and some with exclusion spots. It would be interesting to characterize and identify additional proteins that accumulates at the bulb membrane.

Protein mobility

Previous description of bulbs and prevailing models indicate they are connected to the tonoplast (Saito et al. 2002). On the other hand, a report pointed out the qualitative differences in protein content between the bulb membranes and the tonoplast (Saito et al. 2011). To investigate the connection between the two membranes, protein mobility between the tonoplast and the bulb membrane have recently been assessed using

fluorescence recovery after photobleaching (FRAP) of young *Arabidopsis* leaf epidermal cells expressing Mlp124357-eGFP or γ-TIP-YFP (Madina et al. 2018). We observed the fluorescence of the bleached region of tonoplast recovered completely within 1 minute, whereas the bleached area of the bulb membrane fluorescence did not recover (Madina et al. 2018). This observation can be explained by two mechanisms: 1) something restricts the movement of proteins from the tonoplast to the bulb membrane even though they are still attached or 2) the connection between the bulbs and the tonoplast is severed. Both explanations provide a new perception of the biology of tonoplast-derived substructures, but further investigation is required to validate the molecular mechanisms implicated. Furthermore, as the vacuole plays a crucial role in plant defense, the role of protein distribution and motility in tonoplast and bulbs should also be the focus of more research.

The vacuole in plant-pathogen interaction

The immune system of plants lack antibodies or phagocytosis. As an alternative, they have evolved numerous layers of active defense responses against pathogens including the production of reactive oxygen species (ROS) (Alvarez et al. 1998; Zhang et al. 2003) and of many other defense compounds such as phytoalexins (Neuhaus et al. 1991). Attempted attacks by avirulent pathogens may result in cell death (CD) in the tissues, a reaction known as the hypersensitivity response (HR), which is effective in preventing the spread of pathogens (Mur et al. 2007). These defense responses largely depend on the plant's vacuole because it constitutes a reservoir for many secondary metabolites, hydrolytic enzymes, and defense proteins (Marty et al. 1999; Hara-Nishimura and Hatsugai 2011).

Secondary metabolites

Plant vacuoles accumulate a variety of secondary metabolites including cyanogenic glycosides, benzoxazinoids, and phenolics, some of which are thought to function as direct defenses against pathogens by reducing their performance, survival,

and reproduction (Shitan 2016; Steppuhn et al. 2004). For example, the well-known cyanogenic glycosides are stored in the plant vacuole as inactive precursors and are able to form toxic hydrocyanic acid (HCN) in response to tissue damage by different phytopathogens (Vetter et al 2000; Freeman BC and Beattie GA 2008). A recent study reported that mutation of the cyanogenic 4-hydroxyindole-3-carbonyl nitrile (4-OH-ICN) pathway increases susceptibility to the bacterial pathogen *Pseudomonas syringae* in *Arabidopsis*, suggesting a role in inducible pathogen defense (Rajniak et al. 2015). Benzoxazinoids are among the most important plant defense compounds for grasses (Poaceae) and are also stored as inactive glucosides in the vacuole to avoid toxicity to the plant itself (Niemeyer et al 2009; Handrick et al. 2016, Zhou et al. 2018). While some benzoxazinoids are constitutively present, others are only synthesised followingpathogen infection. Upon tissue damage, they undergo enzymatic and chemical degradation to become the active benzoxazinoid form (Niemeyer et al 2009). Benzoxazinoids have also been shown to act as defense signaling molecules and to induce callose deposition in response to the pathogenic fungal elicitor chitosan in maize (Ahmad et al. 2011). Another large group of secondary metabolites implicated in defense are the flavonoids, which are widely distributed in terrestrial plants and serve as defense compounds in the plant-microbe interaction (Harborne and Williams 2000; Taylor and Grotewold 2006). For example, silencing of a G-type ABC transporter of *M. truncatula* (MtABCG10) results in a lower concentration of isoflavonoids in the roots which in turns results in increased growth of *Fusarium oxysporum*, indicating that flavonoids play an important role in the defense against root-infecting pathogens (Banasiak et al. 2013). Finally, the seed coat accumulates flavonoids to protect the embryo and the endosperm from external stresses such as UV radiation and pathogen infections (Lepiniec et al. 2006; Shimada et al. 2006; Shimada et al. 2018).

Hydrolytic enzymes

Like animal lysosome, plant vacuole contains hydrolytic enzymes (e.g. aspartate proteinases, cysteine proteinases, and nucleases) that play an important role in the crucial events of plant cell death to prevent the spread of biotrophic pathogens (Boller

and Kende 1979; Wada 2013). As first reported by Jones almost two decades ago, the plant vacuole play an important role in the programmed cell death that occurs in response to biotrophic pathogens (Jones 2001). It was also reported that the vacuolar processing enzyme (VPE) is up-regulated during cell death associated with leaf senescence and lateral root formation in *Arabidopsis* (Hatsugai et al. 2004). The same group confirmed that during the defense response plants use the vacuole content in both a destructive and a non-destructive way. The destructive pathway is effective against virus infection, during which the tonoplast collapses and releases vacuolar hydrolytic enzymes called vacuolar processing enzymes (VPE) to suppress virus proliferation in the host cytosol (Hatsugai et al. 2004). The non-destructive way is effective against extracellular bacterial infections and involves the fusion of the plasma membrane to the tonoplast, which allows the discharge of the vacuolar content, including the proteasome subunit PBA1, in the apoplast. This leads to a hypersensitive cell death which suppresses the bacterial proliferation (Hatsugai et al. 2009). Interestingly, although structurally unrelated to caspases, both the vacuolar processing enzyme and the proteasome subunit PBA1 exhibit a caspase-like activity (Hatsugai et al. 2009). As it has been observed that proteasome defects impair the vacuole membrane fusion and VPE deficiency prevents virally induced hypersensitive cell death (Hatsugai et al. 2004, Hatsugai et al. 2009), the identification of PBA1 and VPE substrates would help to unravel the molecular mechanisms of tonoplast breakdown or fusion with the PM.

Defense proteins

The defense proteins, including pathogenesis related proteins (PR proteins) (Neuhaus et al. 1991), myrosinases (Ueda et al. 2006), and lectins (Bowles et al. 1986), are located in the vacuole and act as an effective second line of defense when a pathogen causes tissue damage. For example, overexpression of the pathogen-inducible PR1 genes in tobacco enhances resistance to several fungi, including *Peronospora tabacina* and *Phytophthora parasitica f.sp. nicotianae*, and to the bacteria *Pseudomonas syringae pv. Tabaci* (Broekaert and Terras 2000). The association between PR-1 proteins and enhanced resistance against oomycetes has also been noted when PR1 expression was

transiently silenced by double-stranded RNA interference in barley (Schultheiss et al. 2003). The myrosinases accumulate mainly in the vacuoles of idioblastic myrosin cells, a cell type specific to the abaxial side of the leaf known to accumulate myrosinases (Höglund et al. 1991; Höglund et al. 1992; Thangstad et al. 1991; Thangstad et al. 1990). When plants experience tissue damage, the myrosinases are released from the collapsed vacuoles of the myrosin cells and start the hydrolysis of their glucosinolates substrates to produce isothiocyanates, which are toxic for bacteria. This chemical defense system is known as the myrosinase-glucosinolate system, which is also called the mustard oil bomb (Fuji et al. 2016; Grubb and Abel 2006; Halkier and Gershenzon 2006; Hopkins et al. 2009; Kissen et al. 2009; Rask et al. 2000; Wittstock and Halkier 2002). Moreover, overexpression of Ta-JA1, a jacalin-related lectin gene that resides in vacuole, have been found to increase resistance to bacteria, fungal, and viral pathogens in tobacco plant (Ma et al. 2010).

Vacuole dynamics

The relationship between vacuole dynamics and cell death during the defense response has been discussed for over a decade (Jones 2001). For example, during cell death of the tracheary element in *Zinnia elegans*, disintegration of the tonoplast was observed (Obara et al. 2001). Recent studies have demonstrated that during cell death induced by a pathogenic signal such as the oomycete elicitor cryptogein from *Phytophthora cryptogea* or the bacteria *Erwinia carotovora*, the complex vacuole of BY-2 cells simplified and then ruptured (Higaki et al. 2007; Hirakawa et al. 2015). This seem to be regulated by the vacuolar-localized protease called VPE (Higaki et al. 2011). The structural simplification of vacuoles is also observed in various processes involving program cell death, such as gibberellin-mediated cell death in central aleurone cells (Gao et al. 2015), embryogenesis of gymnosperms (Smertenko et al. 2003), and leaf formation in lace plants (Gunawardena 2007). However, it remains elusive whether simplification of the vacuole is a typical process in defense-related CD.

Tonoplast, TVS, and bulbs in plant-pathogen interaction

Although the vacuole plays an important role in plant defense, little is known about the manipulation of plant vacuolar structures by pathogens. To date, only two effector proteins, one from *H. arabidopsidis* and the other from *M. larici-populina*, have been found to reside in the host tonoplast, TVS, and bulbs (Bozkurt et al. 2015; Caillaud et al. 2012; Madina et al. 2018). Such localization of effector proteins may indicate a pathogenic strategy to modulate the host vacuole and vacuolar structures to suppress the vacuole-mediated defense response. For example, dynamic changes of the vacuolar structures are observed during cryptogein-induced PCD in tobacco BY-2 cells (Higaki et al. 2007). As illustrated in Fig. 2, the initial vacuole is complex and features many TVSs, then the number of strands decreases and bulb structures appear; finally, all those structures are lost before the rupture of the tonoplast membrane, which dilutes and acidifies the cytosol and releases reactive secondary metabolites and hydrolytic enzymes, eventually causing cell death (Higaki et al. 2011). Immediately after cryptogein-treatment, no prominent structural changes of the cells were observed, rather, a complex vacuole structures featuring many transvacuolar strands were seen and the nuclei localizes in the central region of the cell (Fig. 2A). However, after some time the TVSs are gradually decreased in number and complexity and bulb structures appeared (Fig. 2B). Subsequently, bulb structures disappeared resulting the simpler vacuolar structure before the cell death (Fig. 2C-D). The simple-shaped vacuole weakened the tonoplast, leading to its ruptures, which sequentially would be lethal for the cell since it would dilute and acidify the cytosol and release cellular reactive secondary metabolites and hydrolytic enzymes (Higaki et al. 2011). A similar kind of vacuolar simplification was observed in BY-2 cells treated with culture filtrates of *Erwinia carotovora*, a plant pathogenic bacterium (Hirakawa et al. 2015), but in that situation the lysis of the plasma membrane seemed to occur while the vacuole was still intact. It is believed that the simplification of the vacuole is crucial for the vacuolar breakdown, but how these phenomena are orchestrated remains to be elucidated.

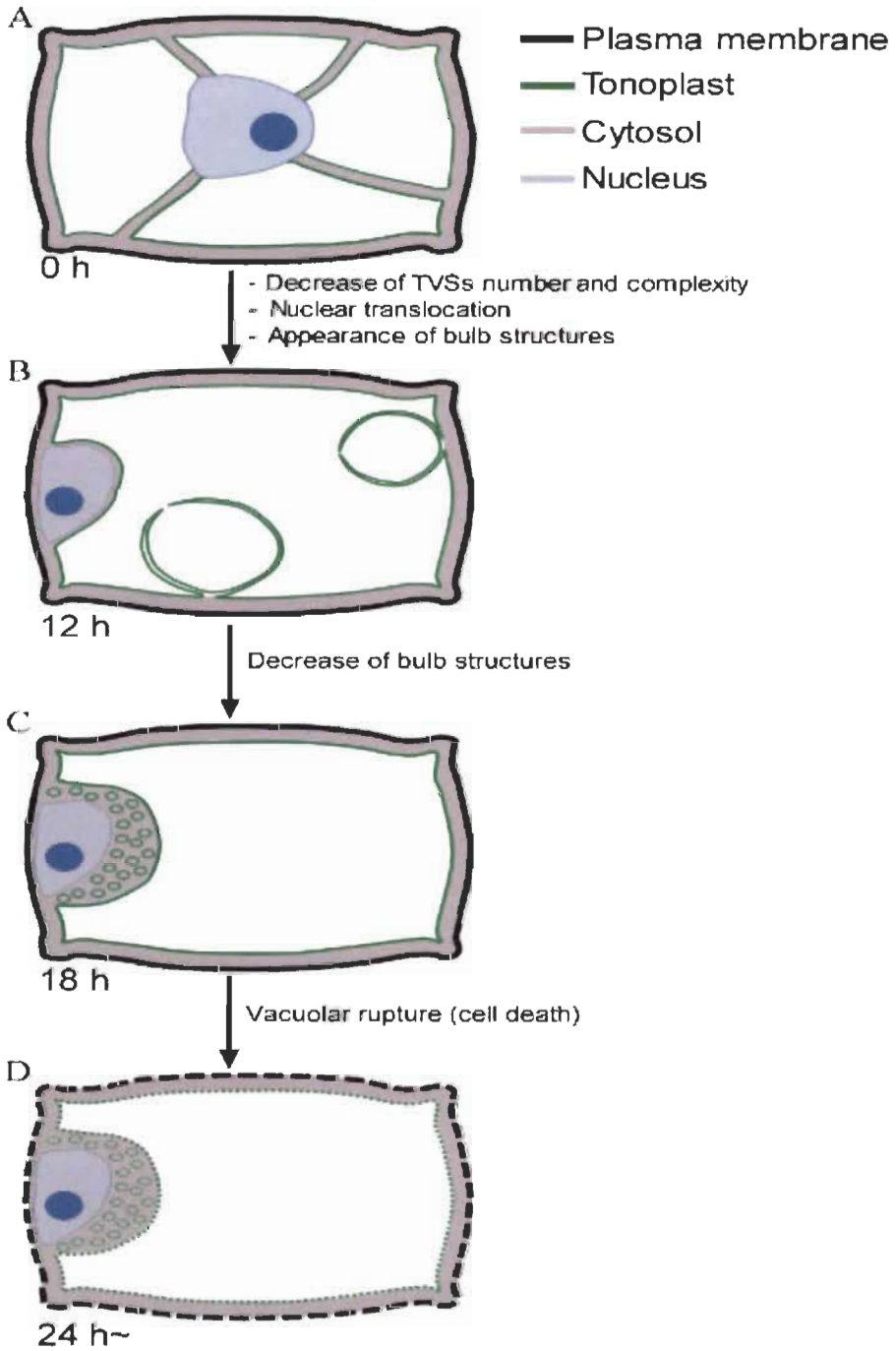

Fig. 2 A schematic illustration of the reorganization of the vacuolar structures during pathogen-induced cell death in BY-2 cells.

A) After cryptogein treatment at 0 h, the vacuole contains many transvacuolar strands and the nucleus localizes at the central region of the cell. B) After 12 h, the nucleus moves from the center to the periphery of the cell and bulb-like structures appear within the vacuole while transvacuolar strands are gradually disrupted. C) After 18 h, the bulb-like structures disappear, and small spherical vacuoles appear. D) After 24 h, the VM and PM lose their integrity. Dashed lines indicate broken membranes.

Conclusions and future perspectives

Although the role of the vacuole in plant-pathogen interactions has recently attracted much attention, our knowledge of the pathogen manipulation of host vacuolar membrane structures and trafficking remains minimal. As we have reviewed here, plant vacuolar structures are highly organized and dynamic, and they are involved in many cellular processes including plant-pathogen interactions. However, further studies are necessary to characterize the biogenesis mechanisms of bulbs and transvacuolar strands and to elucidate which physiological roles they play in the environmental responses of plants. Live-cell imaging using chemical dyes or fluorescently tagged proteins will undoubtedly serve as a critical technique to reveal the underlying mechanisms between vacuolar structural trafficking and plant-pathogen interactions and the use of plants defective in specific transport steps in vacuolar trafficking will help to elucidate the intracellular itinerary of still uncharacterized bulb membrane proteins.

Funding: This work was supported by a NSERC grant number RGPIN/435870-2013 and Canada Research Chair number 950-231790.

Disclosures: All the authors declare that there are no conflicts of interest.

Acknowledgement

We are very thankful to Melodie B. Plourde for critical review of the manuscript.

References

Ahmad et al. (2011) Benzoxazinoid metabolites regulate innate immunity against aphids and fungi in maize. Plant Physiol 157: 317-327

Alvarez ME, Pennell RI, Meijer PJ, Ishikawa A, Dixon RA, Lamb C (1998) Reactive oxygen intermediates mediate a systemic signal network in the establishment of plant immunity. Cell 92:773-784

Banasiak J, Biała W, Staszków A, Swarcewicz B, Kępczyńska E, Figlerowicz M, Jasiński M (2013) A Medicago truncatula ABC transporter belonging to subfamily G modulates the level of isoflavonoids. J of Exp Bot 64:1005-1015

Beebo A et al. (2009) Life with and without AtTIP1; 1, an *Arabidopsis* aquaporin preferentially localized in the apposing tonoplasts of adjacent vacuoles. Plant Mol Biol 70:193-209

Bewley JD, Black M (1994) Seeds: Physiology of Development and Germination, Ed 2. Plenum Press, New York

Boller T, Kende H (1979) Hydrolytic enzymes in the central vacuole of plant cells. Plant Physiol 63:1123-1132

Bottanelli F, Foresti O, Hanton S, Denecke J (2011) Vacuolar transport in tobacco leaf epidermis cells involves a single route for soluble cargo and multiple routes for membrane cargo. The Plant Cell 23:3007-3025

Boursiac Y, Chen S, Luu D-T, Sorieul M, Van den Dries N, Maurel C (2005) Early effects of salinity on water transport in *Arabidopsis* roots. Molecular and cellular features of aquaporin expression. Plant Physiol 139:790-805

Bowles DJ, Marcus SE, Pappin D, Findlay J, Eliopoulos E, Maycox PR, Burgess J (1986) Posttranslational processing of concanavalin A precursors in jackbean cotyledons. The J of cell biol 102:1284-1297

Bozkurt TO, Belhaj K, Dagdas YF, Chaparro-Garcia A, Wu CH, Cano LM, Kamoun S (2015) Rerouting of plant late endocytic trafficking toward a pathogen interface. Traffic 16:204-226

Broekaert WF, Terras FRG, Cammue BPA (2000) Induced and preformed antimicrobial proteins. In A. J. Slusarenko, R. S. S. Fraser, L. C. van Loon (Eds.) Mechanisms of resistance to plant diseases 371-477

Caillaud MC, Piquerez SJ, Fabro G, Steinbrenner J, Ishaque N, Beynon J, Jones JD (2012) Subcellular localization of the Hpa RxLR effector repertoire identifies a tonoplast-associated protein HaRxL17 that confers enhanced plant susceptibility. The Plant J 69:252-265

De Angeli A, Monachello D, Ephritikhine G, Frachisse J, Thomine S, Gambale F, Barbier-Brygoo H (2006) The nitrate/proton antiporter AtCLCa mediates nitrate accumulation in plant vacuoles. Nature 442:939

Emans N, Zimmermann S, Fischer R (2002) Uptake of a fluorescent marker in plant cells is sensitive to brefeldin A and wortmannin. The Plant Cell 14:71-86

Endler A et al. (2006) Identification of a vacuolar sucrose transporter in barley and *Arabidopsis* mesophyll cells by a tonoplast proteomic approach. Plant Physiol 141:196-207

Epimashko S, Meckel T, Fischer-Schliebs E, Lüttge U, Thiel G (2004) Two functionally different vacuoles for static and dynamic purposes in one plant mesophyll leaf cell. The Plant J 37:294-300

Escobar NM, Haupt S, Thow G, Boevink P, Chapman S, Oparka K (2003) High-throughput viral expression of cDNA-green fluorescent protein fusions reveals novel subcellular addresses and identifies unique proteins that interact with plasmodesmata. The Plant Cell 15:1507-1523

Foresti O, Luis L, Denecke J (2006) Overexpression of the *Arabidopsis* syntaxin PEP12/SYP21 inhibits transport from the prevacuolar compartment to the lytic vacuole in vivo. The Plant Cell 18:2275-2293

Freeman BC, Beattie GA (2008) An overview of plant defenses against pathogens and herbivores. The Plant Health Instructor 149

Fuji K, Shirakawa M, Shimono Y, Kunieda T, Fukao Y, Koumoto Y, Takahashi H, Hara-Nishimura I, Shimada T (2016) The adaptor complex AP-4 regulates vacuolar protein sorting at trans-Golgi network by interacting with VACUOLAR SORTING RECEPTOR 1. Plant physiol 170:211-219

Gaffal KP, Friedrichs GJ, El-Gammal S (2007) Ultrastructural evidence for a dual function of the phloem and programmed cell death in the floral nectary of *Digitalis purpurea.* Annals of Bot 99:593-607

Gao C, Zhao Q, Jiang L (2015) Vacuoles protect plants from high magnesium stress. Proceed of the National Acad of Sci 112:2931-2932

Gattolin S, Sorieul M, Hunter PR, Khonsari RH, Frigerio L (2009) In vivo imaging of the tonoplast intrinsic protein family in *Arabidopsis* roots. BMC Plant Biol 9:133

Grolig F, Pierson ES (2000) Cytoplasmic streaming: from flow to track. In: Actin: A dynamic framework for multiple plant cell functions. Springer 89: 165-190

Grotewold E (2006) The genetics and biochemistry of floral pigments. Ann Rev of Plant Biol 57:761-780

Grubb CD, Abel S (2006) Glucosinolate metabolism and its control. Trends in Plant Sci 11:89-100

Gunawardena AH (2007) Programmed cell death and tissue remodelling in plants. J of Exp Bot 59:445-451

Halkier BA, Gershenzon J (2006) Biology and biochemistry of glucosinolates. Ann Rev of Plant Biol 57:303-333

Han SW, Alonso JM, Rojas-Pierce M (2015) REGULATOR OF BULB BIOGENESIS1 (RBB1) is involved in vacuole bulb formation in *Arabidopsis*. PloS ONE 10:e0125621

Handrick V et al. (2016) Biosynthesis of 8-o-methylated benzoxazinoid defense compounds in maize. Plant Cell 28: 1682-1700

Hara-Nishimura I, Hatsugai N (2011) The role of vacuole in plant cell death. Cell Death & Differentiat 18:1298-1304

Harborne JB, Williams CA (2000) Advances in flavonoid research since 1992. Phytochem 55:481-504

Hatsugai N, Hara-Nishimura I (2010) Two vacuole-mediated defense strategies in plants. Plant sig & behav 5:1568-1570

Hatsugai N et al. (2009) A novel membrane fusion-mediated plant immunity against bacterial pathogens. Gen & developm 23:2496-2506

Hatsugai N, Kuroyanagi M, Nishimura M, Hara-Nishimura I (2006) A cellular suicide strategy of plants: vacuole-mediated cell death. Apoptosis 11:905-911

Hatsugai N et al. (2004) A plant vacuolar protease, VPE, mediates virus-induced hypersensitive cell death. Science 305:855-858

Hawes C, Saint-Jore CM, Brandizzi F, Zheng H, Andreeva AV, Boevink P (2001) Cytoplasmic illuminations: *In planta* targeting of fluorescent proteins to cellular organelles. Protoplasma 215:77-88

Hedrich R (2012) Ion channels in plants. Physiol Rev 92:1777-1811

Hicks GR, Rojo E, Hong S, Carter DG, Raikhel NV (2004) Geminating pollen has tubular vacuoles, displays highly dynamic vacuole biogenesis, and requires VACUOLESS1 for proper function. Plant Physiol 134:1227-1239

Higaki T et al. (2007) Elicitor-induced cytoskeletal rearrangement relates to vacuolar dynamics and execution of cell death: In vivo imaging of hypersensitive cell death in tobacco BY-2 cells. Plant and Cell Physiol 48:1414-1425

Higaki T, Kurusu T, Hasezawa S, Kuchitsu K (2011) Dynamic intracellular reorganization of cytoskeletons and the vacuole in defense responses and hypersensitive cell death in plants. J of Plant Research 124:315-324

Higaki T, Kutsuna N, Okubo E, Sano T, Hasezawa S (2006) Actin microfilaments regulate vacuolar structures and dynamics: dual observation of actin microfilaments and vacuolar membrane in living tobacco BY-2 cells. Plant and Cell Physiol 47:839-852

Higaki T, Kutsuna N, Sano T, Hasezawa S (2008) Quantitative analysis of changes in actin microfilament contribution to cell plate development in plant cytokinesis. BMC Plant Biol 8:80

Hirakawa Y, Nomura T, Hasezawa S, Higaki T (2015) Simplification of vacuole structure during plant cell death triggered by culture filtrates of *Erwinia carotovora*. Journal of Integrative Plant Biol 57:127-135

Höglund A-S, Lenman M, Falk A, Rask L (1991) Distribution of myrosinase in rapeseed tissues. Plant Physiol 95:213-221

Höglund A-S, Lenman M, Rask L (1992) Myrosinase is localized to the interior of myrosin grains and is not associated to the surrounding tonoplast membrane. Plant Sci 85:165-170

Hoh B, Hinz G, Jeong B-K, Robinson DG (1995) Protein storage vacuoles form de novo during pea cotyledon development. J of Cell Sci 108:299-310

Hopkins RJ, van Dam NM, van Loon JJ (2009) Role of glucosinolates in insect-plant relationships and multitrophic interactions. Ann Revi of Entomol 54:57-83

Hunter PR, Craddock CP, Di Benedetto S, Roberts LM, Frigerio L (2007) Fluorescent reporter proteins for the tonoplast and the vacuolar lumen identify a single vacuolar compartment in *Arabidopsis* cells. Plant Physiol145:1371-1382

Inada N, Ueda T (2014) Membrane trafficking pathways and their roles in plant-microbe interactions. Plant and Cell Physiol 55:672-686

Jaquinod M, Villiers F, Kieffer-Jaquinod S, Hugouvieux V, Bruley C, Garin J, Bourguignon J (2007) A proteomics dissection of *Arabidopsis thaliana* vacuoles isolated from cell culture. Mol & Cellular Proteo 6:394-412

Jauh G-Y, Phillips TE, Rogers JC (1999) Tonoplast intrinsic protein isoforms as markers for vacuolar functions. The Plant Cell 11:1867-1882

Jiang L, Phillips TE, Rogers SW, Rogers, JC (2000) Biogenesis of the protein storage vacuole crystalloid. J Cell Biol. 150:755-769

Johnson KD, Herman EM, Chrispeels MJ (1989) An abundant, highly conserved tonoplast protein in seeds. Plant Physiol 91:1006-1013

Jones AM (2001) Programmed cell death in development and defense. Plant Physiol 125:94-97

Kamiya T, Akahori T, Ashikari M, Maeshima M (2006) Expression of the vacuolar Ca^{2+}/H^{+} exchanger, OsCAX1a, in rice: cell and age specificity of expression, and enhancement by Ca^{2+}. Plant and Cell Physiol 47:96-106

Kasaras A, Melzer M, Kunze R (2012) *Arabidopsis* senescence-associated protein DMP1 is involved in membrane remodeling of the ER and tonoplast. BMC Plant Biol 12:54

Katsuta J, Hashiguchi Y, Shibaoka H (1990) The role of the cytoskeleton in positioning of the nucleus in premitotic tobacco BY-2 cells. J of Cell Sci 95:413-422

Kim DH et al. (2001) Trafficking of phosphatidylinositol 3-phosphate from the trans-Golgi network to the lumen of the central vacuole in plant cells. The Plant Cell 13:287-301

Kissen R, Rossiter JT, Bones AM (2009) The 'mustard oil bomb': not so easy to assemble?! Localization, expression and distribution of the components of the myrosinase enzyme system. Phytochem Rev 8:69-86

Kluge C et al. (2004) Subcellular distribution of the V-ATPase complex in plant cells, and in vivo localisation of the 100 kDa subunit VHA-a within the complex. BMC Cell Biol 5:29

Kobae Y, Uemura T, Sato MH, Ohnishi M, Mimura T, Nakagawa T, Maeshima M (2004) Zinc transporter of *Arabidopsis thaliana* AtMTP1 is localized to vacuolar membranes and implicated in zinc homeostasis. Plant and Cell Physiol 45:1749-1758

Kovar DR, Staiger CJ, Weaver EA, McCurdy DW (2000) AtFim1 is an actin filament crosslinking protein from *Arabidopsis thaliana*. The Plant J 24:625-636

Kovermann P et al. (2007) The *Arabidopsis* vacuolar malate channel is a member of the ALMT family. The Plant J 52:1169-1180

Koyano T, Kurusu T, Hanamata S, Kuchitsu K (2014) Regulation of vacuole-mediated programmed cell death during innate immunity and reproductive development in plants. in: sexual reproduction in animals and plants. Springer, Tokyo, pp. 431-440

Küfner I, Koch W (2008) Stress regulated members of the plant organic cation transporter family are localized to the vacuolar membrane. BMC Research Notes 1:43

Kumagai F, Hasezawa S (2001) Dynamic organization of microtubules and microfilaments during cell cycle progression in higher plant cells. Plant Biol 3:4-16

Kusumi A et al. (2005) Paradigm shift of the plasma membrane concept from the two-dimensional continuum fluid to the partitioned fluid: high-speed single-molecule tracking of membrane molecules. Ann Rev of Biophysics and Biomol Struct 34:351-378

Kutsuna N, Hasezawa S (2002) Dynamic organization of vacuolar and microtubule structures during cell cycle progression in synchronized tobacco BY-2 cells. Plant and Cell Physiol 43:965-973

Kutsuna N, Kumagai F, Sato MH, Hasezawa S (2003) Three-dimensional reconstruction of tubular structure of vacuolar membrane throughout mitosis in living tobacco cells. Plant and Cell Physiol 44:1045-1054

Lepiniec L, Debeaujon I, Routaboul J-M, Baudry A, Pourcel L, Nesi N, Caboche M (2006) Genetics and biochemistry of seed flavonoids. Ann Rev of Plant Biol 57:405-430

Leshem Y et al. (2006) Suppression of *Arabidopsis* vesicle-SNARE expression inhibited fusion of H_2O_2-containing vesicles with tonoplast and increased salt tolerance. Proceed of the National Acad of Sci 103:18008-18013

Lillemeier BF, Pfeiffer JR, Surviladze Z, Wilson BS, Davis MM (2006) Plasma membrane-associated proteins are clustered into islands attached to the cytoskeleton. Proceed of the National Acad of Sci 103:18992-18997

Ma QH, Tian B, Li YL (2010) Overexpression of a wheat jasmonate-regulated lectin increases pathogen resistance. *Biochimie* 92:187-193

Madina MH, Zheng H, Germain H (2018) New insight into bulb dynamics in the vacuolar lumen of *Arabidopsis* cells. Botany 96:511-520

Maîtrejean M et al. (2011) Assembly and sorting of the tonoplast potassium channel AtTPK1 and its turnover by internalization into the vacuole. Plant Physiol 156:1783-1796

Martinoia E, Meyer S, De Angeli A, Nagy R (2012) Vacuolar transporters in their physiological context. Plant Biol 63:183-213

Marty F (1999) Plant vacuoles. The Plant Cell 11:587-599

Melan MA (1999) Overview of cell fixatives and cell membrane permeants. Methods Mol Biol 115: 45-55

Minami A et al. (2009) Alterations in detergent-resistant plasma membrane microdomains in *Arabidopsis thaliana* during cold acclimation. Plant and Cell Physiol 50:341-359

Mitsuhashi N, Shimada T, Mano S, Nishimura M, Hara-Nishimura I (2000) Characterization of organelles in the vacuolar-sorting pathway by visualization with GFP in tobacco BY-2 cells. Plant and Cell Physiol 41:993-1001

Morita MT, Kato T, Nagafusa K, Saito C, Ueda T, Nakano A, Tasaka M (2002) Involvement of the vacuoles of the endodermis in the early process of shoot gravitropism in *Arabidopsis*. The Plant Cell 14:47-56

Mur LA, Kenton P, Lloyd AJ, Ougham H, Prats E (2007) The hypersensitive response; the centenary is upon us but how much do we know? Jl of Exp Bot 59:501-520

Nebenführ A, Gallagher LA, Dunahay TG, Frohlick JA, Mazurkiewicz AM, Meehl JB, Staehelin LA (1999) Stop-and-go movements of plant Golgi stacks are mediated by the acto-myosin system. Plant Physiol 121:1127-1141

Neuhaus HE, Trentmann O (2014) Regulation of transport processes across the tonoplast. Frontiers in Plant Sci 5:460

Neuhaus J-M, Sticher L, Meins F, Boller T (1991) A short C-terminal sequence is necessary and sufficient for the targeting of chitinases to the plant vacuole. Proceed of the National Acad of Sci 88:10362-10366

Niemeyer HM (2009) Hydroxamic acids derived from 2-hydroxy-2H-1,4-benzoxazin-3(4H)-one: key defense chemicals of cereals. J Agric Food Chem 57: 1677-1696

Obara K, Kuriyama H, Fukuda H (2001) Direct evidence of active and rapid nuclear degradation triggered by vacuole rupture during programmed cell death in Zinnia. Plant Physiol 125:615-626

Okubo-Kurihara E, Sano T, Higaki T, Kutsuna N, Hasezawa S (2008) Acceleration of vacuolar regeneration and cell growth by overexpression of an aquaporin NtTIP1;1 in tobacco BY-2 cells. Plant and Cell Physiol 50:151-160

Opalski KS, Schultheiss H, Kogel KH, Hückelhoven R (2005) The receptor-like MLO protein and the RAC/ROP family G-protein RACB modulate actin reorganization in barley attacked by the biotrophic powdery mildew fungus *Blumeria graminis* f. sp. *hordei*. The Plant J 41:291-303

Otegui MS, Noh YS, Martínez DE, Vila PMG, Andrew SL, Amasino RM, Guiamet JJ (2005) Senescence-associated vacuoles with intense proteolytic activity develop in leaves of *Arabidopsis* and soybean. The Plant J 41:831-844

Ovečka M, Lang I, Baluška F, Ismail A, Illeš P, Lichtscheidl I (2005) Endocytosis and vesicle trafficking during tip growth of root hairs. Protoplasma 226:39-54

Owens T, Poole RJ (1979) Regulation of cytoplasmic and vacuolar volumes by plant cells in suspension culture. Plant Physiol 64:900-904

Ozolina N, Nesterkina I, Nurminsky V, Stepanov A, Kolesnikova E, Gurina V, Salyaev R (2011) Recognition of lipid-protein rafts in vacuolar membrane. Biochem, Biophysics and Mol Biol Springer 438:120-122

Paris N, Stanley CM, Jones RL, Rogers JC (1996) Plant cells contain two functionally distinct vacuolar compartments. Cell 85:563-572

Parton R, Fischer-Parton S, Watahiki M, Trewavas A (2001) Dynamics of the apical vesicle accumulation and the rate of growth are related in individual pollen tubes. J of Cell Sci 114:2685-2695

Peiter E, Maathuis FJ, Mills LN, Knight H, Pelloux J, Hetherington AM, Sanders D (2005) The vacuolar Ca 2+-activated channel TPC1 regulates germination and stomatal movement. Nature 434:404

Rajniak J, Barco B, Clay NK, Sattely ES (2015). A new cyanogenic metabolite in *Arabidopsis* required for inducible pathogen defence. Nature 525: 376-379

Rask L, Andréasson E, Ekbom B, Eriksson S, Pontoppidan B, Meijer J (2000) Myrosinase: gene family evolution and herbivore defense in Brassicaceae. Plant Mol Biol 42:93-114

Reisen D, Marty F, Leborgne-Castel N (2005) New insights into the tonoplast architecture of plant vacuoles and vacuolar dynamics during osmotic stress. BMC Plant Biol 5:1

Robinson DG, Hoh B, Hinz G, Jeong B-K (1995) One vacuole or two vacuoles: do protein storage vacuoles arise de novo during pea cotyledon development? J of Plant Physiol 145:654-664

Ruthardt N, Gulde N, Spiegel H, Fischer R, Emans N (2005) Four-dimensional imaging of transvacuolar strand dynamics in tobacco BY-2 cells. Protoplasma 225:205-215

Saito C (2003) A "bulb" subregion in the vacuolar membrane. Plant Morphol 15:60-67

Saito C, Morita MT, Kato T, Tasaka M (2005) Amyloplasts and vacuolar membrane dynamics in the living graviperceptive cell of the *Arabidopsis* inflorescence stem. The Plant Cell 17:548-558

Saito C et al. (2002) A complex and mobile structure forms a distinct subregion within the continuous vacuolar membrane in young cotyledons of *Arabidopsis*. The Plant J 29:245-255

Saito C et al. (2011a) The occurrence of 'bulbs', a complex configuration of the vacuolar membrane, is affected by mutations of vacuolar SNARE and phospholipase in *Arabidopsis*. The Plant J 68:64-73

Sansebastiano GPD, Barozzi F, Piro G, Denecke J, Lousa CDM (2017) Trafficking routes to the plant vacuole: connecting alternative and classical pathways. J of Exp Bot 69: 79-90

Schaaf G, Honsbein A, Meda AR, Kirchner S, Wipf D, Von Wirén N (2006) *AtIREG2* encodes a tonoplast transport protein involved in iron-dependent nickel detoxification in *Arabidopsis thaliana* roots. J of Biol Chem 281:25532-25540

Schnell U, Dijk F, Sjollema KA, Giepmans BN (2012) Immunolabeling artifacts and the need for live-cell imaging. Nat Methods 9:152-158

Schultheiss H, Dechert C, Kiraly L, Fodor J, Michel K, Kogel KH, Hückelhoven R (2003) Functional assessment of the pathogenesis-related protein PR-1b in barley. Plant Sci 165:1275-1280

Segami S, Makino S, Miyake A, Asaoka M, Maeshima M (2014) Dynamics of vacuoles and H+-pyrophosphatase visualized by monomeric green fluorescent protein in *Arabidopsis*: artifactual bulbs and native intravacuolar spherical structures. The Plant Cell 26:3416-3434

Sheahan MB, Rose RJ, McCurdy DW (2007) Actin-filament-dependent remodeling of the vacuole in cultured mesophyll protoplasts. Protoplasma 230:141-152

Shimada C, Lipka V, O'Connell R, Okuno T, Schulze-Lefert P, Takano Y (2006) Nonhost resistance in *Arabidopsis-Colletotrichum* interactions acts at the cell periphery and requires actin filament function. Mol Plant-Microbe Interact 19:270-279

Shimada T, Takagi J, Ichino T, Shirakawa M, Hara-Nishimura I (2018) Plant Vacuoles. Ann Rev of Plant Biol 69:123-45

Shitan N (2016) Secondary metabolites in plants: transport and self-tolerance mechanisms. Biosci, Biotechnol, and Biochem 80:1283-1293

Silady RA, Ehrhardt DW, Jackson K, Faulkner C, Oparka K, Somerville CR (2008) The GRV2/RME-8 protein of *Arabidopsis* functions in the late endocytic pathway and is required for vacuolar membrane flow. The Plant J 53:29-41

Smertenko AP, Bozhkov PV, Filonova LH, Arnold S, Hussey PJ (2003) Re-organisation of the cytoskeleton during developmental programmed cell death in *Picea abies* embryos. The Plant J 33:813-824

Steppuhn A, Gase K, Krock B, Halitschke R, Baldwin IT (2004) Nicotine's defensive function in nature. PLoS Biol 2:e217

Swanson SJ, Bethke PC, Jones RL (1998) Barley aleurone cells contain two types of vacuoles: characterization of lytic organelles by use of fluorescent probes. The Plant Cell 10:685-698

Tanaka Y, Kutsuna N, Kanazawa Y, Kondo N, Hasezawa S, Sano T (2007) Intra-vacuolar reserves of membranes during stomatal closure: the possible role of guard cell vacuoles estimated by 3-D reconstruction. Plant and Cell Physiol 48:1159-1169

Taylor LP, Grotewold E (2005) Flavonoids as developmental regulators. Current Opinion in Plant Biol 8:317-323

Thangstad O, Evjen K, Bones A (1991) Immunogold-EM localization of myrosinase in *Brassicaceae.* Protoplasma 161:85-93

Thangstad O, Iversen T-H, Slupphaug G, Bones A (1990) Immunocytochemical localization of myrosinase in *Brassica napus* L. Planta 180:245-248

Thomine S, Lelièvre F, Debarbieux E, Schroeder JI, Barbier-Brygoo H (2003) AtNRAMP3, a multispecific vacuolar metal transporter involved in plant responses to iron deficiency. The Plant J 34:685-695

Tominaga M, Yokota E, Vidali L, Sonobe S, Hepler PK, Shimmen T (2000) The role of plant villin in the organization of the actin cytoskeleton, cytoplasmic streaming and the architecture of the transvacuolar strand in root hair cells of *Hydrocharis*. Planta 210:836-843

Toyooka K, Moriyasu Y, Goto Y, Takeuchi M, Fukuda H, Matsuoka K (2006) Protein aggregates are transported to vacuoles by macroautophagic mechanism in nutrient-starved plant cells. Autophagy 2:96-106

Ueda H et al. (2006) AtVAM3 is required for normal specification of idioblasts, myrosin cells. Plant and Cell Physiol 47:164-175

Ueda T, Yamaguchi M, Uchimiya H, Nakano A (2001) Ara6, a plant-unique novel type Rab GTPase, functions in the endocytic pathway of *Arabidopsis thaliana.* The EMBO J 20:4730-4741

Uemura T, Yoshimura SH, Takeyasu K, Sato MH (2002) Vacuolar membrane dynamics revealed by GFP-AtVam3 fusion protein. Genes to Cells 7:743-753

Van der Hoorn RA, Jones JD (2004) The plant proteolytic machinery and its role in defence. Curr Opin in Plant Biol 7:400-407

Van Gestel K, Köhler R, Verbelen JP (2002) Plant mitochondria move on F-actin, but their positioning in the cortical cytoplasm depends on both F-actin and microtubules. J of Exp Bot 53:659-667

Vermeer JE et al. (2006) Visualization of PtdIns3P dynamics in living plant cells. The Plant J 47:687-700

Vetter J (2000) Plant cyanogenic glycosides. Toxicon 38:11-36

Voelker C, Schmidt D, Mueller-Roeber B, Czempinski K (2006) Members of the *Arabidopsis* AtTPK/KCO family form homomeric vacuolar channels *in planta*. The Plant J 48:296-306

Wada Y (2013) Vacuoles in mammals: a subcellular structure indispensable for early embryogenesis. Bioarchitecture 3:13-19

Wang J, Li Y, Lo SW, Hillmer S, Sun SSM, Robinson DG Jiang L (2007) Protein Mobilization in Germinating Mung Bean Seeds Involves Vacuolar Sorting Receptors and Multivesicular Bodies. Plant Physiol 143: 1628-1639.

Williamson RE (1993) Organelle movements. Ann Rev of Plant Biol 44:181-202

Wittstock U, Halkier BA (2002) Glucosinolate research in the *Arabidopsis* era. Trends in Plant Sci 7:263-270

Wormit A et al. (2006) Molecular identification and physiological characterization of a novel monosaccharide transporter from *Arabidopsis* involved in vacuolar sugar transport. The Plant Cell 18:3476-3490

Xu Y, Ishida H, Reisen D, Hanson MR (2006) Upregulation of a tonoplast-localized cytochrome P450 during petal senescence in Petunia inflata. BMC Plant Biol 6:8

Yamaryo Y, Dubots E, Albrieux C, Baldan B, Block MA (2008) Phosphate availability affects the tonoplast localization of PLDζ2, an *Arabidopsis thaliana* phospholipase D. FEBS letters 582:685-690

Yoshida K et al. (2013) Studies on vacuolar membrane microdomains isolated from *Arabidopsis* suspension-cultured cells: Local distribution of vacuolar membrane proteins. Plant and Cell Physiol 54: 1571-1584

Zhang C, Hicks GR, Raikhel NV (2014) Plant vacuole morphology and vacuolar trafficking Frontiers in Plant Sci 5:476

Zhang W, Wang C, Qin C, Wood T, Olafsdottir G, Welti R, Wang X (2003) The oleate-stimulated phospholipase D, PLDδ, and phosphatidic acid decrease H_2O_2-induced cell death in *Arabidopsis*. The Plant Cell 15:2285-2295

Zhou S, Richter A, Jander G (2018) Beyond Defense: Multiple Functions of Benzoxazinoids in Maize Metabolism. Plant Cell Physiol 59: 1528-1537

Chapter III contains a study that demonstrated dynamic characteristics of tonoplast-derived substructures bulbs in *Arabidopsis* using Mlp124357 as a marker protein.

CHAPTER III

NEW INSIGHT INTO BULB DYNAMICS IN THE VACUOLAR LUMEN OF *ARABIDOPSIS* CELLS

Mst Hur Madina, Huanquan Zheng and Hugo Germain

Published on 23rd of May 2018 in *Canadian journal of Botany*

3.1 Author contributions

Madina and Germain conceived and designed the study. Madina performed the experiments. Madina, Zheng, and Germain analyzed the data, prepared the figures, wrote and reviewed the manuscript.

3.2 Résumé de l'article

Les vacuoles végétales sont des organites multifonctionnels qui possèdent des structures membranaires dynamiques et transitoires comme les filaments transvacuolaires et les bulbes. Les bulbes sont des structures hautement mobiles qui voyagent le long des filaments transvacuolaires. Une protéine effectrice candidate de *Melampsora larici-populina* (Mlp124357) fusionnée à la protéine fluorescente verte (eGFP) a été utilisée afin d'examiner les propriétés des vacuoles centrales et leurs bulbes. Les auteurs ont découvert la coexistence de deux populations de bulbes dans les cellules d'*Arabidopsis*. En plus des bulbes précédemment décrits, à la surface desquels la protéine marqueur est distribuée de manière uniforme, ils ont détecté des bulbes sur lesquels la protéine de fusion était distribuée de manière irrégulière. À l'aide de méthode de FRAP, ils ont aussi démontré que les bulbes n'échangeaient pas de protéines avec le tonoplaste une fois formés. Ces résultats montrent que plus d'un type de bulbe peut

coexister dans la même cellule et apportent la preuve de l'existence de microdomaines à la surface des bulbes. Ils révèlent par ailleurs que les protéines ne circulent pas librement du tonoplaste à la membrane des bulbes, apportant éclairage nouveau dans la biologie des structures dérivées du tonoplaste.

3.3 Full article in English: New insight into bulb dynamics in the vacuolar lumen of *Arabidopsis* cells

Abstract

Plant vacuoles are multifunctional organelles with dynamic and transient membranous structures, such as trans-vacuolar strands and bulbs. Bulbs are highly mobile structures that travel along trans-vacuolar strands. A candidate effector protein from *Melampsora larici-populina* (Mlp124357) fused with the enhanced green fluorescent protein (eGFP) was used to investigate the properties of central vacuoles and their bulbs. We discovered the coexistence of two bulb populations in *Arabidopsis* cells. In addition to previously-described bulbs, which present even marker protein distribution on the bulb surface, we discerned bulbs displaying irregular fusion protein distribution. Using fluorescence recovery after photobleaching (FRAP), we also demonstrated that bulbs do not exchange proteins with the tonoplast once they are formed. These results show that more than one type of bulb may co-exist in the same cell and provide evidence of micro-domains on the bulb surface. They also reveal that proteins do not flow freely from the tonoplast to the bulb membrane, giving new insight into the biology of tonoplast-derived substructures.

Introduction

Vacuoles, the largest organelles in plant cells, may occupy more than 90% of total intracellular spaces (Owens and Poole 1979). Studies of plant vacuoles have mostly focused on the large central vacuoles and their functions. The central vacuole maintains turgor pressure against the cell wall, regulates cellular homeostasis, acts as a storage compartment for nutrients, chemicals, waste products, and breaks down complex molecules (Owens and Poole 1979). Moreover, vacuoles are involved in plant defense responses to pathogens (Hara-Nishimura and Hatsugai 2011) and the recycling of misfolded proteins (Melkikh and Sutormina 2013).

Vacuoles are composed of dynamic compartments diverse in morphology, size, and content (Marty 1999). Vacuole morphology changes in response to environmental conditions, cell type and developmental stage (Marty 1999). Extensive research has shown that vacuoles are formed by the fusion of multiple membrane vesicles, and single cells may contain more than one vacuole type. Initially, they were known as protein storage vacuoles and lytic vacuoles (Hoh et al. 1995; Paris et al. 1996; Jauh et al. 1999). As plant cells develop, protein storage vacuoles fuse with lytic vacuoles to become central vacuoles (Inoue et al. 1995; Paris et al. 1996).

Vacuoles are surrounded by a membrane, the tonoplast. It is a unique membrane relative to other cellular membranes: very active and dynamic, it separates vacuolar contents from the cell cytoplasm. The tonoplast is a semi-permeable membrane that allows certain molecules and substrates to pass through and reach the vacuolar lumen or exit to the cytosol. Most vacuole functions depend directly or indirectly on the tonoplast. For instance, it regulates the movement of water and ions in and out of vacuoles to maintain proper turgor pressure inside cells. In addition, the tonoplast contains many transporters and channels that control molecule transport (Martinoia et al. 2012; Zhang et al. 2015).

Furthermore, the tonoplast forms additional transient and dynamic structures, such as trans-vacuolar strands (TVS), sheets, and bulbs. TVS are tubular structures that traverse the central vacuole. Their putative function is the distribution of cytosol and small organelles between the perinuclear cytosol and cortical cytosol. The emergence and dynamics of TVS are poorly known; however, the use of inhibiting actin polymerization was shown to affect TVS (Hoffmann and Nebenführ 2004).

Bulbs are small spherical structures present in the lumen of central vacuoles and abundant in rapidlyexpanding cells (Saito et al. 2002). They came to be called "bulbs" because of their spherical shape and brightness in confocal microscopy. They consist of a double tonoplast layer, coherent with the brightness of bulb membranes, which is generally twice that of the tonoplast (Saito et al. 2002; Oda et al. 2009; Segami et al.

2014). Bulb size varies between 1 and 10μm in diameter (Saito et al. 2002; Maîtrejean et al. 2011). Bulbs present dynamic behavior, moving along the tonoplast or on TVS in vacuoles across cells. Bulb number and dynamics are affected by drought stress (Reisen et al. 2005), drugs such as cytochalasin-D and latrunculin, which inhibit actin polymerization (Escobar et al. 2003; Beebo et al. 2009), and mutation of the genes involved in the biogenesis/development of the endomembrane system. For example, mutation of VACUOLESS, SNARE, and ATPases decreases the number of bulbs per cell (Saito et al. 2011a; Kasaras et al. 2012), while mutation of REGULATOR of BULB BIOGENESIS1 (a gene of unknown function) has the opposite outcome (Han et al. 2015).

Bulbs were first noted in the epidermal cells of young *Arabidopsis* cotyledons expressing tonoplast intrinsic protein fused to a fluorescent protein (FP), as viewed by confocal laser scanning microscopy (Saito et al. 2002). Later, they were visualized with several tonoplast markers and in multiple cell types. For instance, bulbs were reported in epidermis cells of tobacco leaf expressing FP fusion with Vam3/SYP22 (Bottanelli et al. 2011), the phosphate transporter NtPT1 (Escobar et al. 2003), SYP22 (Foresti et al. 2006), and AtRabG3c (Bozkurt et al. 2015).

In *Arabidopsis*, bulbs have been detected in many tissues, including epidermal cells expressing green fluorescent protein (GFP)-AtVam3/SYP22 (Kutsuna and Hasezawa 2002; Uemura et al. 2002), Tonoplast Intrinsic Protein (TIP) 1;1-GFP, or FP fusion with other intrinsic tonoplast proteins (Saito et al. 2002; Hicks et al. 2004; Boursiac et al. 2005; Hunter et al. 2007;Beebo et al. 2009; Gattolin et al. 2009; Bozkurt et al. 2015), 2 pore potassium channel 1 (TPK1)-GFP (Maîtrejean et al. 2011), YFP-2xFYVE (Saito et al. 2011a), Cauliflower tonoplast intrinsic protein (BobTIP) 26-1::GFP (Reisen et al. 2005), DUF679 Membrane Protein 1 (Dmp1)-enhanced GFP (eGFP) (Kasaras et al. 2012), and VHP1-GFP (Segami et al. 2014). Bulbs can also be viewed without fluorescent protein, they are naturally present in *Arabidopsis* wild-type cotyledon cells and can be seen using transmission electron microscopy (Saito et al. 2002).

On observing that bulbs disappear in expanded cells or seedlings grown in poor medium, Saito et al. (2002) suggested that they may act as tonoplast membrane reservoirs for quick expansion of vacuoles (Saito et al. 2002). To date, however, no clear function has been proposed. Although it is believed that bulbs are connected to the vacuolar membrane, the bulb membrane is qualitatively distinct from the tonoplast on the basis of fluorescence intensity and protein segregation (Saito et al. 2002, 2011a). For example, the well-known tonoplast marker γ-Tonoplast Intrinsic Protein (γ-TIP) displays fluorescent signals in both the tonoplast and bulbs, whereas another tonoplast marker, Rab75c, manifests fluorescent signals only in the tonoplast, establishing that bulb membranes are intrinsically different from the tonoplast (Saito et al. 2011a). To date, however, a clear mechanism of protein segregation still needs to be elaborated.

Our laboratory has carried out a functional screen for fungal effectors in the model plant *Arabidopsis thaliana*. Interestingly, those effectors were shown to target various cellular compartments: most were observed in the nucleus and cytosol, one targeted the plasmodesmata, one accumulated in undefined cytosolic punctae, one accumulated in the chloroplast and finally, one was observed in the plasma membrane and the tonoplast (Gaouar et al. 2016; Germain et al. 2018). In the present study, a fungal candidate effector protein (Mlp124357) of *Melampsora larici-populina* (the causal agent of poplar leaf rust) was isolated and used as a marker to investigate bulb diversity and dynamics inside vacuoles of *Arabidopsis*. This effector does not have any transmembrane domain, but we observed that it targets the tonoplast, TVS, and bulbs. We confirmed that bulbs are very transient structures that travel across the vacuolar lumen, and we quantified their speed. In addition, the coexistence of two bulb populations was identified in cells, suggesting the existence of micro-domains on the bulb surface. Fluorescent recovery after photobleaching (FRAP) analysis demonstrated that once bulbs are formed, their membranes do not exchange proteins with the tonoplast.

Materials and Methods

Plasmid constructs, transformation, and growth conditions

The lyophilized-DNA coding sequence of the candidate effector protein of the rust fungus *Melampsora larici-populina* (Mlp124357) was obtained from GenScript (Piscataway, New Jersey, USA). It was inserted into pB7FWG2.0 Gateway destination vector (Karimi et al. 2002) to generate the Mlp124357 construct fused with C-terminus eGFP (Mlp124357-eGFP). The construct was introduced into *Arabidopsis thaliana* (Col-0), according to the modified floral dip method (Mireault et al. 2014). The tonoplast markers γ-TIP-YFP and γ-TIP-CFP were used as a control in most of the experiments and in the co-localization experiment to avoid overlap of the excitation and emission spectra between YFP and GFP, respectively (Nelson et al. 2007). All of the plants were soil-grown and maintained throughout the experiments in a growth chamber at a controlled temperature of 23 °C with 60% relative humidity and a 14 h light/10 h dark regime.

Confocal laser scanning microscopy

All live-cell imaging was performed on *Arabidopsis* leaves. Before the observation, 4-day-old *Arabidopsis* leaves were cut and mounted in water under a coverslip and observed with a Leica TCS SP8 confocal laser scanning microscope (Leica Microsystems) and a 40×/1.40 oil immersion objective. Excitation/emission wavelengths during acquisition were 405 nm/450-460 nm for CFP, 488 nm/505-525 nm (or 488 nm/530-535 nm with spectral subtraction when used with CFP) for eGFP and 488 nm/530-550 nm for YFP, respectively. For colocalization images, GFP and CFP were taken sequentially, using the sequential scanning mode. Fluorescence intensities were acquired by drawing a one-pixel-wide line over the fluorescent membrane (white lines). Pearson correlation and overlap coefficients were calculated using the Leica LASX quantify co-localization module. The Pearson correlation describes the strength of the correlation between the two-color channel shown in Figs. 1 D-E. The overlap coefficient indicates the overlap of the fluorescence signals in both color channels.

Z-stacks of between 50 and 100 confocal images were acquired and three-dimensional (3-D) reconstructions were generated using Leica TCS SP8 software. Images were analyzed using LAS AF Lite software (version 3.3) and Adobe Photoshop CS6. Ratios of fluorescent intensity for the vacuolar membrane versus TVS or bulb membrane were calculated as described previously (Saito et al. 2002).

Crosses

The Mlp124357-eGFP marker line was used as the male parent and the γ-TIP-CFP line as the female parent. Successfully crossed F1 seeds were harvested, sowed, and screened for phosphinothricin (Basta) resistance. The F1-resistant plantlets were transplanted, further grown on soil, and observed under a confocal laser scanning microscope for both fluorescence markers (CFP and GFP), as described above.

Fluorescence recovery after the FRAP experiments

We performed FRAP experiments using a Leica TCS SP8 confocal laser scanning microscope with a 40×/1.40 oil immersion objective and a 488 nm laser for GFP or YFP excitation. For each FRAP experiment, one image was taken of the regions of interest (ROIs) of tonoplast (a portion) and nonmoving bulbs (white rectangles box) both in Mlp124357-eGFP and γ-TIP-YFP before bleaching: it was then bleached at 100% laser intensity, after which a series of 60-120 images were captured at 1 s intervals. To measure the fluorescence recovery percentage of ROIs that were completely bleached, only colored rectangles (blue) were selected for quantification over time.

Results

The candidate effector Mlp124357 labels the tonoplast, TVS, and bulbs, enabling bulb speed quantification

We and others recently reported that candidate secreted effector proteins (CSEPs) of *Melampsora larici-populina* (*Mlp*) are distinctly localized in a variety of cellular

compartments of *Nicotiana benthamiana* and *Arabidopsis thaliana*. For instance, the plasma membrane, the chloroplast, the plasmodesmata, the nucleolus, the cytosol, and the nucleus are all targeted organelles (Petre et al. 2015; Gaouar et al. 2016; Germain et al. 2018). Here, we investigated the subcellular localization of an additional CSEP of *Mlp* termed Mlp124357. Toward this end, we fused Mlp124357 to eGFP (Mlp124357-eGFP) and transformed the resulting fusion protein into wild-type *Arabidopsis* Col-0 to develop a stable transgenic line. Localization was ascertained in young leaf epidermal cells by confocal laser scanning microscopy. We found that the fluorescent signal of Mlp124357-eGFP accumulates in vacuolar membranes (tonoplast), TVS, and bright circular structures in the vacuolar lumen of *Arabidopsis* epidermal cells (Fig. 1A, arrowheads).

We hypothesized that these bright circular structures are the same as the "bulbs" reported previously by (Saito et al. 2002). To test this premise, we used the tonoplast marker line expressing γ-TIP fused with Yellow Fluorescent Protein (γ-TIP-YFP) and observed a similar appearance of bulbs in both lines (Fig. 1A-B, arrowheads). We undertook three-dimensional (3D) image reconstruction from the Z-stack series, which showed that the bulbs are spherical and dispersed in vacuoles (Fig. 1C). The tonoplast marker line expressing FP with γ-TIP often accumulates in bulbs (Saito et al. 2002; Hunter et al. 2007; Beebo et al. 2009). To ascertain that the spherical structures fluorescently labeled in Mlp124357-eGFP were the same as the ones seen in the γ-TIP-YFP plants, we crossed the Mlp124357-eGFP (male phosphinothricin-resistant) line with the γ-TIP-CFP (female) line. The F_1 plantlets expressing both Mlp124357-eGFP and γ-TIP-CFP and resistant to phosphinothricin were subjected to confocal microscopy. Fluorescence of γ-TIP-CFP is shown in Fig. 1D and Mlp124357-eGFP in Fig. 1E. Co-localization can be observed in the merge of both channels is shown in Fig. 1F and was also plotted as signal overlay shown in Fig. 1G, overlap coefficient (0.8) and Pearson correlation (0.7) are shown in the Supplementary data, Fig. S1 (Pearson scatter plot).

Although bulbs have been portrayed as very dynamic and fast-moving structures (Saito et al. 2002), we could not find any reports of their actual speed. Therefore, we sought to quantify bulb speed in the vacuolar lumen of Mlp124357-eGFP epidermal cells. Time-lapse images were captured at 1 s intervals for 60 s by confocal microscopy, and the average bulb speed across vacuoles was quantified. Fig. 1H depicts how speed was calculated between each frame, enabling us to establish that the maximum speed reached by bulbs was 3.23 μm/s, while the average speed was 1.30 μm/s (n = 76, Supplementary data, Fig. S2). The average bulb size was slightly larger than that described previously (ranging from 1 to 10μm). Bulbs of both the Mlp124357-eGFP and γ-TIP-YFP lines ranged between 1 and 22μm (Supplementary data, Fig. S3).

Table 1. Average fluorescence intensity ratios between TVS or bulb and the tonoplast

	γ-TIP-YFP		Mlp124357-eGFP		Sample No.
	Mean ratios	SEM	Mean ratios	SEM	
TVS/tonoplast	1.7	0.2	2.8	0.8	34
Bulbs/tonoplast	2.6	0.2	3.1	0.6	34

Note: TVS, trans-vacuolar strands.

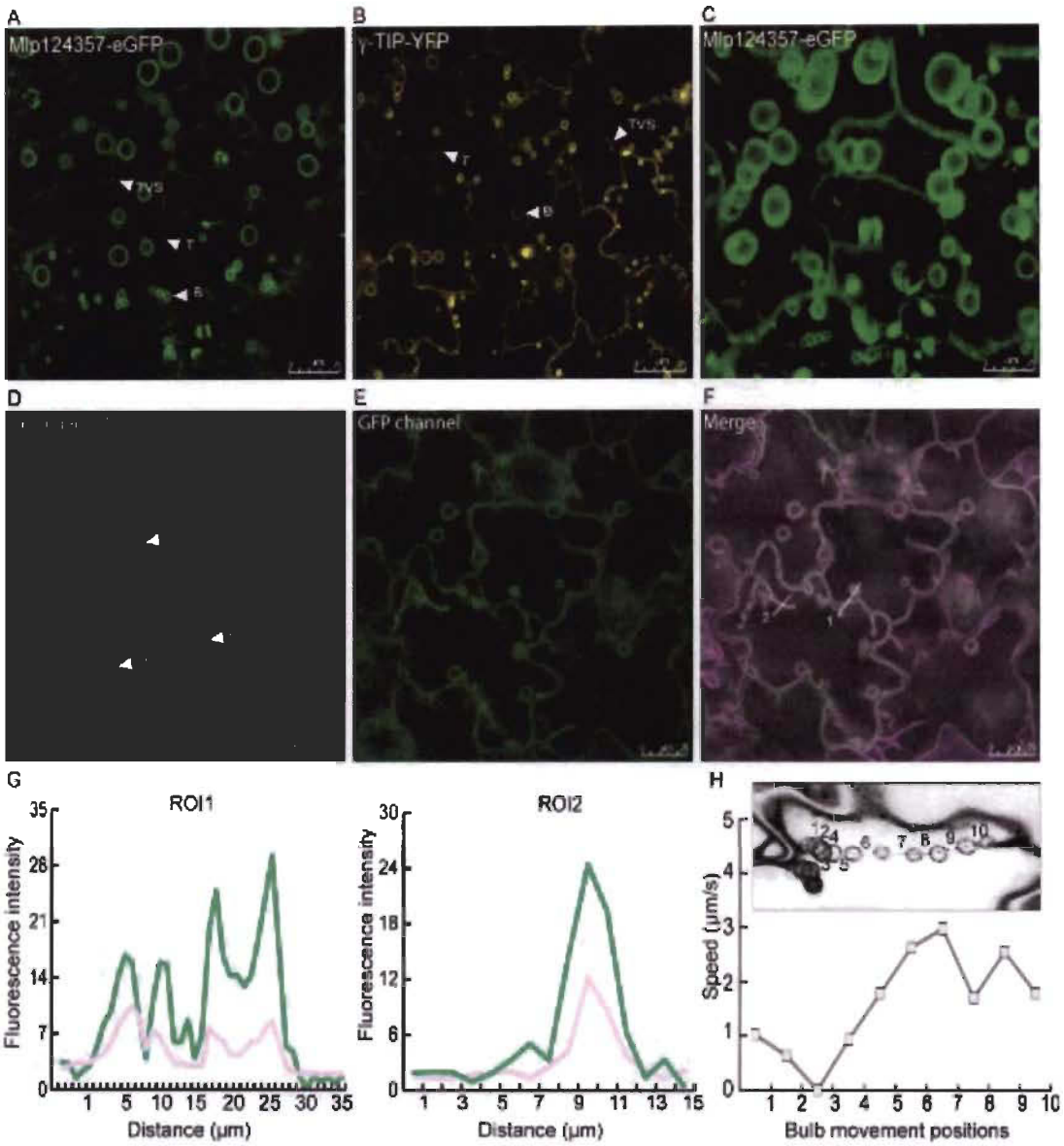

Fig. 1 The effector Mlp124357 labels the tonoplast, TVS, and bulbs, enabling the quantification of bulb speed.

Representative images showing: A) the subcellular localization of eGFP-tagged Mlp124357 to the tonoplast, TVS, and bulbs (white arrowheads) in *Arabidopsis* leaf epidermal cells; B) γ-TIP-YFP bulb appearance (white arrowhead); C) 3-D reconstruction giving a clear view of bulbs in Mlp124357-eGFP, and co-localization of both markers in F1 progeny seedlings of γ-TIP-CFP crossed with Mlp124357-eGFP by confocal microscopy; D) CFP channel for γ-TIP-CFP; E) GFP channel for Mlp124357-eGFP; F) Merged image of the CFP and GFP channels; G) Histogram of co-localization level in the region of interest depicted in the merged images (white lines). T, tonoplast; TVS, transvacuolar strand; B, bulb; ROI, region of interest. Scale bars = 25 μm (A–B) and 50 μm (C-D). H) Diagram of bulb speed calculation.

Bulbs are highly fluorescent structures within the vacuolar lumen (Saito et al. 2002). To assess whether the distribution of these two marker proteins is the same

between vacuolar subcellular structures, we investigated the accumulation intensity of Mlp124357-eGFP in the tonoplast, TVS, and bulbs. We quantified the maximum fluorescence intensity of the tonoplast, TVS, and bulb membrane from 34 randomly-selected images in leaf epidermal cells expressing Mlp124357-eGFP or γ-TIP-YFP. In Mlp124357-eGFP plants, the average fluorescence ratio of TVS/tonoplast was 2.8, whereas the mean bulb membrane/tonoplast ratio was 3.1. In the γ-TIP-YFP line, the fluorescence ratio of TVS/tonoplast and bulb membrane/ tonoplast was 1.7 and 2.6, respectively (Table 1). This observation indicates that Mlp124357-eGFP and γ-TIP-YFP accumulate in the same vacuolar sub-compartment at different levels, for example, Mlp124357-eGFP accumulates at higher levels than γ-TIP in bulbs or TVS. This observation also suggests that protein distribution is qualitatively different between structures in both lines. In addition to fluorescence intensity, we also calculated the number of bulbs per cell from 60 randomly-selected confocal images of leaf epidermal cells expressing Mlp124357-eGFP or γ-TIP-YFP and found no significant differences between the two lines (Supplementary data, Fig. S4). These results indicate that, overall, structures labeled with γ-TIP-CFP are the same as those labeled with Mlp124357-eGFP, and that our FP marker does not induce neomorphic bulb formation, as has been suggested for some markers (Segami et al. 2014).

Marker proteins are not distributed evenly on the bulb surface

It has been reported that GFP fusion proteins are not evenly distributed along the tonoplast but remain concentrated at attachment points between the tonoplast and bulbs in AtTIP1;1-GFP (Beebo et al. 2009). Therefore, we investigated the distribution of our fusion proteins in the tonoplast and bulbs. To better visualize protein distribution on the bulbs, we reconstructed high-resolution 3-D images from the Z-stack series of *Arabidopsis* leaf epidermal cells expressing Mlp124357-eGFP or γ-TIP-YFP. We observed regular distribution (Fig. 2A), as discerned previously on many bulbs and in the tonoplast, but also observed the irregular distribution of fusion proteins on the bulb membrane (Fig. 2B arrowhead). We found cells with both distribution types of these marker proteins in bulbs (Fig. 2C, arrowhead). In the γ-TIP-YFP line, we also saw

coexistence of the two bulb types in the same cells, displaying both even and uneven FP distribution (Fig. 2D, arrowhead). This suggests that two distinct bulb types exist in this cell type, one with regular marker protein distribution, and a novel bulb type with irregular protein distribution, hinting that microdomains occur on the bulb surface.

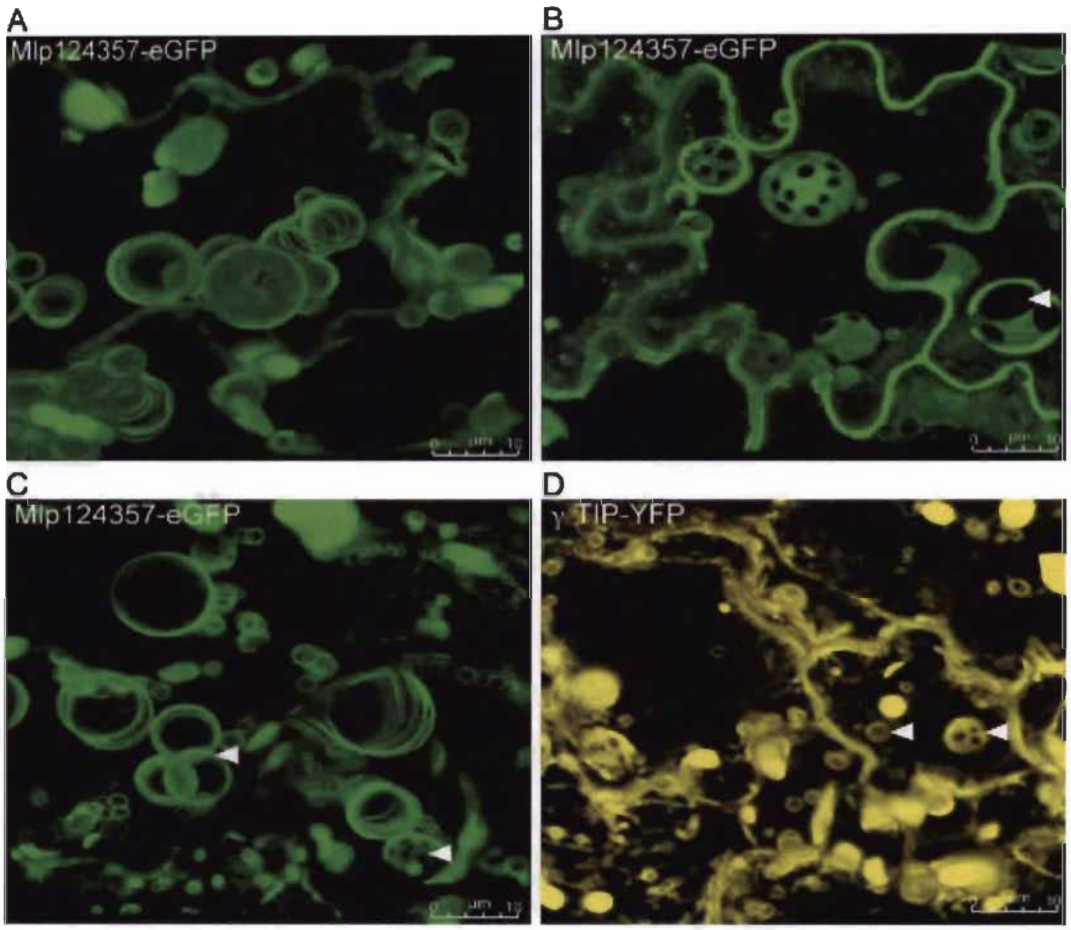

Fig. 2 Marker proteins are not distributed evenly on the bulb surface.
3-D confocal images of *Arabidopsis* leaf epidermal cell showing A) Regular appearance of bulbs. B) Uneven protein distribution of markers on bulbs in a single cell of the Mlp124357-eGFP line. C) and D) Coexistence of bulb populations with irregular fusion protein distribution in both lines: Mlp124357-eGFP and γ-TIP-YFP. Three-dimensional images reconstructed from 60 optical sections. White arrowheads indicate the hole for uneven protein distribution. Scale bars = 10 μm.

Once bulbs are formed they no longer exchange protein with the tonoplast

Previous descriptions of bulbs and prevailing models indicate that they are connected to the vacuolar membrane (Saito et al. 2002). We investigated whether

tonoplast-associated proteins travel freely between the tonoplast and bulb membrane. To answer this question, we conducted FRAP analysis of young *Arabidopsis* leaf epidermal cells expressing Mlp124357-eGFP or γ-TIPYFP. Recovery of eGFP and YFP fluorescence was quantified over time. When the tonoplast of cells expressing Mlp124357-eGFP was bleached, its fluorescence recovered completely within 60 seconds (Fig. 3A-B). However, the bleached region of bulb membrane fluorescence did not recover in 60 seconds (Fig. 3A-B) and not even after a 120-second period (Supplementary data, Fig. S5 A-B).

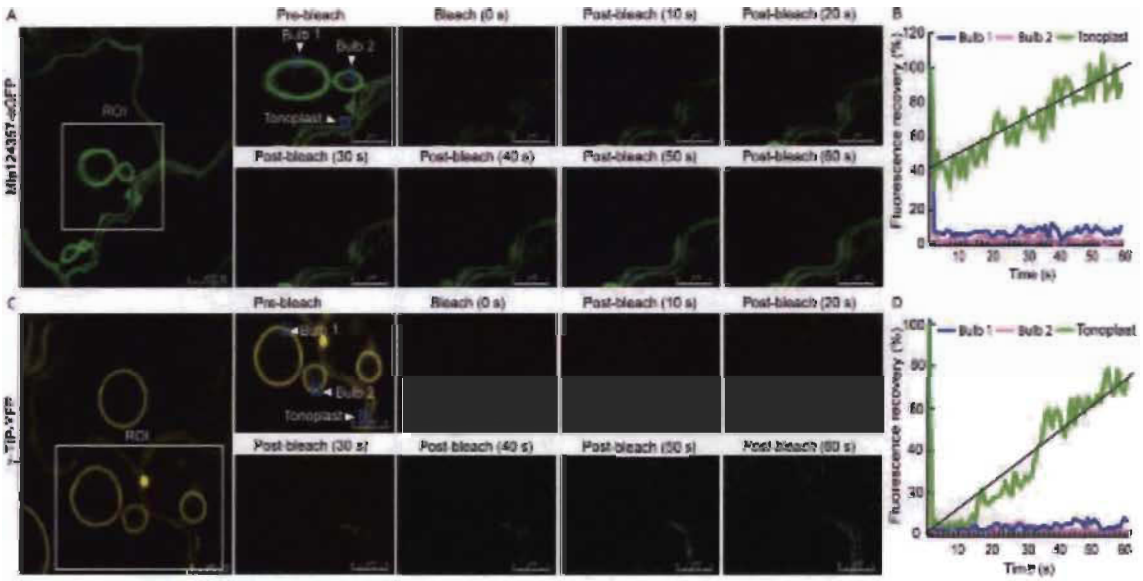

Fig. 3 Once bulbs are formed they no longer exchange protein with the tonoplast.
A) FRAP image of leaf epidermal cell expressing Mlp124357-eGFP. B) Fluorescence recovery curve of photobleached area in Mlp124357-eGFP. C) FRAP image of leaf epidermal cells expressing γ-TIP-YFP. D) Fluorescence recovery curve of the photo-bleached area in γ-TIP-YFP. Images were taken before (prebleach), immediately after (bleach 0) and 1-second interval for 1 min after bleaching from 6-day old seedlings. ROI for the bleached area is shown with white rectangles. To measure fluorescence recovery of ROIs are shown in colored rectangles (blue). To measure the fluorescence recovery of tonoplast that were completely bleached, only the membrane adjacent to the bulb was selected for quantification (blue rectangles). The experiment was repeated three times with similar results.

Similar results were obtained after bleaching the bulb membrane and tonoplast in cells expressing γ-TIP-YFP (Fig. 3C-D; Supplementary data, Fig. S5 C-D), indicating that neither Mlp124357-eGFP nor γ-TIP-YFP can be displaced from the tonoplast to the bulbs once they are formed. More precisely, our findings demonstrate that protein exchange from the tonoplast to bulb, or from bulb to bulb, does not occur.

Discussion

This study focused on an *Arabidopsis thaliana* stable transgenic line expressing a candidate effector of *Melampsora larici-populina* (Mlp124357) fused to eGFP and γ-TIP-FP, which strongly labels the tonoplast, TVS, and bulbs-to visualize and understand intra-vacuolar membrane structure dynamics. The results confirmed that *Arabidopsis* leaf epidermal cells contained many bulbs in the vacuolar lumen and revealed that some bulbs displayed irregular marker protein distribution. In addition, FRAP experiments demonstrated that the tonoplast and bulb membrane do not exchange proteins, as demonstrated by the absence of bulb recovery after photo-bleaching.

Confocal microscopy disclosed that eGFP fusion of the reporter protein accumulated in the tonoplast and vacuolar membranous structures, such as TVS and bulbs in the vacuolar lumen of *Arabidopsis* leaf epidermal cells.

Considering morphology and localization, we confirmed that these spherical structures are known as bulbs, as reported by (Saito et al. 2002). Therefore, we compared the bulb structures of our reporter line with the well-known tonoplast marker expressing γ-TIP and found them to be similar as the two markers co-localized. Several reports confirmed the occurrence of bulbs in a broad spectrum of tissue types in *Arabidopsis* and tobacco (Saito et al. 2002; Uemura et al. 2002; Escobar et al. 2003; Hicks et al. 2004; Tian et al. 2004; Vera-Estrella et al. 2004; Boursiac et al. 2005; Reisen et al. 2005; Beebo et al. 2009; Mohanty et al. 2009; Saito et al. 2011a). All these markers that label bulbs were integral membrane proteins with transmembrane domains, while two other marker proteins were identified as soluble cytosolic GFP and YFP-2xFYVE, which lacked a transmembrane domain (Saito et al. 2011a). However, in the present study, we used Mlp124357-eGFP, a fungal protein that lacks a transmembrane domain, to visualize bulbs.

It was proposed recently that bulbs can be artifactual structures, formed by dimerization of GFP tags when fused to tonoplast markers (Segami et al. 2014). We ruled out the notion that the bulbs observed in our transgenic line were artifacts,

based on the fluorescence ratio between the bulbs and the tonoplast. Further, we did not find additional bulbs in F1 seedlings of the cross between γ-TIP-CFP and Mlp124357-eGFP, we noted perfect co-localization, and the bulb numbers were similar in both the Mlp124357-eGFP and the γ-TIP-YFP lines.

Our results indicate that our marker accumulates in bulbs and TVS more abundantly and strongly in the tonoplast than γ-TIP, making it a great tool with which to analyze these structures. It has been proposed that bulbs are formed by multiple layers of tonoplast membranes, which explains the increased intensity of bulbs in fluorescently labeled tonoplasts (Saito et al. 2002; Saito et al. 2011a). Several reports have confirmed that the fluorescence intensity of bulb membrane is higher than that of the tonoplast (Beebo et al. 2009; Segami et al. 2014; Han et al. 2015). Although numerous studies hold that bulbs are highly mobile structures, there is no data on their actual speed. Therefore, we took advantage of time-lapse imaging to calculate bulb speed and found that the maximum speed was 3.23 μm/s, and the average speed was 1.30 μm/s.

Our results highlight the coexistence of bulb populations in the same cell, as demonstrated in either Mlp124357-eGFP or γ-TIP-YFP stable transgenic plants. Uneven distribution of aquaporins in the plasma membrane and AtTIP1;1-GFP fusion protein in the tonoplast of plant cells has already been reported (Siefritz et al. 2001; Hachez et al. 2006; Beebo et al. 2009), but not in bulb membranes. Irregular protein distribution may imply the membrane micro-domain concept. According to this concept, membrane lipids and proteins move unevenly and are distributed non-uniformly in the membrane, which is considered to be dependent on sphingolipids and sterols (Kusumi et al. 2005; Lillemeier et al. 2006; Minami et al. 2009). This would be coherent with our observations.

FRAP is widely exploited to quantify the dynamics of fluorescently-labeled proteins in cell membranes (Martinière et al. 2012; Takagi et al. 2013). The current model supports the fact that bulbs remain attached to TVS or the tonoplast at all times, and we do not have data that would prove otherwise (Saito et al. 2002). However,

reports point to qualitative differences in protein content between bulb membranes and the tonoplast (Saito et al. 2011b). Therefore, we undertook FRAP experiments to assess protein dynamics between the tonoplast and bulb membrane. We disclosed that the fluorescence of bleached areas of the tonoplast in cells expressing either Mlp124357-eGFP or γ-TIP-YFP recovered completely within 60 seconds, while the membrane fluorescence of bulbs, even those attached with the tonoplast did not recuperate at all, not even after 120 seconds.

Although evidence indicates that membrane connections exist between the tonoplast and bulbs, the results of our investigation suggest that neither Mlp124357-eGFP nor γ-TIP-YFP translocate between the tonoplast and bulb membrane once bulbs are formed (Saito et al. 2002). An additional explanation could be that the bulb-to-tonoplast connections are severed, making fluorescence recovery of bulbs impossible. However, we do not have evidence to support this hypothesis.

Our results demonstrate the fact that Mlp124357-eGFP is an excellent marker with which to study tonoplast and bulb dynamics. Further studies are necessary to understand bulb emergence and the fate of bulb proteins when they merge with the tonoplast.

Acknowledgments

We thank the Natural Sciences and Engineering Research Council of Canada (NSERC), Fonds de recherche du Québec-Nature et technologies (FRQNT) and an Institutional Research Chair to HG for funding this work. Manuscript editing by Mélodie B. Plourde was much appreciated.

References

Beebo, A., Thomas, D., Der, C., Sanchez, L., Leborgne-Castel, N., Marty, F., Schoefs, B., and Bouhidel, K. 2009. Life with and without AtTIP1;1, an *Arabidopsis* aquaporin preferentially localized in the apposing tonoplasts of adjacent vacuoles. Plant Mol. Biol. 70(1-2): 193-209. doi: https://doi.org/10.1007/s11103-009-9465-2.

Bottanelli, F., Foresti, O., Hanton, S., and Denecke, J. 2011. Vacuolar transport in tobacco leaf epidermis cells involves a single route for soluble cargo and multiple routes for membrane cargo. The Plant Cell, 23(8): 3007-3025. doi: https://dx.doi.org/ 10.1105/tpc.111.085480.

Boursiac, Y., Chen, S., Luu, D.-T., Sorieul, M., van den Dries, N., and Maurel, C. 2005. Early effects of salinity on water transport in *Arabidopsis* roots. Molecular and cellular features of aquaporin expression. Plant Physiology, 139(2): 790-805. doi: https://doi.org/10.1104/pp.105.065029.

Bozkurt, T.O., Belhaj, K., Dagdas, Y.F., Chaparro-Garcia, A., Wu, C.H., Cano, L.M., and Kamoun, S. 2015. Rerouting of plant late endocytic trafficking toward a pathogen interface. Traffic, 16(2): 204-226. doi: https://doi.org/10.1111/tra.12245.

Escobar, N.M., Haupt, S., Thow, G., Boevink, P., Chapman, S., and Oparka, K. 2003. High throughput viral expression of cDNA-green fluorescent protein fusions reveal novel subcellular addresses and identifies unique proteins that interact with plasmodesmata. The Plant Cell, 15(7): 1507-1523. doi: https://dx.doi.org/10.1105/tpc.013284.

Foresti, O., Luis, L., and Denecke, J. 2006. Overexpression of the *Arabidopsis* syntaxin PEP12/SYP21 inhibits transport from the prevacuolar compartment to the lytic vacuole in vivo. The Plant Cell, 18(9): 2275-2293. doi: https://dx.doi.org/10.1105/tpc.105.040279.

Gaouar, O., Morency, M.-J., Letanneur, C., Séguin, A., and Germain, H. 2016. The 124202 candidate effector of *Melampsora larici-populina* interacts with membranes in Nicotiana and *Arabidopsis*. Can. J. Plant Pathol. 1-12. doi: https://doi.org/10.1080/07060661.2016.1153523.

Gattolin, S., Sorieul, M., Hunter, P.R., Khonsari, R.H., and Frigerio, L. 2009. In vivo imaging of the tonoplast intrinsic protein family in *Arabidopsis* roots. BMC Plant Biology, 9(1): 1-9. doi: https://doi.org/10.1186/1471-2229-9-133.

Germain, H., Joly, D.L., Mireault, C., Plourde, M.B., Letanneur, C., Stewart, D., Morency, M.J., Petre, B., Duplessis, S., and Séguin, A. 2018. Infection assays in *Arabidopsis* reveal candidate effectors from the poplar rust fungus that promote susceptibility to bacteria and oomycete pathogens. Mol. Plant Pathol. 19(1): 191-200. doi: https://doi.org/10.1111/mpp.12514.

Hachez, C., Moshelion, M., Zelazny, E., Cavez, D., and Chaumont, F. 2006. Localization and quantification of plasma membrane aquaporin expression in maize primary root: a clue to understanding their role as cellular plumbers. Plant Mol. Biol. 62(1-2): 305-323. doi: https://doi.org/10.1007/s11103-006-9022-1.

Han, S.W., Alonso, J.M., and Rojas-Pierce, M. 2015. Regulator of Bulb Biogenesis1 (RBB1) Is Involved in Vacuole Bulb Formation in *Arabidopsis*. PLoS One, 10(4): 1-20. doi: https://doi.org/10.1371/journal.pone.0125621.

Hara-Nishimura, I., and Hatsugai, N. 2011. The role of vacuole in plant cell death. Cell Death Differ. 18(8): 1298-1304. doi: https://dx.doi.org/10.1038/cdd.2011.70.

Hicks, G.R., Rojo, E., Hong, S., Carter, D.G., and Raikhel, N.V. 2004. Geminating pollen has tubular vacuoles, displays highly dynamic vacuole biogenesis, and requires Vacuoless1 for proper function. Plant Physiology, 134(3): 1227-1239. doi: https://doi.org/10.1104/pp.103.037382.

Hoffmann, A., and Nebenführ, A. 2004. Dynamic rearrangements of transvacuolar strands in BY-2 cells imply a role of myosin in remodeling the plant actin cytoskeleton. Protoplasma, 224(3-4): 201-210. doi: http://dx.doi.org/10.1007/s00709-004-0068-0.

Hoh, B., Hinz, G., Jeong, B.-K., and Robinson, D.G. 1995. Protein storage vacuoles form de novo during pea cotyledon development. J. Cell Sci. 108(1): 299-310.

Hunter, P.R., Craddock, C.P., Di Benedetto, S., Roberts, L.M., and Frigerio, L. 2007. Fluorescent reporter proteins for the tonoplast and the vacuolar lumen identify a single vacuolar compartment in *Arabidopsis* cells. Plant physiology, 145(4): 1371-1382. doi: https://doi.org/10.1104/pp.107.103945.

Inoue, K., Motozaki, A., Takeuchi, Y., Nishimura, M., and Hara-Nishimura, I. 1995. Molecular characterization of proteins in protein-body membrane that disappear most rapidly during transformation of protein bodies into vacuoles. The Plant Journal, 7(2): 235-243. doi: https://doi.org/10.1046/j.1365-313X.1995.7020235.x.

Jauh, G.-Y., Phillips, T.E., and Rogers, J.C. 1999. Tonoplast intrinsic protein isoforms as markers for vacuolar functions. The Plant Cell, 11(10): 1867-1882. doi: https://doi.org/10.1105/tpc.11.10.1867.

Karimi, M., Inzé, D., and Depicker, A. 2002. GATEWAY™ vectors for Agrobacterium mediated plant transformation. Trends Plant Sci. 7(5): 193-195. doi: https://doi.org/10.1016/S1360-1385(02)02251-3.

Kasaras, A., Melzer, M., and Kunze, R. 2012. *Arabidopsis* senescence-associated protein DMP1 is involved in membrane remodeling of the ER and tonoplast. BMC Plant Biology, 12(1): 1-13. doi: https://doi.org/10.1186/1471-2229-12-54.

Kusumi, A., Nakada, C., Ritchie, K., Murase, K., Suzuki, K., Murakoshi, H., Kasai, R.S., Kondo, J., and Fujiwara, T. 2005. Paradigm shift of the plasma membrane concept from the two-dimensional continuum fluid to the partitioned fluid: high-speed single-molecule tracking of membrane molecules. Annu. Rev. Biophys. Biomol. Struct. 34: 351-378. doi: https://doi.org/10.1146/annurev.biophys.34.040204.144637.

Kutsuna, N., and Hasezawa, S. 2002. Dynamic organization of vacuolar and microtubule structures during cell cycle progression in synchronized tobacco BY-2 cells. Plant and Cell Physiology, 43(9): 965-973. doi: https://doi.org/10.1093/pcp/pcf138.

Lillemeier, B.F., Pfeiffer, J.R., Surviladze, Z., Wilson, B.S., and Davis, M.M. 2006. Plasma membrane-associated proteins are clustered into islands attached to the cytoskeleton. Proc. Natl. Acad. Sci. U.S.A. 103(50): 18992-18997. doi: https://dx.doi.org/10.1073/pnas.0609009103.

Maîtrejean, M., Wudick, M.M., Voelker, C., Prinsi, B., Mueller-Roeber, B., Czempinski, K., Pedrazzini, E., and Vitale, A. 2011. Assembly and sorting of the tonoplast potassium channel AtTPK1 and its turnover by internalization into the vacuole. Plant Physiology, 156(4): 1783-1796. doi: https://doi.org/10.1104/pp.111.177816.

Martinière, A., Lavagi, I., Nageswaran, G., Rolfe, D.J., Maneta-Peyret, L., Luu, D.-T., Botchway, S.W., Webb, S.E., Mongrand, S., and Maurel, C. 2012. Cell wall constrains lateral diffusion of plant plasma-membrane proteins. Proc. Natl. Acad. Sci. U.S.A. 109(31): 12805-12810. doi: https://doi.org/10.1073/pnas.1202040109.

Martinoia, E., Meyer, S., De Angeli, A., and Nagy, R. 2012. Vacuolar transporters in their physiological context. Plant Biology, 63(1): 183. doi: https://doi.org/10.1146/annurev-arplant-042811-105608.

Marty, F. 1999. Plant vacuoles. The Plant Cell, 11(4): 587-599. doi: https://doi.org/10.1105/tpc.11.4.587.

Melkikh, A., and Sutormina, M. 2013. Developing synthetic transport systems. Springer Science & Business Media, Dordrecht.

Minami, A., Fujiwara, M., Furuto, A., Fukao, Y., Yamashita, T., Kamo, M., Kawamura, Y., and Uemura, M. 2009. Alterations in detergent-resistant plasma membrane microdomains in *Arabidopsis thaliana* during cold acclimation. Plant and Cell Physiology, 50(2): 341-359. doi: https://doi.org/10.1093/pcp/pcn202.

Mireault, C., Paris, L.-E., and Germain, H. 2014. Enhancement of the *Arabidopsis* floral dip method with XIAMETER OFX-0309 as alternative to Silwet L-77 surfactant. Botany, 92(7): 523-525. doi: https://doi.org/10.1139/cjb-2014-0048.

Mohanty, A., Luo, A., DeBlasio, S., Ling, X., Yang, Y., Tuthill, D.E., Williams, K.E., Hill, D., Zadrozny, T., and Chan, A. 2009. Advancing cell biology and functional genomics in maize using fluorescent protein-tagged lines. Plant Physiology, 149(2): 601-605. doi: https://dx.doi.org/10.1104/pp.108.130146.

Nelson, B.K., Cai, X., and Nebenführ, A. 2007. A multicolored set of in vivo organelle markers for co-localization studies in *Arabidopsis* and other plants. The Plant Journal, 51(6): 1126-1136. doi: https://doi.org/10.1111/j.1365-313X.2007.03212.x.

Oda, Y., Higaki, T., Hasezawa, S., and Kutsuna, N. 2009. New insights into plant vacuolar structure and dynamics. Int. Rev. Cell Mol. Biol. 277: 103-135. doi: https://doi.org/10.1016/S1937-6448(09)77003-0.

Owens, T., and Poole, R.J. 1979. Regulation of cytoplasmic and vacuolar volumes by plant cells in suspension culture. Plant Physiology, 64(5): 900-904. doi: https://doi.org/10.1104/pp.64.5.900.

Paris, N., Stanley, C.M., Jones, R.L., and Rogers, J.C. 1996. Plant cells contain two functionally distinct vacuolar compartments. Cell, 85(4): 563-572. doi: https://doi.org/10.1016/S0092-8674(00)81256-8.

Petre, B., Saunders, D.G., Sklenar, J., Lorrain, C., Win, J., Duplessis, S., and Kamoun, S. 2015. Candidate effector proteins of the rust pathogen *Melampsora larici-populina* target diverse plant cell compartments. Molecular Plant-Microbe Interactions, 28(6): 689-700. doi: https://doi.org/10.1094/MPMI-01-15-0003-R.

Reisen, D., Marty, F., and Leborgne-Castel, N. 2005. New insights into the tonoplast architecture of plant vacuoles and vacuolar dynamics during osmotic stress. BMC Plant Biology, 5(1): 1-13. doi: https://doi.org/10.1186/1471-2229-5-13.

Saito, C., Ueda, T., Abe, H., Wada, Y., Kuroiwa, T., Hisada, A., Furuya, M., and Nakano, A. 2002. A complex and mobile structure forms a distinct subregion within the continuous vacuolar membrane in young cotyledons of *Arabidopsis*. The Plant Journal, 29(3): 245-255. doi: https://doi.org/10.1046/j.0960-7412.2001.01189.x.

Saito, C., Uemura, T., Awai, C., Tominaga, M., Ebine, K., Ito, J., Ueda, T., Abe, H., Morita, M.T., and Tasaka, M. 2011a. The occurrence of 'bulbs', a complex configuration of the vacuolar membrane, is affected by mutations of vacuolar SNARE and phospholipase in *Arabidopsis*. The Plant Journal, 68(1): 64-73. doi: https://doi.org/10.1111/j.1365-313X.2011.04665.x.

Saito, C., Uemura, T., Awai, C., Ueda, T., Abe, H., and Nakano, A. 2011b. Qualitative difference between "bulb" membranes and other vacuolar membranes. Plant Signaling & Behavior, 6(12): 1914-1917. doi: https://dx.doi.org/10.4161/psb.6.12.18061.

Segami, S., Makino, S., Miyake, A., Asaoka, M., andMaeshima, M. 2014. Dynamics of vacuoles and H+-pyrophosphatase visualized by monomeric green fluorescent protein in *Arabidopsis*: artifactual bulbs and native intravacuolar spherical structures. The Plant Cell, 26(8): 3416-3434. doi: https://dx.doi.org/10.1105/tpc.114.127571.

Siefritz, F., Biela, A., Eckert, M., Otto, B., Uehlein, N., and Kaldenhoff, R. 2001. The tobacco plasma membrane aquaporin NtAQP1. J. Exp. Bot. 52(363): 1953-1957. doi: https://doi.org/10.1093/jexbot/52.363.1953.

Takagi, J., Renna, L., Takahashi, H., Koumoto, Y., Tamura, K., Stefano, G., Fukao, Y., Kondo, M., Nishimura, M., and Shimada, T. 2013. MAIGO5 functions in protein export from Golgiassociated endoplasmic reticulum exit sites in *Arabidopsis*. The Plant Cell, 25(11): 4658-4675. doi: https://doi.org/10.1105/tpc.113.118158.

Tian, G.-W., Mohanty, A., Chary, S.N., Li, S., Paap, B., Drakakaki, G., Kopec, C.D., Li, J., Ehrhardt, D., and Jackson, D. 2004. High-throughput fluorescent tagging of full-length *Arabidopsis* gene products *in planta*. Plant Physiology, 135(1): 25-38. doi: https://doi.org/10.1104/pp.104.040139.

Uemura, T., Yoshimura, S.H., Takeyasu, K., and Sato, M.H. 2002. Vacuolar membrane dynamics revealed by GFP-AtVam3 fusion protein. Genes to Cells, 7(7): 743-753. doi: https://doi.org/10.1046/j.1365-2443.2002.00550.x.

Vera-Estrella, R., Barkla, B.J., Bohnert, H.J., and Pantoja, O. 2004. Novel regulation of aquaporins during osmotic stress. Plant Physiology, 135(4): 2318-2329. doi: https://doi.org/10.1104/pp.104.044891.

Zhang, C., Hicks, G.R., and Raikhel, N.V. 2015. Molecular Composition of Plant Vacuoles: Important but Less Understood Regulations and Roles of Tonoplast Lipids. Plants,4(2): 320-333. doi: https://dx.doi.org/10.3390/plants4020320.

Supplementary data

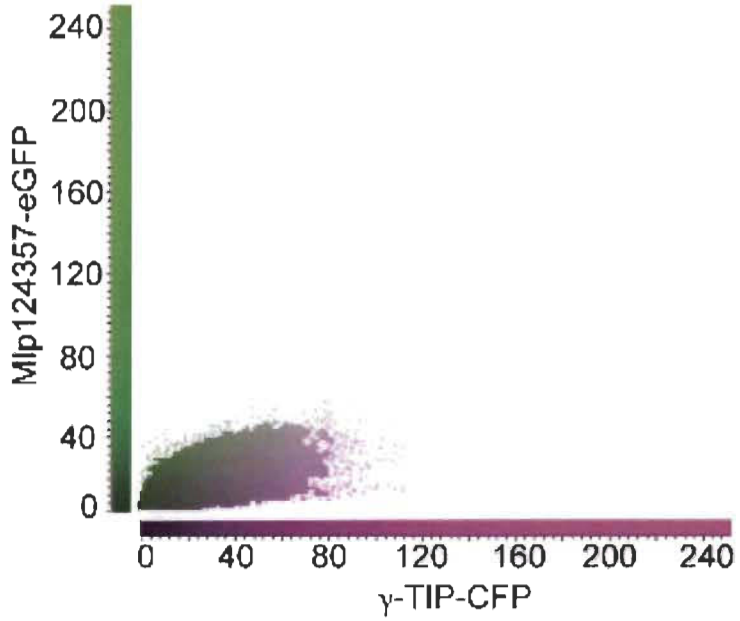

Fig. S1 Intensity scatter plot graph of the co-localization between γ-TIP-CFP and Mlp124357-eGFP.

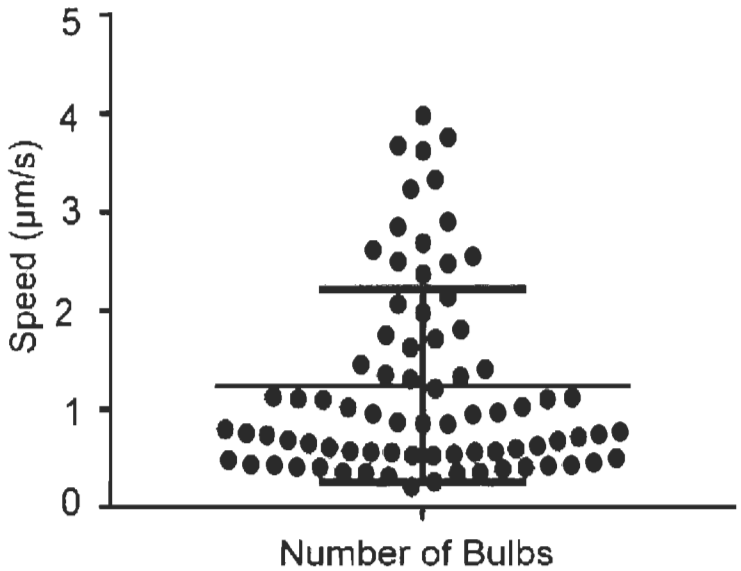

Fig. S2 Bulb size of leaf epidermal cells expressing Mlp124357-eGFP or γ-TIP-YFP. N = 30.

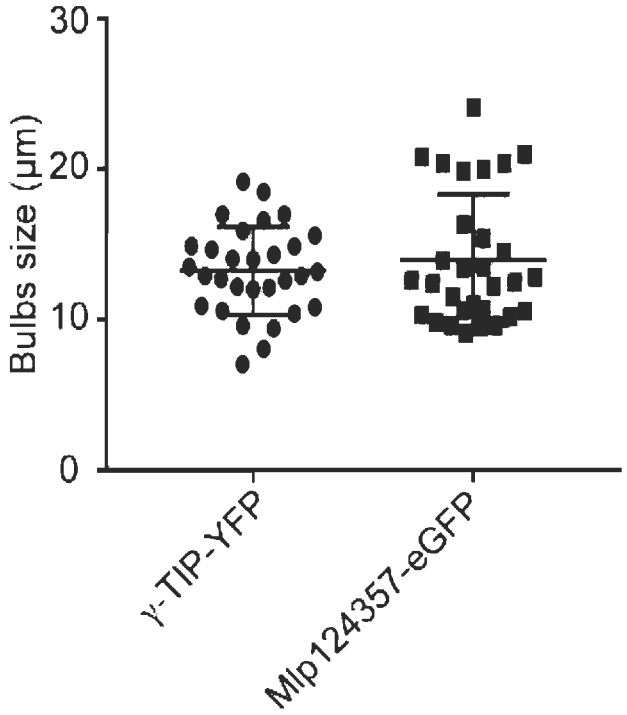

Fig. S3 Bulb speed of leaf epidermal cells expressing Mlp124357-eGFP. N = 76.

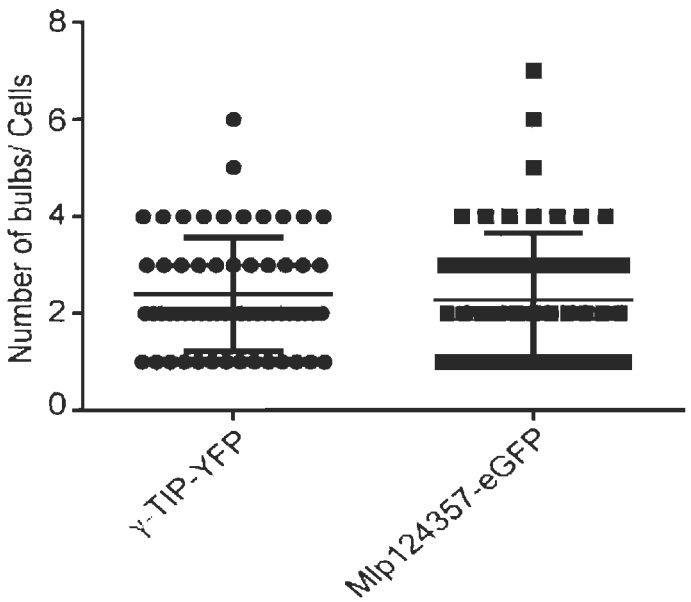

Fig. S4 The frequency of bulbs in the leaf epidermal cells expressing Mlp124357-eGFP or γ-TIP-YFP.
Images were taken from 4-day old seedling leaf epidermal cells and counted the bulbs number per cell. N = 60.

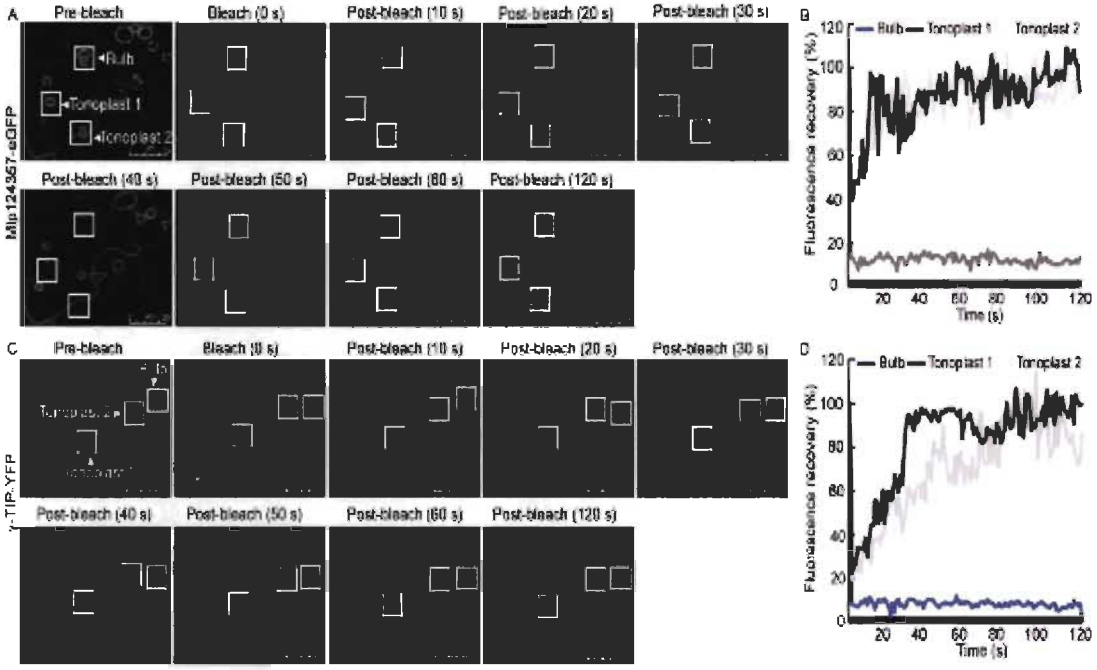

Fig. S5 FRAP image of leaf epidermal cell expressing Mlp124357-eGFP or γ-TIP-YFP. Images were taken before (pre-bleach), immediately after (bleach 0) and 1-second interval for 2 min after bleaching from 6-day old seedlings.

Chapter IV contains a study that demonstrates the Mlp124357 effector of poplar rust pathogen protein interacts with protein disulfide isomerase and promotes plant susceptibility to pathogen.

CHAPTER IV

A POPLAR RUST EFFECTOR PROTEIN ASSOCIATES WITH PROTEIN DISULFIDE ISOMERASE AND ENHANCE PLANT SUSCEPTIBILITY IN *ARABIDOPSIS*

Mst Hur Madina, Md Saifur Rahman, Huanquan Zheng and Hugo Germain

Will be submitted on 1st December 2019 in *Plant Communications*

4.1 Authors contributions

Madina and Germain conceived and designed the study. Madina performed the experiments. Rahman carried out the *in silico* docking study. Madina, Zheng, Germain analyzed the data, prepared the figures, wrote and reviewed the manuscript.

4.2 Résumé de l'article

Melampsora larici-populina (*Mlp*), l'agent responsable de la rouille foliaire du peuplier, secrète une série d'effecteurs dans l'hôte par l'intermédiaire de son haustorium. Les mécanismes spécifiques par lesquels ces effecteurs favorisent la virulence demeurent mal compris. Pour tenter de comprendre le rôle de l'un de ces effecteurs, nous avons développé une lignée d'*Arabidopsis* transgénique stable exprimant l'effecteur candidat Mlp124357 en fusion avec la GFP. La microscopie confocale a révélé que Mlp124357 cible le tonoplaste, les filaments transvacuolaires et les bulbes; l'expression constitutive de l'effecteur augmente la susceptibilité de la plante aux agents pathogènes. Un motif GxxxG présent dans la séquence protéique de Mlp124357 est nécessaire pour une localisation subcellulaire appropriée, car le remplacement des

résidus glycine par des alanines a entraîné la délocalisation de Mlp124357 dans le noyau et le cytoplasme. Nous avons utilisé l'immunoprécipitation et la spectrométrie de masse (MS) pour identifier les partenaires d'interaction Mlp124357. Nous avons testé cinq protéines issues de la liste MS qui ont une localisation tonoplastique et évalué si leur absence dans les plantes conduirait à une délocalisation de Mlp124357. Une seule ligne de knock-out ayant provoquée la délocalisation de l'effecteur confirmant que la protéine disulfure isomérase-1 (AtPDI-11) est nécessaire pour la localisation tonoplastique de l'effecteur, ce qui a été confirmé par un test de complémentation et un test de double hybride dans la levure-deux. De plus, le test d'infection suggère qu'AtPDI-11 agit comme un auxiliaire pour Mlp124357. Nos résultats ont établi qu'un effecteur de *Mlp* réside à la surface de la vacuole et module la sensibilité des plantes tout en requérant la présence d'une protéine disulfure isomérase pour cette localisation.

Mots-clés : rouille, effecteur, motif GxxxG, protéine disulfure isomérase, auxiliaire, sensibilité des plantes

4.3 Full text in English: A poplar rust effector protein associates with protein disulfide isomerase and enhances plant susceptibility in *Arabidopsis*

Abstract

Melampsora larici-populina (Mlp), the causal agent of the leaf rust in *Populus*, secretes an array of effectors into the host through a specialized structure, the haustorium. The specific mechanisms by which these effectors promote virulence remains unclear. To address this question, we developed a stable transgenic *Arabidopsis* line expressing the candidate effector Mlp124357 in fusion with GFP. Confocal microscopy revealed that Mlp124357 targets the tonoplast, transvacuolar strands, and bulbs and constitutive expression of the effector increases plant susceptibility to pathogens. A predicted GxxxG motif present in the protein sequence of Mlp124357 is required for proper subcellular localization since replacement of the glycine residues with alanine led to the delocalization of Mlp124357 into the nucleus and cytoplasm. We used immunoprecipitation and mass spectrometry (MS) to identify Mlp124357 interaction partners. We tested five proteins obtained from the MS list and assessed if their absence *in planta* would lead to a delocalization of Mlp124357. A single knock-out line caused delocalization of the effector confirming that *Arabidopsis* protein disulfide isomerase-1 1 (AtPDI-11) is required for the effector tonoplastic localization, which was further confirmed by a complementation test, yeast-two hybrid assay and *in silico* docking experiment. Moreover, localization results and infection assay suggest that AtPDI-11 act as a helper for Mlp124357. Our findings established that an effector of *Mlp* resides at the vacuole surface and modulates plant susceptibility.

Keywords: rust, effector, GxxxG motif, protein disulfide isomerase, helper, plant susceptibility

Introduction

During infection, plant pathogenic microbes deliver virulence proteins, known as effectors, into host cells to overcome plant immunity and promote parasitic colonization

through manipulation of cellular processes (Dodds and Rathjen 2010). Once inside host tissues, effectors traffic to various cellular compartments including plasma membrane, tonoplast, nucleus, chloroplast, mitochondria and interact with DNA or protein where they exert their virulence function (Ahmed et al. 2018; Caillaud et al. 2012; Petre et al. 2016; Petre et al. 2015; Vargas et al. 2016). To target these destinations, effectors possess domains or motif in their sequence, for example, nucleus localized effectors can contain nuclear localized signal (NLS) and chloroplast localized effector carry a transit peptide (Petre et al. 2016; Schornack et al. 2010; Wirthmueller et al. 2015). Uncovering how effector proteins function inside the plant is key to understanding the pathogenicity mechanism and to developing more resistant crops (Dangl et al. 2013). Because investigating pathogenesis on crop species can be challenging, alternative approaches using heterologous expression in *Arabidopsis thaliana* and *Nicotiana benthamina* are extensively used in effector biology for functional investigation (Bombarely et al. 2012; Caillaud et al. 2012; Germain et al. 2018; Goodin et al. 2008; Petre et al. 2015).

Host proteins that associate with effectors can be targets or helpers (Win et al. 2012). Target proteins are directly targeted and modulated by effectors to alter host cellular processes. For example, bacterial effector HopZ1a interacts with positive regulators of immunity to inhibit their activity (Deslandes and Rivas 2012). The *Pseudomonas syringae* T3E AvrB effector binds with the *Arabidopsis* mitogen activated protein kinase MAP KINASE 4 (MPK4), a suppressor of immunity, to induce plant susceptibility (Cui et al., 2010). The helper proteins may act as a co-factor to enable effector to function, mature or enable trafficking of an effector to their final subcellular destination. Unlike targets, less information is available for the helper so far, perhaps since mutation in the helpers may not result in enhance susceptibility yto pathogens. For instance, the effectors AvrRPM1 and AvrPto both require myristoylation for their activity suggesting they interact with a myristoyl transferase which would serve as the helper for their maturation (Nimchuk et al. 2000; Anderson et al. 2006). A well-known helper is the importin-α, a protein whose function is to mediate nuclear entry of NLS-containing proteins; several TAL effectors and Crinklers were shown to require importin-α for their proper nuclear accumulation (Szurek et al. 2001; Bai et al.

2009; Schornack et al. 2010). Regardless whether host proteins act as an effector target or helper, they are consider as host susceptibility factor (Win et al. 2012).

Rust fungi (Basidiomycetes, Pucciniales) are obligate biotrophic parasite, infect numerous plants families and the largest group of fungal pathogens (Duplessis et al. 2012). Several rust species are devastating pathogens of plants that affect agricultural crops and food security (Pennisi 2010). *Melampsora larici-populina (Mlp* causes rust disease on poplar leaf and leads a major yield loss in poplar plantation worldwide (Duplessis et al. 2009; Hacquard et al. 2011; Major et al. 2010). Genome and transcriptome analysis have revealed that the *M. larici-populina* may contains as much as 1,184 small secreted proteins (SSPs) (Duplessis et al. 2011). Among these SSPs, selected candidate secreted effector proteins (CSEPs) have been selected based on features such as expression in poplar leaves during infection and specificity to Pucciniales order (Hacquard et al. 2010; Hacquard et al. 2012; Saunders et al. 2012). When expressed in *N. benthamiana* or *A. thaliana,* several CSEPs of *Mlp* have been shown to accumulate in diverse cell compartments in leaf tissues such as nucleus, chloroplast, mitochondria, plasmodesmata, nucleolus (Germain et al. 2018; Petre et al. 2015; Ahmed et al. 2018). To date, a number of *Mlp* effectors have been identified that affect *Mlp* virulence and promote plant susceptibility as determined by *in planta* assays, such as MLP124497, MLP124499, and MLP124478 (Ahmed et al. 2018; Germain et al. 2018).

We recently published that the candidate effector Mlp124357, accumulates in tonoplast, transvacuolar strands (TVS), and bulbs (Madina et al. 2018). In this study, we further exploited the *A. thaliana* experimental system, discovered that this tonoplast-localized effector affects plant susceptibility to pathogens and tried to elucidate the mechanisms through which it does so. We used the combined methods of genetics, live cell-imaging, immunoprecipitation, and biochemical analysis to investigate interaction partners of Mlp124357 at the tonoplast. We show that a specific motif of Mlp124357 is necessary for the tonoplast localization. Constitutive expression of the effector increases plant susceptibility to bacterial and oomycete pathogen. We also

provide evidence through mass-spectrometry, a complementation test, a yeast-two hybrid assay and *in silico* modeling that the Mlp124357 associates with protein disulfide-isomerase (PDI) which act as a helper protein for this effector but not for other *Mlp* effectors having similar numbers of disulfide bridges.

Materials and Methods

Plants material and growth conditions

A. thaliana and *N. benthamiana* plants were grown in soil, in a growth chamber after seed underwent a stratification period of 48 h at 4°C. The plant growth chamber was maintained at 22°C, 60% relative humidity, and with a 16 h/8 h light/dark cycle. *In vitro* culture of *Arabidopsis* was performed onto Petri dish containing ½ Murashige and Skoog medium (½ MS) and 0.7% agar. For selection of the single-insertion homozygous transgenic plants, appropriate selection on Basta 15 mg/ml or Kanamycin 50 mg/ml was used.

Cloning procedures and plasmid constructs

The open reading frame (ORF) of *Mlp124357* without the portion coding for its signal peptide was amplified through polymerase chain reaction (PCR) after resuspending and diluting lyophilized-*Mlp124357* obtained from GenScript. The *PDI-11* coding sequence weas amplified from *Arabidopsis*. Amplicons were inserted into the pDONR221 vector (Invitrogen) by BP recombination reactions and then into plant expression vectors pB7FWG2 or pK7WG2 by LR recombination reactions using Gateway technology (Karimi et al. 2002). All the constructs were sequenced and verified before transformation in *Agrobacterium*.

Expression of proteins in *N. benthamiana* and *A. thaliana*

For transient protein expression, constructs were introduced into *A. tumefaciens* strain C58C1 by electroporation and delivered into leaf cells of 4-weeks-old *N. benthamiana* using agroinfiltration method previously described (Sparkes et al. 2006). Briefly, recombinant bacterial strains were grown overnight in yeast extract peptone (YEP) medium with spectinomycin (50 mg/L) antibiotics, then harvested, and resuspended into an infiltration buffer (10 mM $MgCl_2$ and 150 μM acetosyringone) to obtain 0.5 unit of optical density at 600 nm. One hour after resuspension, the abaxial side of leaves were infiltrated. The agro-infected leaves were collected at 2-days post infiltration for confocal microscopy. Stable *A. thaliana* transgenics were developed by introducing the constructs into *A. thaliana* (Col-0) using the *A. tumefaciens*-mediated floral dip transformation (same strain as used for agroinfiltration) method as previously described (Mireault et al. 2014).

Pathogen infections assay

Bacterial infections were performed with 4-weeks-old *Arabidopsis* plants. *Pseudomonas syringae* pv. *tomato* (*Pst*) DC3000 grown overnight at 28°C and infiltrated with a needle-less syringe on the abaxial side of the leaves at 0.001 optical density at 600 nm as previously described (Germain et al. 2018). *Hyaloperonospora arabidopsidis* (*Hpa*) Noco2 infections were performed with the 2-weeks-old *Arabidopsis* plants using spray inoculation method as described by Dong et al. (2016).

Membrane fractionation

Membrane fractionation experiment was carried out according to the method of Lundborg et al. (1981) and Widell and Larsson et al. (1981) with the modification applied in Germain et al. (2013). Briefly, two-phase separation method was used to separate membrane fraction of plant cells, and all preparation steps were maintained at 4°C or on the ice. 3-5 g fresh leaves of 3-weeks old Col-0, and Mlp124357-GFP was

homogenized with a knife blender in the homogenization buffer. The homogenized sample was filtered twice through four layers of cheesecloth and centrifuged at 10,000 g for 10 min. Then, the supernatant was transferred to an ultracentrifuge tube and centrifuged at 50,000 g for 1 h. The supernatant, containing soluble proteins was discarded and the membranal pellet was resuspended in immunoprecipitation buffer. The membranal pellet was used for immunoprecipitation. The membranal pellet was resuspended in IP lysate buffer (10 mM MgCl2, 50 mM Tris-HCl (pH 7.5), 100 mM NaCl, 0.1% triton, 1 mM PMSF, and 1X Coctail (Roche)) and followed the protocol by Serino G and Deng XW (2002). Affinity chromatrography of the protein complexes were performed with GFP-A beads. Then, proteins eluted from the beads by heating the samples at 95°C for 10 minutes and analyzed by standard SDS-PAGE and Western blotting.

Sample preparation for mass spectrometry

For mass spectrometry analysis, bands of interest were extracted from gels and washed with water. Tryptic digestion was performed by following the protocol of Shevchenko et al. (1996) with the modification described in Havlis et al. (2003). Briefly, proteins were reduced in 10 mM DTT for 30 min and alkylated with 55 mM iodoacetamide for another 30 min. After extensive washing, trypsin digestion was carried out with the modified porcine trypsin (Sequencing grade, Promega, Madison, WI) at 37°C for overnight. Peptide were recovered with 1% formic acid, 2% acetonitrile followed by 1% formic acid, 50% acetonitrile (ACN). The recovered extracts were pooled, evaporated to dryness, dissolved in 12 µl of 0.1% formic acid and then 5 µl were analyzed by mass spectrometry.

LC/ES-MS/MS, data processing, and protein identification

Sample preparation and liquid chromatography/electrospray mass spectrometry (ES-MS/MS) were performed as described in Gaillet et al. (2010). Briefly, the peptides were applied to reverse-phase nanoscale capillary liquid chromatography (Nano LC) and

analyzed by electrospray mass spectrometry. The LC-ES MS/MS data were processed and analyzed using Mascot (Matrix Science, London, UK; version 2.5.1) and Scaffold (version Scaffold-4.7.1, Proteome Software Inc., Portland, OR) as previously described (Liu et al. 2016).

Western blot analysis

Leaf tissue was harvested from the 2-3 weeks of stable transgenic plants and protein extracts were prepared as described by Germain et al. (2007). The presence of Mlp124357-GFP, GFP and AtPDI-11-GFP were determined by SDS-PAGE and western blotting was carried out as described (Germain et al. 2008). The blot was probed with an α-GFP-HRP antibody (1:500 dilution, Molecular Probes, Santa Cruz Biotechnolgy, USA). The bands were revealed with the Clarity™ western ECL substrate (Bio-Rad) according to the manufacturer's recommendations.

Confocal Microscopy

Small pieces of young leaves from *Arabidopsis* or *N. benthamiana* were mounted in water between a slide and a coverslip and were immediately observed. Live-cell imaging was performed on Leica TCS SP8 confocal laser scanning microscope (Leica Microsystems) with a 40X/1.40 oil immersion objective. Images were taken at 1024 x 1024 resolution using line-by-line and using sequential scanning (when appropriate). The excitation wavelength for GFP was 488 nm and its emission was collected from 500 to 525 nm. Z-stacks of between 50 and 100 confocal images were acquired and used to generate three-dimensional (3-D) reconstructions using Leica TCS SP8 software (when required). The LAS AF Lite software (Version 3.3) and Adobe Photoshop CS6 were used for the post-acquisition images processing.

Y2H reporter assays

Coding sequences of *Mlp124357* and *AtPDI-11* without their signal peptide were cloned into pGBKT7 (binding domain) and pGADT7 (activation domain), respectively, by homologous recombination in yeast strain Y187 or Y2H gold. Bait-protein encoding vector pGBKT7 expressing Mlp124357 and the prey-protein encoding vector pGADT7 expressing AtPDI-11 were transformed into the yeast strain Y2H gold according to the Clontech yeast-two hybrid protocol. Transformants were plated along with negative control onto yeast synthetic double drop-out medium (DDO) lacking Leu and Trp and quadruple drop-out selective medium (QDO) lacking Trp, Leu, His and Ade (Sigma-Aldrich) and incubated at 30°C for 3 to 4 day. For photographing, series of dilution (10^{-0}, 10^{-1}, 10^{-2}) were prepared for each transformants and 10µl were placed onto DDO and QDO medium and incubated at 30°C for 3 to 4 day.

RNA extraction and transcriptome analysis

RNA isolation was carried out as described previously (Ahmed et al. 2018). Briefly, total RNA was extracted from four-days-old *Arabidopsis* plants grown in Petri and quantified before sending for sequencing. Ion Torrent Technology was used for library construction and sequencing (Université Laval, Quebec City, Canada). Transcriptomics data were processed as reported previously (Ahmed et al. 2018). Gene Ontology (GO) enrichment of both up- and down-regulated genes (having Q-value $\leq$ 0.05 and a fold-change $\geq$ 3) were investigated using the Cytoscape software (version 3.1.1) with the plug-in ClueGO and CluePedia (Bindea et al. 2013).

Molecular modeling of the proteins

Three-dimensional structures of the Mlp124357 were produced through homology modeling using online tool I-TASSER (Yang et al. 2015). PDI-11 3D structure homology-modeling was obtained from sequence alignment against homology template of Protein disulfide-isomerase A3 (PDB: 6eny). The binding efficiency of the effector to

the AtPDI-11 was determined using four different protein-protein docking servers Cluspro, Grammx, Patchdock, ZDock (Kozakov et al. 2017; Pierce et al. 2011; Schneidman-Duhovny et al. 2005; Tovchigrechko and Vakser 2006). The generated protein-protein complexes were visualized and analyzed through PyMOL (DeLano 2002; Yuan et al. 2017).

Results

Identification/ selection and phylogenetic analysis of Mlp124357

The genome analysis of *M. larici-populina* revealed that more than one thousand potential small-secreted proteins are present in *Mlp* (Duplessis et al. 2011). In order to select candidate secreted effector protein (CSEP) for functional investigations, we followed various criteria that were previously described (Petre et al. 2015); these included that expressed sequences must be detected in infection structures, the sequences must be short, possess a signal peptide, conserved cysteines and they must not have conserved sequences outside the order Pucciniales. One of the small secreted peptides that met these criteria is Mlp124357. The small secreted protein Mlp124357 belongs to the family CPG4890, which contains 10 members and appears to be under a positive selective pressure. Each member carries a N-terminal signal peptide region (1-22 aa in the case of 124357) and encodes a short peptide of 80-98 amino acids (molecular weight 9-10 kDa) (Fig. 1A-B). The amino acid identity ranges from 40-60% between Mlp124357 and the other family members (Fig. 1C). In addition, this peptide contains eight conserved cysteine residues and expressed sequence tag (EST) have not been detected in spores but are abundant in infected poplar leaves, supporting infection specific expression. Beyond the member of its close family, Mlp124357 has no similarity with other proteins, whether in Pucciniales or in any other genus, indicating that it is a fairly unique protein in all kingdoms. Hence, the infection specific expression of *Mlp124357* and its uniqueness across the kingdoms triggered us to investigate its localization and putative a role *in planta* during infection.

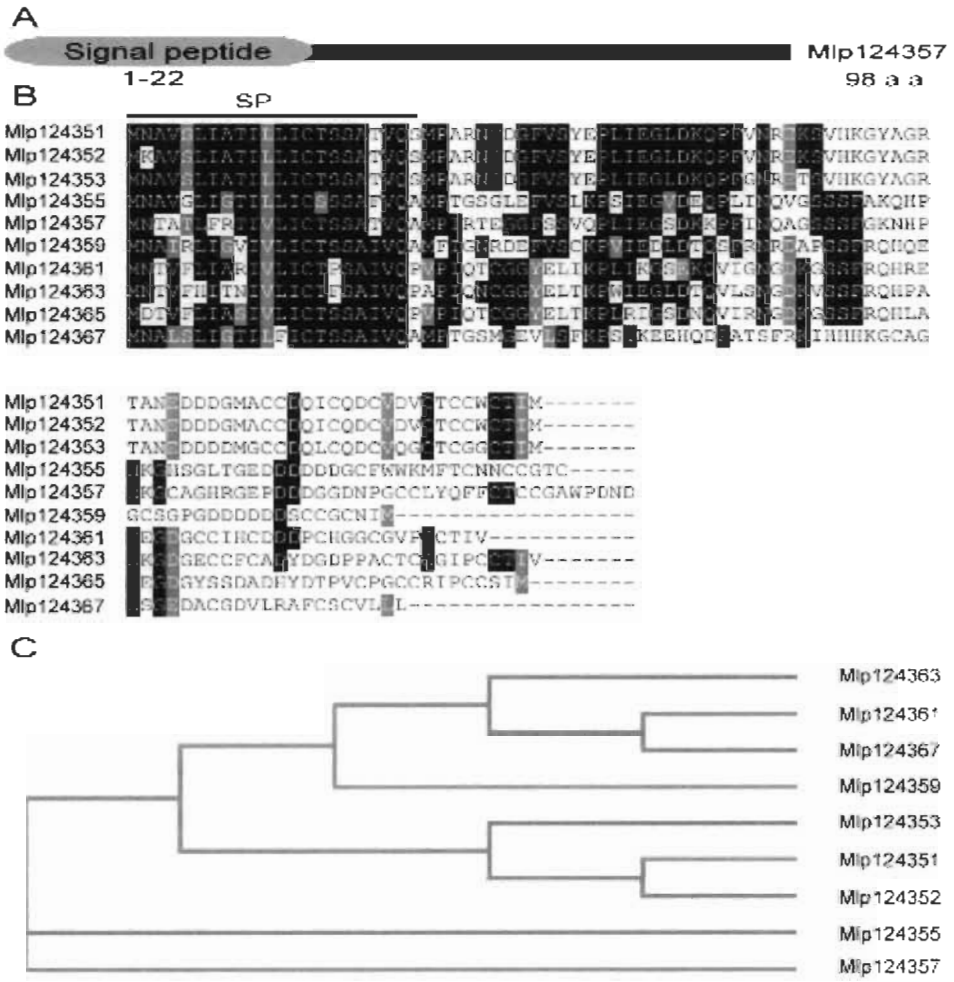

Fig. 1 Multiple sequence alignment and phylogenetic tree of the *M. larici-populina* CPG4890 SSP family.
A) Schematic representation of protein topology of Mlp124357 effector of *M. larici-populina*. N-terminus of Mlp124357 contains a secretory signal peptide (SP) B) Multiple sequence alignment of the ten effector proteins that are the members of the *M. larici-populina* CPG4890 SSP family. Predicted Signal peptides (SP) are marked with a line. Black boxes indicate conserved residues and grey boxes indicate similar residues. C) Phylogenetic tree of the ten effector proteins that are the members of the CPG4890 gene family obtained with Clustal Omega using neighbor-joining tree method.

Mlp124357 expression *in planta* affects the plant susceptibility to bacterial and oomycete pathogens

To express and determine the Mlp124357 localization *in planta*, we cloned the coding sequence without its signal peptide tagged with C-terminal eGFP (enhanced Green Fluorescent Protein; to avoid masking the potential N-terminal chloroplast or mitochondrial signal) under the control of a CaMV35S promoter in a Gateway

expression vector (Fig. 2A). Then, we expressed the Mlp124357 fusion construct in the wild-type *Arabidopsis* (Col-0) as a stable transgenic line and also developed a control line expressing GFP under the control of the same promoter. We then assessed whether Mlp124357 was in frame with the GFP using immunoblot. Fig. 2B shows that both proteins (GFP and 124357-GFP) show at the expected molecular weight. This result confirms that Mlp124357-GFP can be expressed *in planta*, that it is not further processed and can be used for further investigation. The resulting transgenic plants are shown in Fig. 2C. The plant expressing only GFP appeared wild-type looking while the plant overexpressing Mlp124357-GFP displayed narrower leaves, darker green leaves, and chlorosis and drying of the leave tips (Fig. 2C).

To evaluate if Mlp124357 could interfere with the plant susceptibility to pathogens, we subjected control plants and plants expressing Mlp124357 to bacterial and oomycete pathogens. The plants expressing Mlp124357 supported nearly 10-fold more *Pseudomonas syringae* pv *tomato* DC3000 bacteria after 3-days than control plants indicating that it is hypersusceptible to this bacterial hemibiotrophic pathogen (Fig. 2D). Since rusts cannot infect *Arabidopsis thaliana*, we used *Hyaloperonospora arabidopsidis* (*H.a.)* for our infection assays. Although *H.a.* is not a rust (it is an oomycete) it is also an obligate biotrophic pathogen which infects the plants by making haustoria. Seven days following *H. arabidopsidis* spore's inoculation, we quantified the number of spores and detected a significantly increased susceptibility in Mlp124357-GFP transgenic plants compared to Col-0 ($P < 0.0001$) (Fig. 2E) which was not as pronounced as the one observed in the hypersusceptible mutant line *eds1*.

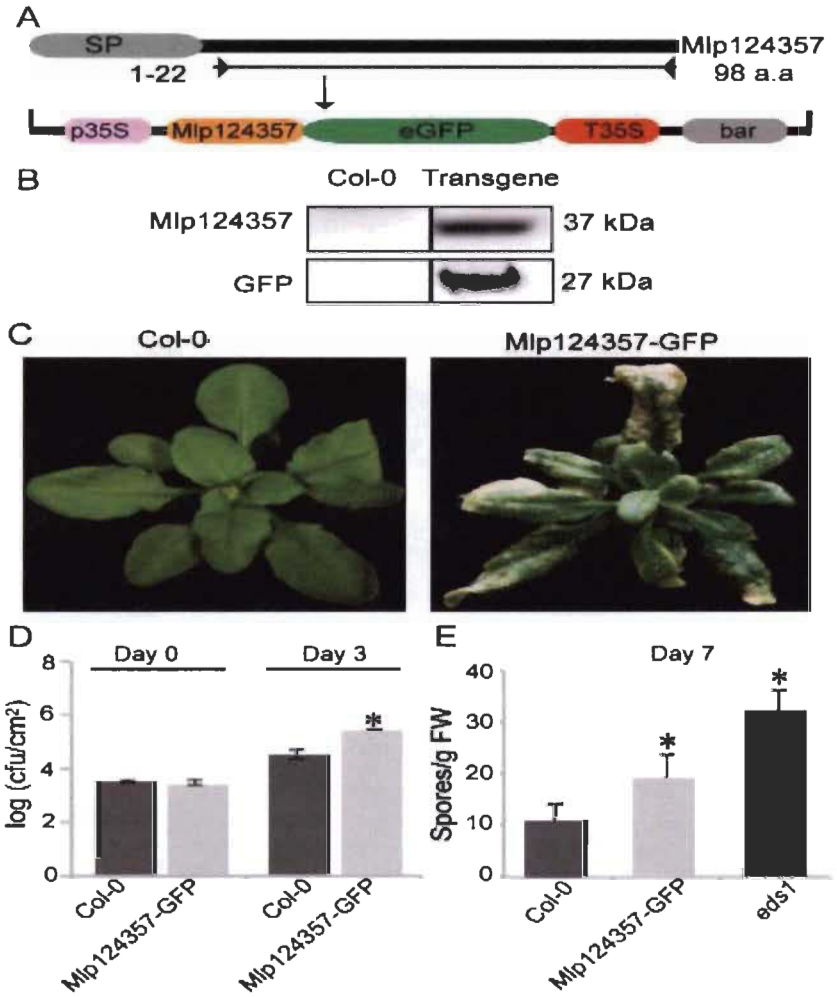

Fig. 2 Expression of Mlp124357 in *Arabidopsis* alters plant morphology and susceptibility to pathogens.

A) Schematic representation of the T-DNA construct that used for *in planta* expression of the Mlp124357 mature coding sequence (without signal peptide) in frame with the green fluorescent protein (GFP). B) Immunodetection of GFP protein in wild-type (Col-0) and stable transgenic seedlings expressing Mlp124357 from 14 days old plantlets. C) Morphology of wild-type (Col-0) and transgenic *Arabidopsis* plants expressing Mlp124357. Photographs were taken from 4-week-old soil grown plants. D) Growth of *Pst*DC3000 bacteria in *Arabidopsis*. Four-week-old soil-grown wild type Col-0 and transgenic plants expressing Mlp124357 leaves were infiltrated with *Pst*DC3000 bacterial suspension (OD_{600} = 0.001) and the bacterial growth was measured on day 0 and day 3 after the infection. Statistical significance was evaluated using Student's t-test ($P<0.05$); asterisk indicates statistically significant difference between plants carrying effector and Col-0 expressing GFP. For each genotype five replicates were used. cfu, colony forming unit. E) Growth of *Hyaloperonospora arabidopsidis* Noco2 oomycete in *Arabidopsis*. Two-weeks-old soil-grown wild type Col-0, stable transgenic Mlp124357 and *eds1* plants were inoculated with *H. arabidopsidis* Noco2 spores (20,000 conidiospores/ml) using spray method and the number of conidiophores were quantified 7 days after inoculation. Statistical significance was evaluated using student's test ($P<0.05$). Asterisk denotes significant difference between Col-0 and Mlp124357 or eds1. FW, fresh weight.

Both bacterial and oomycete infection experiments were repeated at least three times and a representative data is shown.

Mlp124357 possesses a GxxxG motif that is required for the interaction with tonoplast

We have previously reported that Mlp124357 targets the tonoplast *in planta* (Madina et al. 2018), however, Mlp124357 does not possess any transmembrane domain. Thus, we rationalized that Mlp124357 must interact with an integral tonoplast protein. We investigated the primary sequence of Mlp124357 and discovered a GxxxG motif (Fig. 3A) which is known for membrane protein interaction (Bronnimann et al. 2013; Cabanillas et al. 2018). The secondary structure of Mlp124357 sequence was modeled as an alpha-helical wheel projection using helix prediction software (http://kael.net/helical.htm). The presence of two glycines of the GxxxG motif at position 76, and 80 was found on the same side of the α-helix structure (Fig. 3B, pink box). This amino acid orientation of the GxxxG motif is involved in protein interactions between membrane proteins (Teese and Langosch 2015).

To investigate whether these glycines were implicated in Mlp124357 localization we carried out site-directed mutagenesis to substitute the two glycine (Gly) with alanines (Ala). We generated a mutant construct Mlp124357$^{G76A\text{-}G80A}$ fused to the C-terminal GFP, which is thereafter referred to as Mlp124357^{GA}. The fusion protein was transiently expressed in *N. benthamiana* leaves and the subcellular localization was assessed by confocal laser microscopy. Expression of wild type Mlp124357-GFP, was still detected in tonoplast and bulbs of epithelial cells (Fig. 3C). However, replacement of glycine residues with alanine led to the delocalization of the effector (Fig. 3C).

Subsequently, to test whether the delocalization of Mlp124357 affects the activity of the effector, we developed a stable *Arabidopsis* transgenic line (Fig. 3D) with the glycine mutant construct. The glycine mutant line no longer displayed the chlorotic phenotype on the leaves; rather, it was undistinguishable from WT plants (Fig. 3D). We then confirmed that Mlp124357^{GA} localization in *A. thaliana* supported with the ones observed in *N. benthamiana* that is the Mlp124357-GFP effector accumulates in the tonoplast, TVS, and bulb while the Mlp124357^{GA} accumulates in the nucleus and cytoplasm (Fig. S1). Further, these transgenic lines were used to perform infection

assays to evaluate their susceptibility to pathogens. The plants expressing Mlp124357^{GA} showed a level of bacterial growth which was similar to the control plants Col-0 and Col-GFP (Fig. 3E). Similarly, inoculation experiment of *H. arabidopsidis* spores demonstrated wild-type like susceptibility on Mlp124357^{GA}-GFP compared to that of Mlp124357-GFP ($P < 0.0001$) (Fig. 3F). From these experiments, we conclude that the GxxxG motif is required for the Mlp124357 localization and function of the effector.

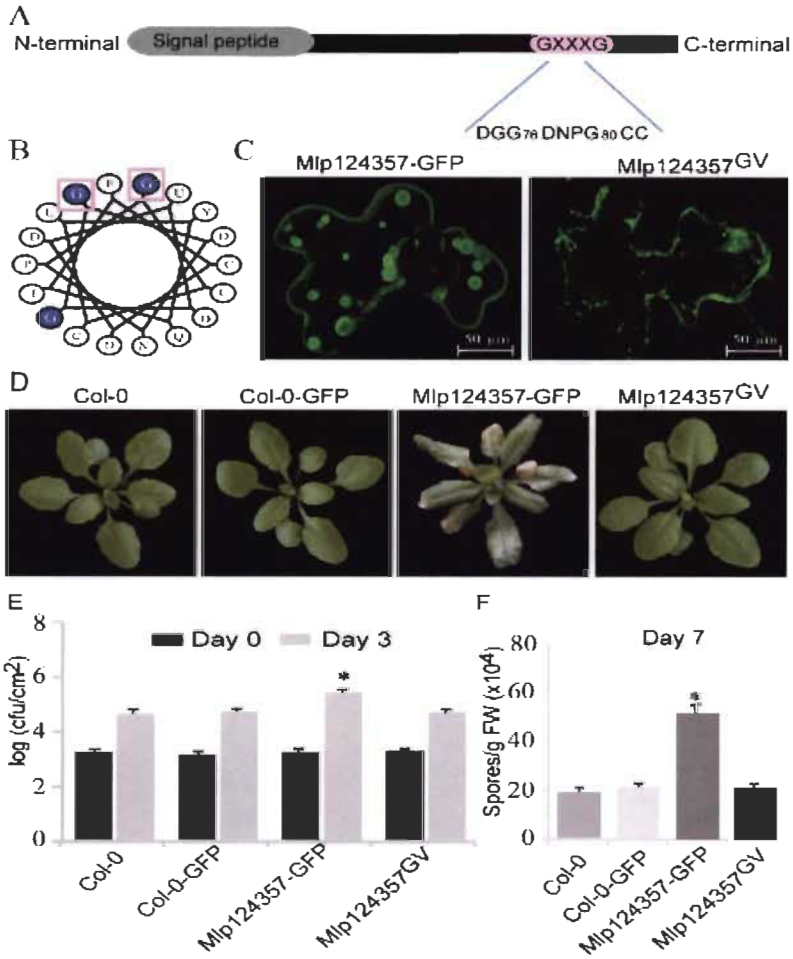

Fig. 3 The GxxxG motif is essential for effector localization and plant susceptibility in *Arabidopsis*.

A) Schematic representation shows the presence of GXXXG motif in the C-terminus region of Mlp124357. B) A predicted helical wheel projection of the Mlp124357. The glycine residues located at position 76 and 80 are indicated by square boxes. C) Fluorescence imaging of *N. benthamiana* cells expressing GFP fusions of Mlp124357 and the indicated Mlp124357 ^{GA} mutants at 2 dpi using confocal microscopy of epidermal cells. These images are three-dimensional renderings stacks of 50 z-section. D) Morphology of wild-type (Col-0), Col-0 expressing GFP, and transgenic *Arabidopsis* plants expressing Mlp124357 or Mlp124357^{GA}. Photographs were taken from 4-week-old soil grown plants. E) Four-week-old soil-grown wild type Col-0, Col-GFP, and transgenic plants expressing Mlp124357 leaves were infiltrated with *Pst*DC3000 bacterial suspension at concentration of OD_{600} = 0.001 and quantified the colony forming unit (cfu) for the bacterial growth on the day 0 and day 3 after infection. Statistical significance was evaluated using Student's t-test ($P < 0.05$); asterisk indicates statistically significant difference between plants carrying effector and Col-0 expressing GFP. For each genotype five replicates were used. F) Two-weeks-old soil-grown wild type Col-0, Col-GFP, Mlp124357-GFP and eds1 plants were spray inoculated with *H. arabidopsidis* Noco2 spores (20,000 conidiospores/ml) and the number of conidiophores was quantified 7 days after inoculation. Statistical significance was evaluated using student's test ($P<0.05$). Asterisk denotes significant difference between Col-0-GFP and Mlp124357 or eds1. FW, fresh weight.

Both bacterial and oomycete infection experiments were repeated at least three times and a representative data is shown.

Immunoprecipitation and mass spectrometry reveal potential plant interactor protein of Mlp124357

Since no transmembrane domain was detected in the Mlp124357 peptide sequence using the TMHMM software (http://www.cbs.dtu.dk/services/TMHMM/), we rationalized that the small secreted peptide must interact with an integral plant protein to achieve its tonoplastic localization. In order to identify putative interaction partners of Mlp124357 protein in membranes, we first assessed if it could be isolated from membranes. It appears that Mlp124357 association with the membranes was not very strong as it could also be detected in the supernatant of membranal fraction (Fig. S2). However, since Mlp124357 was partly retained in the membrane, we immunoprecipitated it from the membranal fractions using anti-GFP beads and subjected gel bands to mass spectrometry to identify potential plant protein interactors. From the MS analysis, 40 *A. thaliana* proteins were identified as potential interactor of the Mlp124357 effector (Table S1). However, since the Mlp124357 accumulates in the tonoplast, we screened and selected only tonoplastic protein for further investigation (Fig. 4A).

Mlp124357 associates with *Arabidopsis* and poplar protein disulfide-isomerase

To verify the potential interacting protein partner, we crossed the knock out (KO) lines of those five tonoplast proteins from MS lists with Mlp124357-GFP transgenic line and assessed their fluorescence localization using confocal microscopy (Fig. 4A). We hypothesized that if one of those proteins is the interactor and serves as an anchor protein to Mlp124357 at the tonoplast, the effector would change localization in the knock-out line when its anchor is absent. Interestingly, the absence of one tonoplast protein named protein disulfide isomerase 11 (*PDI-11*; gene id: *AT2G47470*) led to the delocalization of Mlp124357-GFP (Fig. 4 B and Fig. S3). Since the host of the poplar rust is poplar we also assessed if the effector could interact with the *Populus trichocarpa* PDI (the *At*PDI-11and *Pt*PDI share about 87% identity (Fig. S4). A genetic complementation test was performed to confirm the interaction between the effector and *At*PDI-11 or PtPDI. Hence, both the *Arabidopsis PDI-11* and poplar *PDI* could restore

the tonoplastic localization of 124357-GFP in the *pdi-11* ko background (Fig. 4B panels IV and V). In addition, to verify the cellular localization of AtPDI-11, it was cloned in fusion with eGFP protein (*At*PDI-11-GFP) and transiently overexpressed in *N. benthamiana* leaf cells by *Agro*-infltration and observed by confocal microscopy. The GFP signal suggested a localization in both the tonoplast and ER structures (Fig. S5). These results suggest that PDI is required for the localization of 124357 at the tonoplast.

Further confirmation of the interaction between Mlp124357 and AtPDI-11 or PtPDI was carried out using yeast-two hybrid assay. Independent co-transformation experiments showed that yeast co-expressing a bait-Mlp124357 construct with a prey-AtPDI-11 or prey-PtPDI construct were able to grow on quadruple dropout medium (Fig. 4C), whereas bait-Mlp124357^{GA} construct did not grow (Fig. 4C). Both the complementation and Y2H results provide evidence that the Mlp12357 associates with protein disulfide isomerase. The results demonstrate that PDI is required for the localization of the effector *in planta*.

A

Gene name	Functions in	SALK name
AT2G33210	ATP binding, copper ion binding	SALK_120568
AT5G15650	Intramolecular transferase activity	SALK_132152
AT2G47470	Protein disulfide isomerase activity	SALK_135268
AT1G04040	Acid phosphatase activity	SALK_068225
AT4G29810	Kinase activity	SALK_200520

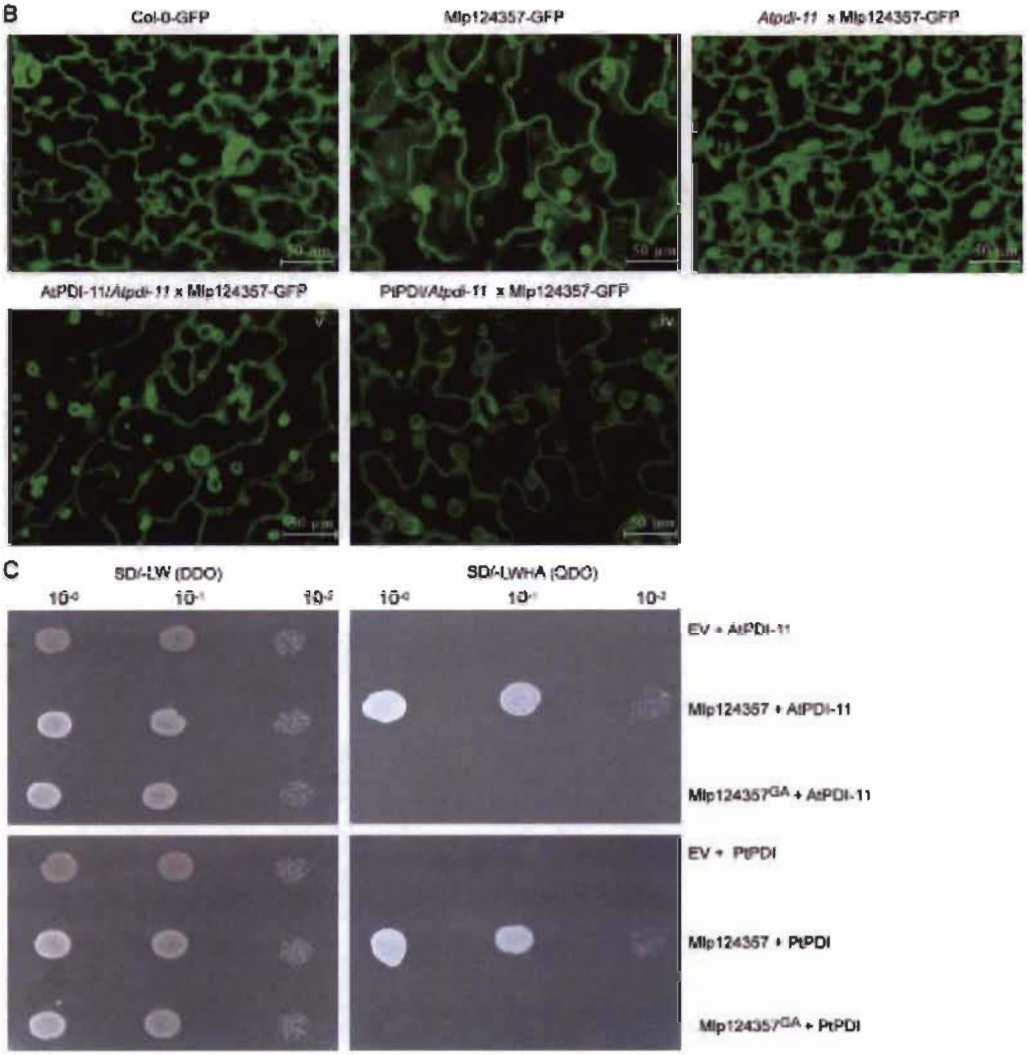

Fig. 4 Mlp124357 associate with both AtPDI-11 and PtPDI in *Arabidopsis*.
A) Selected five-tonoplast localized protein from IP/MS list. B) Interaction between Mlp124357 and AtPDI-11 or PtPDI was detected by a genetic analysis/complementation test. Live-cell imaging of leaf epidermal cells of Col-0-GFP and Mlp124357-GFP in *Atpdi-11* x Mlp124357-GFP, AtPDI-11/Atpdi-11 x Mlp124357-GFP, and PtPDI/Atpdi-11 x Mlp124357-GFP lines with a laser-scanning confocal microscopy. C) Interaction between Mlp124357 and AtPDI-11 was evaluated by Y2H. AtPDI-11 and Mlp124357 or Mlp124357^{GA} were cloned into pGBKT7 and pGADT7 vectors, respectively. The plates were photographed 2 days after inoculation.

Molecular modeling also supports the association of AtPDI-11 and Mlp124357 effector

To further assess the interaction between PDI-11 and the effector we sought to use molecular modeling to investigate if the interaction was supported by molecular modeling using I-TASSER. Three-dimensional structures of Mlp124357 were produced through homology modeling using online tool I-TASSER. AtPDI-11 3D structure homology-modeling was obtained from sequence alignment against homology template of Protein disulfide-isomerase A3 (PDB: 6eny) and the generated protein-protein complexes were visualized and analyzed through PyMOL. To select the final or best models of Mlp124357 and AtPDI-11 from I-TASSER simulation (Fig. 5A-B) for docking, we selected the model with the highest confidence score (C-score), higher TM-score and lower RMSD. Our docking results from four different servers have shown a similar conformational binding affinity of Mlp124357 to AtPDI-11 (Fig. 5C-D). Commonly, these residues, C30GHC33, and C149GHC152 located in the catalytic sites of both AtPDI-11 and PtPDI are also involved in hydrogen bonding with Mlp124357 (Fig. 5D); catalytic 30 positioned residue CYS of PDI makes bond with GLU 6 of effector. As the crystalline structure of AtPDI-11, PtPDI and Mlp124357 has not yet been obtained, we conducted an in-silico study of AtPDI-11, PtPDI and Mlp124357 for 3D structure prediction and docking using four different servers. All the different server simulation gives relatively similar results for mooring Mlp124357-PDI-11. Hence, the IP data, the complementation results, the yeast-two hybrid interaction all support an interaction between Mlp124357 and PDI. Moreover, the molecular modeling suggests that the interaction between the two proteins occurs through the catalytic site of PDI-11 suggesting that 124357 may be a substrate for PDI-11.

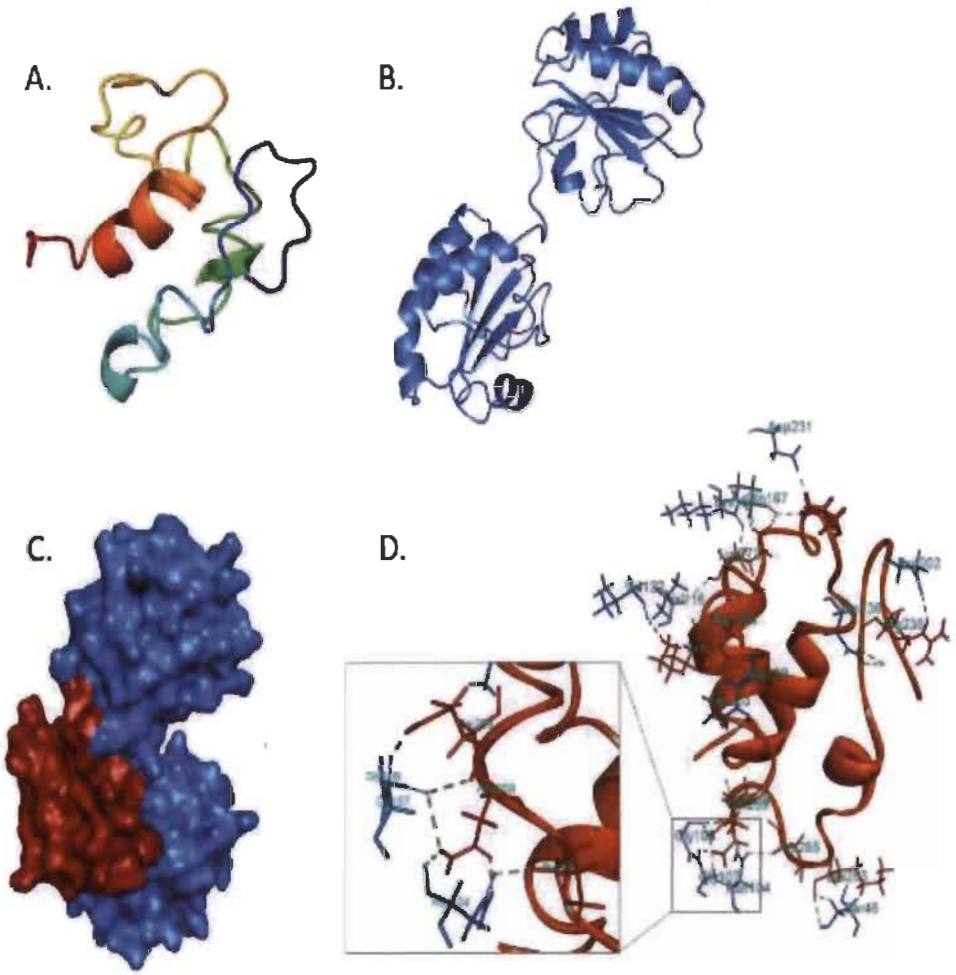

Fig. 5 Functional approach of docking between *M. larici-populina* Mlp124357 and AtPDI-11.
A) Predicted structure Mlp124357 and B) AtPDI-11. C) Prepared AtPDI-11 monomer by deleting chains and ligands. AtPDI-11 monomer with B-chain is prepared for further docking. Red colored residues indicate binding pocket sites of AtPDI-11. The general scheme of docking between AtPDI-11 (blue) and Mlp124357 (red) using different servers. D) The orientation and interactions of AtPDI-11-Mlp124357 complex.

The Mlp124357-PDI association takes place in an effector-specific manner

Since protein disulfide-isomerase catalyze the formation of disulfide bond between cysteine residues within protein and most effector protein contains several cysteine residues (5-8), we considered that the PDI-11 interaction could be a general interaction between all (or many) effectors and PDI-11. To determine whether the interaction between Mlp124357 and AtPDI-11 was specific or general, we use the yeast two-hybrid

system to assess the interaction between AtPDI-11 prey and eight *Mlp*-effectors also having several predicted disulfide intramolecular bridges. The yeasts co-expressing effectors (Mlp1104486, Mlp51108708, Mlp772983, Mlp3351690, Mlp1123281, Mlp752166, Mlp3353845 and Mlp151107359) did not grow on quadruple drop out medium like the negative control (Fig. 6). This result suggests that the interaction between PDI-11 and Mlp124357 is specific and PDI-11 does not serves as a general effector maturation interactor.

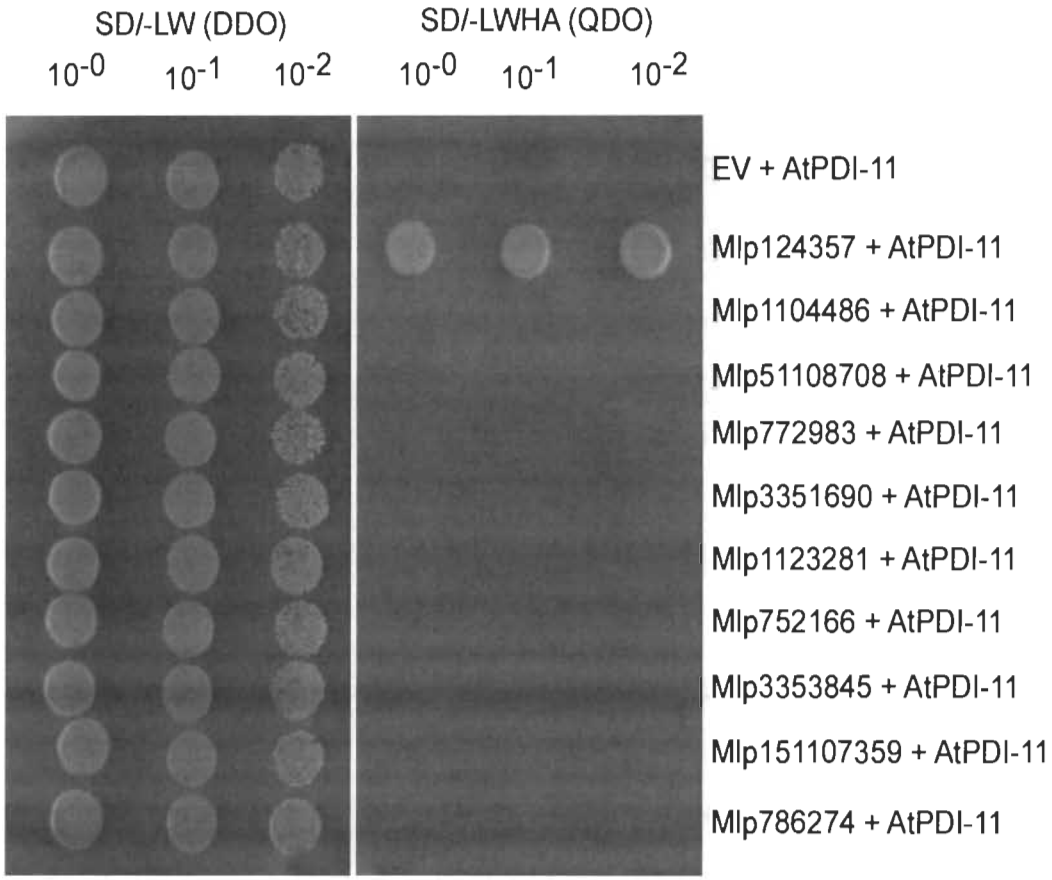

Fig. 6 AtPDI-11 specifically associates with Mlp124357 effector but no other *M. larici-populina* effectors.
Co-expression of AtPDI-11 with Mlp124357, Mlp1104486, Mlp51108708, Mlp772983, Mlp3351690, Mlp1123281, Mlp752166, Mlp3353845, Mlp151107359, or Mlp786274 in yeast show interaction assay between PDI at several cysteine containing effectors. Yeast co-expressing the indicated combination of bait and prey were spotted on the synthetic double dropout medium lacking leucine and tryptophan (SD/-LW (DDO)) and quadruple dropout medium lacking leucine, tryptophan, histidine, and adenine (SD/-LWHA (QDO)). Only those co-expressing AtPDI-11 and Mlp124357 grew on SD/-LWHA plates. The plates were photographed 2 days after inoculation.

Protein disulfide-isomerase act as a helper of Mlp124357

In order to assess whether AtPDI-11 is a target or helper to Mlp124357, we conducted infection assays with two different pathogens (*Pst*DC3000 and *H. arabidopsidis*). It should be noted that the leaf phenotypes of *Atpdi-11* and AtPDI-11/*Atpdi-11* were similar to control plant Col-0 or Col-0-GFP, but in the presence of the Mlp124357 effector, the *Atpdi-11* and AtPDI-11/ *Atpdi-11* complemented line exhibited chlorotic symptoms on their leaves (Fig. 7A). This result suggests that although the effector is mislocalized in the *pdi-11* line it seems to retain its phenotype-altering activity. We then used these lines for the infection assay with *Pst*DC3000 and *H. arabidopsidis*. Comparing to the control wild-type Col-0 or Col-0-GFP, the line *Atpdi-11* and AtPDI-11/*Atpdi-11* showed similar pathogen growth (Fig. 7B-C). This result suggests that PDI-11 does not contribute significantly to the plant immunity and hence that Mlp124357 would not target it to increase the pathogen virulence. The Mlp124357 promoted bacterial and oomycete growth, but interestingly, in the absence of AtPDI-11, it was unable to do so. As such, PDI-11 appears to be required for the localization and the virulence activity of 124357 although the effector capacity to affects the phenotype appears to be uncoupled from its virulence activity.

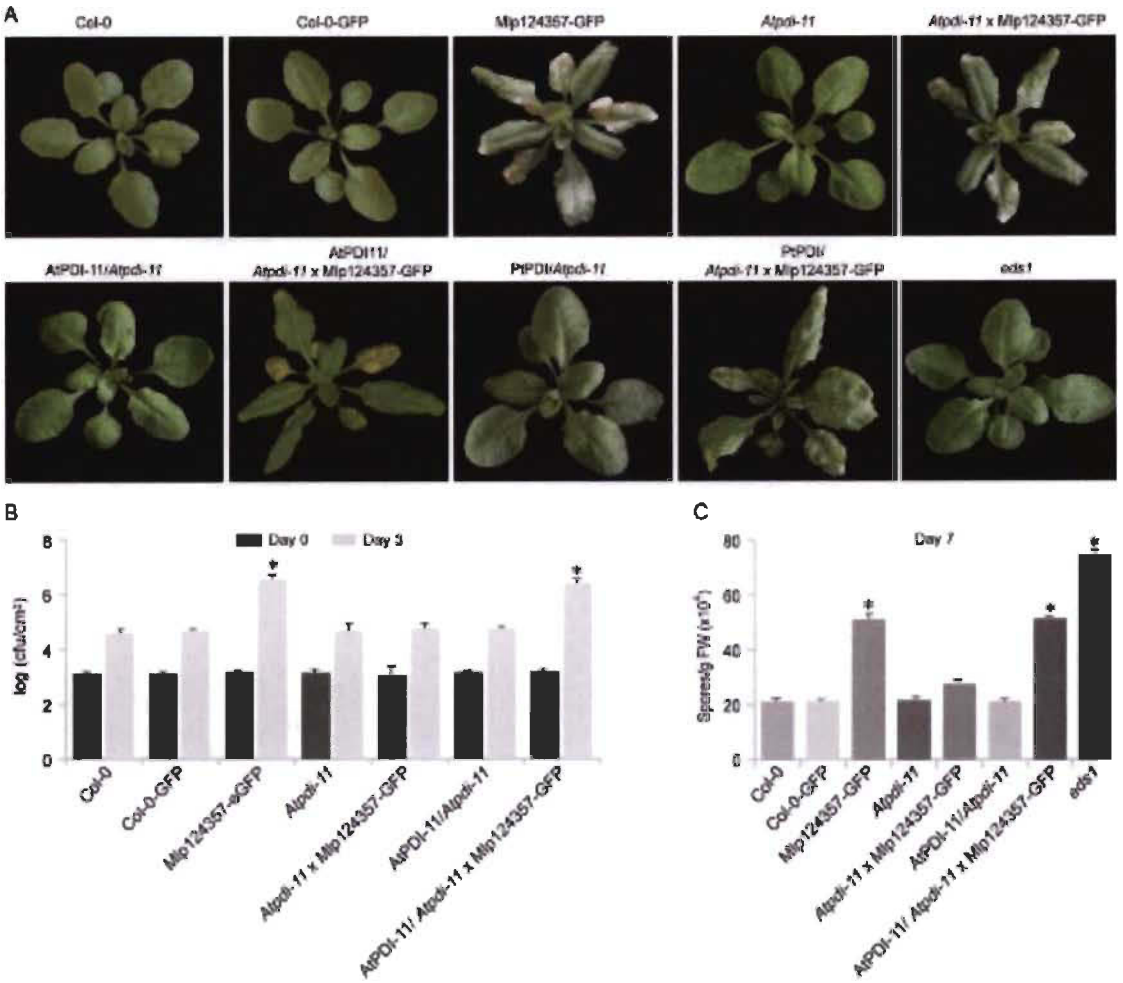

Fig. 7 Protein disulfide-isomerase does not affect plant susceptibility to pathogens.
A) Morphology of each genotypes that were used for the infection assays. Photographs were taken from 4-week-old soil grown plants. B) Growth of *Pst*DC3000 bacteria in *Arabidopsis*. Four-week-old soil-grown plants leaves were infiltrated with *Pst*DC3000 bacterial suspension (OD_{600} = 0.001) and quantified at day 0 and day 3. Statistical significance was evaluated using Student's t-test ($P<0.05$); asterisk indicates statistically significant difference between plants carrying effector and Col-0 expressing GFP. For each genotype five replicates were used. cfu, colony forming unit. C) Growth of *H. arabidopsidis* Noco2 oomycete in *Arabidopsis*. Two-weeks-old soil-grown plants were inoculated with *H. Arabidopsidis* Noco2 spores (20,000 conidiospores/ml) using spray method and the number of conidiophores were quantified at 7 days after inoculation. Statistical significance was evaluated using Student's test ($P<0.05$). Asterisk denotes significant difference between Col-0 and Mlp124357 or eds1. FW, fresh weight.
Both bacterial and oomycete infection experiments were repeated at least three times and a representative data is shown.

Transcriptome analysis of Mlp124357-expressed *Arabidopsis*

To identify host molecular pathways altered by Mlp124357, we performed genome-wide gene expression analysis using RNA-seq of 4-days-old *A. thaliana* Mlp124357 stable transgenic line and control plants expressing GFP. In the Mlp124357 transgenic line, 268 and 353 genes were up- and down-regulated by 2-fold or greater, respectively, in comparison with control plants (Table S2). Next, we performed GO term enrichment analysis of genes that were up- and down-regulated in Mlp124357 to determine the relevant biological process altered by Mlp124357. Four functional groups of GO terms significantly enriched were noted; cellular response to iron ion starvation, indole-containing compound biosynthetic process, organ senescence, and small molecule catabolic process (Fig. 8). Remarkably, multiple defense-related genes such as YLS9, CHI, CYP79B2, BGLU21 were down-regulated in the Mlp124357-GFP transgenic lines compared to the GFP transgenic plants. Several genes of BHLH transcription factor, for instance, BHLH038, BHLH039, BHLH040, and the GLK2 are involved in the plant Fe deficiency response and plant susceptibility to fungus, respectively, were up-regulated in Mlp124357-GFP transgenic line (Fig. 8). These results add support for our observations of the leaf chlorosis (Fig. 2C) and plant susceptibility to pathogens (Fig. 3D-E).

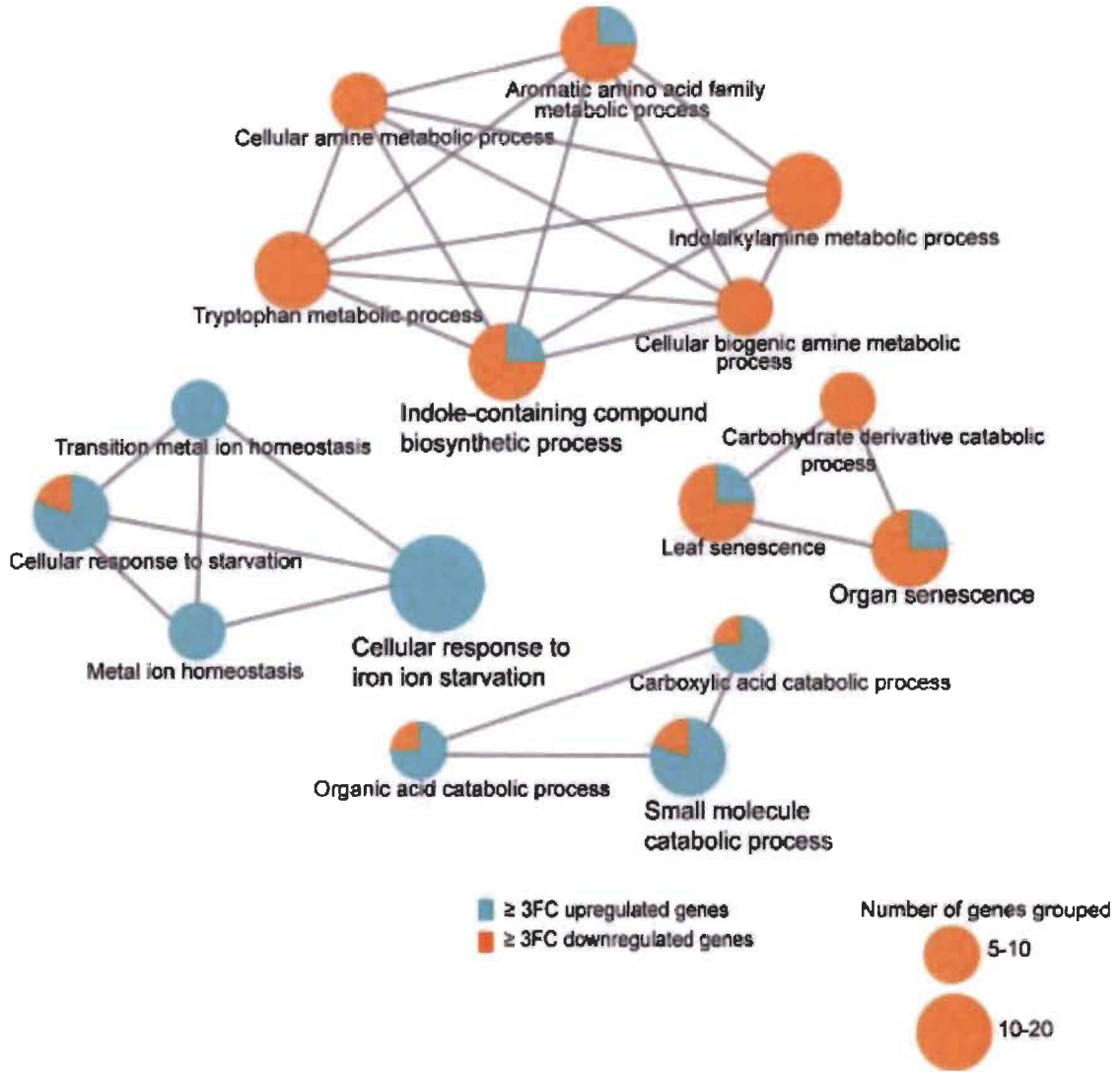

Fig. 8 The expression Mlp124357 in *Arabidopsis* deregulates groups of genes associated with senescence, Fe homeostasis and defense to fungus.
Go term enrichment analysis was performed with both up and deregulated genes filtered with Q-value ≤ 0.05 and fold-change ≥ 3 using the Cytoscape software (version 3.1.1). ClueGO plug-in of Cytoscape was used to visualize enriched functions for the both up- and down regulated genes.

Discussion

Effectors play a key role in plant-microbe interactions (Jones and Dangl 2006) and many of them are shown to act as a virulence factor that are capable to suppress plant defense response and enhance pathogenesis (Speth et al. 2007). However, little is known about effector functions of *Melampsora larici-populina,* a devastating pathogen of

poplar worldwide. In this study, we used *A. thaliana* and *N. benthamiana* as heterologous systems and a poplar leaf rust effector, Mlp124357, as a probe to understand the potential function of this *Mlp* effectors in plants. We identified protein disulfide isomerase as a putative helper of Mlp124357 and determined their specific physical interaction both in yeast and *in planta.* This interaction is required for the virulence of the *Mlp* pathogen. Moreover, we identified a GxxxG motif in the Mlp124357 sequence that mediate the interaction with PDI. Normally, WT Mlp124357 accumulates in the tonoplast, TVS, and bulb, however, when the Gly residues of GxxxG motif were replaced with Ala residues, *in planta* expression of Mlp124357^{GA} mutant lost its tonoplastic localization and is no longer able to enhance pathogen growth. To our knowledge, a connection between rust pathogens and tonoplast has not previously been established.

When *Arabidopsis* was exposed to different pathogens having different lifestyle, i.e. bacteria and oomycetes, we observed that Mlp124357 enhanced the susceptibility to pathogen growth. *Hpa* and *Mlp* both are obligate biotrophic filamentous pathogens of dicot plants and possesses a similar type of infection strategies in leaf tissues. However, Mlp124357 also increased the bacterial *Pst* growth. We conclude that Mlp124357 altered a host mechanism that is active against both bacteria and biotrophic filamentous pathogens.

The morphology of the plants expressing Mlp124357 is altered, the plants show narrower leaves, chlorosis and yellowing of the leave tips. Expression of bacterial as well as filamentous pathogen effectors can affect host immune response and induce a variety of phenotypes in plants including chlorosis (Cunnac et al. 2009; Torto et al. 2003). For instance, fungal effectors SnTox (Faris et al. 2010; Liu et al. 2012), FvTox1 (Brar et al. 2011) and bacterial effectors AvrB (Shang et al. 2006), HOPQ-1 (Kanneganti et al. 2006) induce chlorosis symptoms in plants. Chlorotic phenotype has previously been reported to associate with the plant susceptibility (Chang et al. 2016), thus, induction of chlorosis and plant susceptibility by Mlp124357 can reflect a genuine effector activity. However, when we inserted mutation of Gly residues of GxxxG motif

of Mlp1224357 in *Arabidopsis*, we could no longer observed chlorosis in leaves of plants, suggesting that the GxxxG linked to chlorosis and virulence activity of the effector, supporting this result which could caused by the mislocalization in the mutated effector. On the other hand, the Mlp124357 effector was still capable to induce chlorosis in *pdi-ko* but the effector is unable to suppress plant immunity in *pdi-ko* plant, suggesting they could be uncoupled.

Recently, we reported that Mlp124357 localize to tonoplast, bulbs, and TVS (Madina et al. 2018). However, how would the *Mlp* pathogen benefit from manipulating host tonoplast and vacuolar sub-structures is unclear. To our knowledge, besides Mlp124357, an effector of *Hpa,* HaRxL17, is also reported to localizes to the tonoplast and has the ability to enhance plant susceptibility (Caillaud et al. 2012). Therefore, pathogen effectors may target tonoplast to modulate the host tonoplast to suppress the vacuole-mediated defense response. Further mechanistic investigations of the pathogen effector/tonoplast interplay should shed light on the biological significance of this phenomenon.

The fact that no transmembrane is present in the effector protein sequence, led us to investigate how does Mlp124357 interact with membranes. We discovered a GxxxG motif present in Mlp124357. Many reports have shown that the GxxxG motifs are responsible for membrane protein interaction (Cymer et al. 2012; Fink et al. 2012; Li et al. 2012). Through mutagenesis and pathogen assay, we reveal that the GxxxG motif within Mlp124357 sequence is required for plant susceptibility and tonoplast localization, thereby allowing the effector to interact with tonoplast-localized AtPDI-11.

We identified protein disulfide isomerase, a member of the Protein Disulfide Isomerase (PDI) gene family, as a plant interactor partner of Mlp124357 in *Arabidopsis*. The PDI gene family have been shown to contain more than ten members in distinct eukaryotic species; for example; there are 20 genes in *Homo sapiens*, 18 in rice, 12 in *Arabidopsis*, and 12 in *Populus* (Ellgaard and Ruddock 2005; Houston et al. 2005; Kozlov et al. 2010; Zhu et al. 2014). Similar to human, the major function of PDIs in

plants is to contribute to the formation of disulfide bonds by induction, oxidization, and isomerization; all of which are essential for the proper folding and maturation of proteins (Ellgaard and Ruddock 2005; Houston et al. 2005; Kozlov et al. 2010; Meyer et al. 2019). PDIs have also been shown to play an important role as chaperones in the quality control system for accurate protein folding (Määttänen et al. 2010). For example, HSP70, HSP90, and DNAJ-like proteins have been shown to perform similar functions as chaperones in plant-pathogen interaction (Verchot 2012). Since, like other effector, cysteine-rich Mlp124357 is expected to translocate as an unfolded protein in plant cell, thus, we speculated that PDI could have been recruited by *Mlp* in poplar/*Arabidopsis* to act as cellular chaperone (protein folding, stabilization, or facilitating transport) during infection. The functional motifs and tertiary structures of AtPDI-11 or PtPDI and its homologs in other plants and animals are found to be highly conserved (Yuen et al. 2013). By identifying AtPDI-11 or PtPDI to mediate of *Mlp* virulence activity in poplar, it gives the impression that other members of the PDI gene family might play the same role in other plant-rust interactions, however we have clear evidence that this PDI is a specific, not a general interactor for *Mlp* effector since it did not interact with the other 8 tested effectors.

Variation has been reported in the subcellular localization of PDIs in *Arabidopsis* (Yuen et al. 2013). Most PDI were shown to localize to the ER lumen (Cho et al. 2011; Ondzighi et al. 2008; Wittenberg et al. 2014), while several isoforms of PDI have been localize to other cellular organelles, such as Golgi, chloroplasts, nucleus, and tonoplast (Cho et al. 2011; Ondzighi et al. 2008; Wittenberg et al. 2014). Our result indicates that the AtPDI-11 accumulates both in ER and tonoplast and interact with Mlp124357, however, we did not see any accumulation of this effector in ER.

Host proteins that are targeted by pathogen effectors could act as "helpers" to enable effector functions, while others are "target" (Rovenich et al. 2014). Previous studies demonstrated that folding of pathogens effector facilitated by host protein might be important to modulate effector functions in host cells during pathogenesis. For instance, cyclophilin ROC1 (*Arabidopsis*) and GmCYP1 (soybean) is required to

activate the bacterial effector AvrRpt2 (Coaker et al. 2005; Coaker et al. 2006) and fungal effector Avr3b, respectively (Kong et al. 2015). Our study demonstrated that PDI absence does not affect plant susceptibility, suggesting PDI is not directly involved in immunity but may be responsible for the activation of *Melampsora larici-populina* effector Mlp124357. In another word, AtPDI-11 is likely the host helper recruited by Mlp124357 to enhance plant susceptibility. These results suggest that recruitments of host factor as "helper" is a common pathogenesis mechanism shared by pathogens.

The GO term of transcriptomic analysis revealed that the largest groups of deregulated genes were significantly enriched for defense response and indole-containing compound biosynthetic process in *Arabidopsis* Mlp124357-GFP transgenic line. The most down-regulated genes belonged to defense response are YLS9, CHI, CYP79B2, BGLU21 and chitinase. Similar results were recently reported for Mlp124478 effector by Ahmed and colleagues (Ahmed et al. 2018), suggesting that suppression of defense response genes by effectors is a common shared phenomenon during *Mlp* infection. However, the next most enriched GO term is cellular response to iron ion starvation which is different from Ahmed et al. (2018) findings followed by small molecule catabolic process and organ senescence. Of the most up-regulated genes, several belonged to the transcription factor bHLH (BHLH038, BHLH039, BHLH040) and GLK2. We believe, Mlp124357-induced chlorosis may result from upregulation of the expression of bHLH transcription factors such as bHLH038, bHLH039, and bHLH101, which are involved in the plant Fe deficiency response that leads to chlorotic leaves.

Until recently, the molecular interaction of poplar with the economically important pathogen *Melampsora larici-populina* remained largely mysterious. The research presented here increases our knowledge of the poplar- *Melampsora larici-populina* pathosystem and highlights importance of helper proteins as susceptibility factors. Future work will be directed toward the investigation of understanding whether Mlp124357 has another target protein in host cell and the specific mechanism by which

Mlp124357 affects plant defense, which could be helpful in planning control strategies of rust pathogens.

Acknowledgements

We thank the Natural Sciences and Engineering Research Council of Canada (NSERC) for Discovery Grants for funding this project to HG. The project in HG's laboratory was also partially funded by an institutional research chair held by HG. MHM was funded by an international PhD scholarship from the Fonds de Recherche du Québec sur la Nature et les Technologies (FRQNT-PBEEE).

References

Ahmed MB, dos Santos KCG, Sanchez IB, et al. (2018) A rust fungal effector binds plant DNA and modulates transcription. Scientific reports 8(1):14718

Anderson JC, Pascuzzi PE, Xiao F, Sessa G, Martin GB (2006). Host-mediated phosphorylation of type III effector AvrPto promotesPseudomonasvirulence and avirulence in tomato. Plant Cell18:502-514

Bai X, Correa VR, Toruno TY, Ammar el D, Kamoun S, Hogenhout SA. 2009. AY-WB phytoplasma secretes a protein that targets plant cell nuclei. Mol Plant Microbe Interact 22: 18-30

Bindea G, Galon J, Mlecnik B (2013) CluePedia Cytoscape plugin: pathway insights using integrated experimental and *in silico* data. Bioinformatics 29(5):661-663

Bombarely A, Rosli HG, Vrebalov J, Moffett P, Mueller LA, Martin GB (2012) A draft genome sequence of Nicotiana benthamiana to enhance molecular plant-microbe biology research. Molecular Plant-Microbe Interactions 25(12):1523-1530

Brar HK, Swaminathan S, Bhattacharyya MK (2011) The Fusarium virguliforme toxin FvTox1 causes foliar sudden death syndrome-like symptoms in soybean. Molecular plant-microbe interactions 24(10):1179-1188

Bronnimann MP, Chapman JA, Park CK, Campos SK (2013) A transmembrane domain and GxxxG motifs within L2 are essential for papillomavirus infection. Journal of virology 87(1):464-473

Cabanillas DG, Jiang J, Movahed N, et al. (2018) Turnip mosaic virus uses the SNARE protein VTI11 in an unconventional route for replication vesicle trafficking. The Plant Cell 30(10):2594-2615

Caillaud MC, Piquerez SJ, Fabro G, et al. (2012) Subcellular localization of the Hpa RxLR effector repertoire identifies a tonoplast-associated protein HaRxL17 that confers enhanced plant susceptibility. The Plant Journal 69(2):252-265

Chang H-X, Domier LL, Radwan O, Yendrek CR, Hudson ME, Hartman GL (2016) Identification of multiple phytotoxins produced by Fusarium virguliforme including a phytotoxic effector (FvNIS1) associated with sudden death syndrome foliar symptoms. Molecular Plant-Microbe Interactions 29(2):96-108

Cho EJ, Yuen CY, Kang B-H, Ondzighi CA, Staehelin LA, Christopher DA (2011) Protein disulfide isomerase-2 of *Arabidopsis* mediates protein folding and localizes to both the secretory pathway and nucleus, where it interacts with maternal effect embryo arrest factor. Molecules and cells 32(5):459-475

Coaker G, Falick A, Staskawicz B (2005) Activation of a phytopathogenic bacterial effector protein by a eukaryotic cyclophilin. Science 308(5721):548-550

Coaker G, Zhu G, Ding Z, Van Doren SR, Staskawicz B (2006) Eukaryotic cyclophilin as a molecular switch for effector activation. Molecular microbiology 61(6):1485-1496

Cui H, Wang Y, Xue L, et al. (2010) A Pseudomonas syringae protein perturbs *Arabidopsis* hormone signaling by activating MAP KINASE 4. Cell host microbe 7(2):164-175

Cunnac S, Lindeberg M, Collmer A (2009) Pseudomonas syringae type III secretion system effectors: repertoires in search of functions. Current opinion in microbiology 12(1):53-60

Cymer F, Veerappan A, Schneider D (2012) Transmembrane helix–helix interactions are modulated by the sequence context and by lipid bilayer properties. Biochimica et Biophysica Acta (BBA)-Biomembranes 1818(4):963-973

Dangl JL, Horvath DM, Staskawicz BJ (2013) Pivoting the plant immune system from dissection to deployment. Science 341(6147):746-751

DeLano WL (2002) PyMOL.

Deslandes L, Rivas S (2012) Catch me if you can: bacterial effectors and plant targets. Trends in plant science 17(11):644-655

Dodds PN, Rathjen JP (2010) Plant immunity: towards an integrated view of plant–pathogen interactions. Nature Reviews Genetics 11(8):539

Duplessis S, Cuomo CA, Lin Y-C, et al. (2011) Obligate biotrophy features unraveled by the genomic analysis of rust fungi. Proceedings of the National Academy of Sciences 108(22):9166-9171

Duplessis S, Joly DL, Dodds PN (2012) Rust effectors. Effectors in plant-microbe interactions:155-193

Duplessis S, Major I, Martin F, Séguin A (2009) Poplar and pathogen interactions: insights from Populus genome-wide analyses of resistance and defense gene families and gene expression profiling. Critical Reviews in Plant Science 28(5):309-334

Ellgaard L, Ruddock LW (2005) The human protein disulphide isomerase family: substrate interactions and functional properties. EMBO reports 6(1):28-32

Faris JD, Zhang Z, Lu H, et al. (2010) A unique wheat disease resistance-like gene governs effector-triggered susceptibility to necrotrophic pathogens. Proceedings of the National Academy of Sciences 107(30):13544-13549

Fink A, Sal-Man N, Gerber D, Shai Y (2012) Transmembrane domains interactions within the membrane milieu: principles, advances and challenges. Biochimica et Biophysica Acta (BBA)-Biomembranes 1818(4):974-983

Germain H, Gray-Mitsumune M, Lafleur E, Matton DP (2008) ScORK17, a transmembrane receptor-like kinase predominantly expressed in ovules is involved in seed development. Planta 228(5):851-862

Germain H, Joly DL, Mireault C, et al. (2018) Infection assays in *Arabidopsis* reveal candidate effectors from the poplar rust fungus that promote susceptibility to bacteria and oomycete pathogens. Molecular plant pathology 19(1):191-200

Goodin MM, Zaitlin D, Naidu RA, Lommel SA (2008) Nicotiana benthamiana: its history and future as a model for plant–pathogen interactions. Molecular plant-microbe interactions 21(8):1015-1026

Hacquard S, Delaruelle C, Legué V, et al. (2010) Laser capture microdissection of uredinia formed by *Melampsora larici-populina* revealed a transcriptional switch between biotrophy and sporulation. Molecular Plant-Microbe Interactions 23(10):1275-1286

Hacquard S, Joly DL, Lin Y-C, et al. (2012) A comprehensive analysis of genes encoding small secreted proteins identifies candidate effectors in *Melampsora larici-populina* (poplar leaf rust). Molecular Plant-Microbe Interactions 25(3):279-293

Hacquard S, Petre B, Frey P, Hecker A, Rouhier N, Duplessis S (2011) The poplar-poplar rust interaction: insights from genomics and transcriptomics. Journal of pathogens 2011

Houston NL, Fan C, Schulze J-M, Jung R, Boston RS (2005) Phylogenetic analyses identify 10 classes of the protein disulfide isomerase family in plants, including single-domain protein disulfide isomerase-related proteins. Plant Physiology 137(2):762-778

Jones JD, Dangl JL (2006) The plant immune system. nature 444:323.

Kanneganti T-D, Huitema E, Cakir C, Kamoun S (2006) Synergistic interactions of the plant cell death pathways induced by Phytophthora infestans Nep1-like protein PiNPP1. 1 and INF1 elicitin. Molecular plant-microbe interactions 19(8):854-863

Karimi M, Inzé D, Depicker A (2002) GATEWAY™ vectors for Agrobacterium-mediated plant transformation. Trends in plant science 7(5):193-195

Kong G, Zhao Y, Jing M, et al. (2015) The activation of Phytophthora effector Avr3b by plant cyclophilin is required for the nudix hydrolase activity of Avr3b. PLoS pathogens 11(8):e1005139

Kozakov D, Hall DR, Xia B, et al. (2017) The ClusPro web server for protein–protein docking. Nature protocols 12(2):255

Kozlov G, Määttänen P, Thomas DY, Gehring K (2010) A structural overview of the PDI family of proteins. The FEBS journal 277(19):3924-3936

Li E, Wimley WC, Hristova K (2012) Transmembrane helix dimerization: beyond the search for sequence motifs. Biochimica et Biophysica Acta (BBA)-Biomembranes 1818(2):183-193

Liu M, Zheng H, Chen J, Li S, Huang J, Zhou C (2016) Chitosan-chitin nanocrystal composite scaffolds for tissue engineering. Carbohydrate polymers 152:832-840

Liu Z, Zhang Z, Faris JD, et al. (2012) The cysteine rich necrotrophic effector SnTox1 produced by Stagonospora nodorum triggers susceptibility of wheat lines harboring Snn1. PLoS Pathogens 8(1):e1002467

Määttänen P, Gehring K, Bergeron JJ, Thomas DY Protein quality control in the ER: the recognition of misfolded proteins. In: Seminars in cell & developmental biology, 2010. vol 21. Elsevier, p. 500-511

Madina MH, Zheng H, Germain H (2018) New insight into bulb dynamics in the vacuolar lumen of *Arabidopsis* cells. Botany 96(8):511-520

Major IT, Nicole M-C, Duplessis S, Séguin A (2010) Photosynthetic and respiratory changes in leaves of poplar elicited by rust infection. Photosynthesis Research 104(1):41-48

Meyer AJ, Riemer J, Rouhier N (2019) Oxidative protein folding: state-of-the-art and current avenues of research in plants. New Phytologist 221(3):1230-1246

Mireault C, Paris L-E, Germain H (2014) Enhancement of the *Arabidopsis* floral dip method with XIAMETER OFX-0309 as alternative to Silwet L-77 surfactant. Botany 92(7):523-525

Nimchuk Z, Marois E, Kjemtrup S, Leister RT, Katagiri F, Dangl JL (2000). Eukaryotic fatty acylation drives plasma membrane targeting and enhances function of several type III effector proteins from Pseudomonas syringae. Cell101:353-363

Ondzighi CA, Christopher DA, Cho EJ, Chang S-C, Staehelin LA (2008) *Arabidopsis* protein disulfide isomerase-5 inhibits cysteine proteases during trafficking to vacuoles before programmed cell death of the endothelium in developing seeds. The Plant Cell 20(8):2205-2220

Pennisi E (2010) Armed and dangerous. Science 327(5967): 804-5

Petre B, Lorrain C, Saunders DG, et al. (2016) Rust fungal effectors mimic host transit peptides to translocate into chloroplasts. Cellular microbiology 18(4):453-465

Petre B, Saunders DG, Sklenar J, et al. (2015) Candidate effector proteins of the rust pathogen *Melampsora larici-populina* target diverse plant cell compartments. Molecular Plant-Microbe Interactions 28(6):689-700

Pierce BG, Hourai Y, Weng Z (2011) Accelerating protein docking in ZDOCK using an advanced 3D convolution library. PloS one 6(9):e24657

Rovenich H, Boshoven JC, Thomma BP (2014) Filamentous pathogen effector functions: of pathogens, hosts and microbiomes. Current opinion in plant biology 20:96-103

Saunders DG, Win J, Cano LM, Szabo LJ, Kamoun S, Raffaele S (2012) Using hierarchical clustering of secreted protein families to classify and rank candidate effectors of rust fungi. PloS one 7(1):e29847

Schneidman-Duhovny D, Inbar Y, Nussinov R, Wolfson HJ (2005) PatchDock and SymmDock: servers for rigid and symmetric docking. Nucleic acids research 33(suppl_2):W363-W367

Schornack S, van Damme M, Bozkurt TO, et al. (2010) Ancient class of translocated oomycete effectors targets the host nucleus. Proceedings of the National Academy of Sciences 107(40):17421-17426

Shang Y, Li X, Cui H, et al. (2006) RAR1, a central player in plant immunity, is targeted by Pseudomonas syringae effector AvrB. Proceedings of the National Academy of Sciences 103(50):19200-19205

Sparkes IA, Runions J, Kearns A, Hawes C (2006) Rapid, transient expression of fluorescent fusion proteins in tobacco plants and generation of stably transformed plants. Nature protocols 1(4):2019

Speth EB, Lee YN, He SY (2007) Pathogen virulence factors as molecular probes of basic plant cellular functions. Current Opinion in Plant Biology 10:580-586.

Szurek B, Marois E, Bonas U, Van den Ackerveken G (2001). Eukaryotic features of theXanthomonastype III effector AvrBs3: Protein domains involved in transcriptional activation and the interaction with nuclear import receptors from pepper. Plant J 26:523-534.

Teese MG, Langosch D (2015) Role of GxxxG motifs in transmembrane domain interactions. Biochemistry 54(33):5125-5135

Torto TA, Li S, Styer A, et al. (2003) EST mining and functional expression assays identify extracellular effector proteins from the plant pathogen Phytophthora. Genome research 13(7):1675-1685

Tovchigrechko A, Vakser IA (2006) GRAMM-X public web server for protein–protein docking. Nucleic acids research 34(suppl_2):W310-W314

Vargas WA, Sanz-Martín JM, Rech GE, et al. (2016) A fungal effector with host nuclear localization and DNA-binding properties is required for maize anthracnose development. Molecular Plant-Microbe Interactions 29(2):83-95

Verchot J (2012) Cellular chaperones and folding enzymes are vital contributors to membrane bound replication and movement complexes during plant RNA virus infection. Frontiers in plant science 3:275

Win J, Chaparro-Garcia A, Belhaj K, et al. Effector biology of plant-associated organisms: concepts and perspectives. In: Cold Spring Harbor symposia on quantitative biology, 2012. vol 77. Cold spring harbor laboratory press, p. 235-247

Wirthmueller L, Roth C, Fabro G, et al. (2015) Probing formation of cargo/importin-α transport complexes in plant cells using a pathogen effector. The Plant Journal 81(1):40-52

Wittenberg G, Levitan A, Klein T, Dangoor I, Keren N, Danon A (2014) Knockdown of the A rabidopsis thaliana chloroplast protein disulfide isomerase 6 results in reduced levels of photoinhibition and increased D 1 synthesis in high light. The plant journal 78(6):1003-1013

Yang J, Yan R, Roy A, Xu D, Poisson J, Zhang Y (2015) The I-TASSER Suite: protein structure and function prediction. Nature methods 12(1):7

Yuan S, Chan HS, Hu Z (2017) Using PyMOL as a platform for computational drug design. Wiley Interdisciplinary Reviews: Computational Molecular Science 7(2):e1298

Yuen C, Matsumoto K, Christopher D (2013) Variation in the subcellular localization and protein folding activity among *Arabidopsis thaliana* homologs of protein disulfide isomerase. Biomolecules 3(4):848-869

Zhu C, Luo N, He M, et al. (2014) Molecular characterization and expression profiling of the protein disulfide isomerase gene family in Brachypodium distachyon L. PLoS One 9(4):e94704

Supplementary data

Table S1 List of possible interactor proteins of Mlp124357 from IP/MS

	TAIR name	Located in
1	*AT3G14420	cytosol
2	AT2G21330	apoplast, chloroplast, chloroplast envelope, chloroplast stroma, chloroplast thylakoid, cytosolic ribosome, plastoglobule, thylakoid, thylakoid lumen
3	AT3G13360	nuclear envelope, nucleus
4	AT1G16070	cytosol, nucleus
5	**AT5G26742	chloroplast, chloroplast envelope, chloroplast stroma, membrane, nucleus
6	AT1G23190	chloroplast, chloroplast stroma, cytoplasm, cytosol, nucleus, plasma membrane, stromule
7	AT2G33210	chloroplast, chloroplast envelope, chloroplast stroma, cytoplasm, mitochondrion,plasma membrane, vacuolar membrane
8	AT1G12900	apoplast, chloroplast, chloroplast envelope, chloroplast stroma, cytoplasm,membrane
9	AT2G31060	chloroplast, mitochondrion, plasma membrane
10	AT3G17970	chloroplast, chloroplast envelope, integral to chloroplast outer membrane, plastid
11	ATCG00020	chloroplast, chloroplast thylakoid, chloroplast thylakoid membrane, light-harvesting complex, membrane, photosystem II, plastoglobule, thylakoid
12	AT4G31180	cytoplasm, cytosol, endoplasmic reticulum
13	***AT3G53230	Golgi apparatus, cytosol, nucleolus, nucleoplasm, plasma membrane
14	AT3G16290.1	chloroplast, chloroplast envelope, plasma membrane
15	AT5G60600	chloroplast, chloroplast envelope, chloroplast stroma, nucleus
16	AT1G72730	cytoplasm, cytosol, plant-type cell wall, vacuolar membrane
17	AT3G13300	cytoplasmic mRNA processing body, cytosol, nucleus
18	AT3G60750	chloroplast, chloroplast envelope, chloroplast stroma, plastid
19	AT5G56000	Golgi apparatus, apoplast, cell wall, chloroplast stroma, cytoplasm, cytosol, nucleus, plasma membrane, vacuolar membrane
20	****AT4G25630.1	cajal body, box C/D snoRNP complex, cytosol, mediator complex, nucleolus, nucleus, small-subunit processome
21	AT3G56940	chloroplast, chloroplast envelope, chloroplast inner membrane, chloroplast thylakoid, chloroplast thylakoid membrane

	TAIR name	Located in
22	AT2G27680	chloroplast, chloroplast envelope, chloroplast stroma, peroxisome
23	AT4G01100.2	cytosol, integral component of membrane, mitochondrial inner membrane, mitochondrion, plastid
24	AT5G25460	extracellular region, plant-type cell wall, plasmodesma, plastid
25	AT5G45620	proteasome complex
26	AT1G23740	stromule
27	AT3G47800	cytoplasm
28	AT5G17990	chloroplast, chloroplast envelope, chloroplast stroma, plastid
29	AT5G37640	Golgi apparatus, cell wall, intracellular, nucleolus, vacuolar membrane
30	AT5G15650	cell junction, cell wall, cytosolic ribosome, membrane, nucleus
31	AT5G51970	cytoplasm, cytosol, plasmodesma
32	AT2G47470	endoplasmic reticulum, extracellular region, plant-type cell wall, vacuolar membrane
33	AT1G80380	chloroplast, chloroplast envelope, chloroplast stroma, nucleus
34	AT1G04040	cell wall, plant-type cell wall, plasmodesma, vacuolar membrane, vacuole
35	AT4G29810	cytoplasm, plasma membrane
36	AT2G18710	chloroplast, membrane
37	AT1G53880	chloroplast
38	AT4G10340	chloroplast, chloroplast stromal thylakoid, chloroplast thylakoid, chloroplast thylakoid membrane, light-harvesting complex, membrane, plastoglobule, thylakoid
39	AT2G40290	chloroplast, cytosol, eukaryotic translation initiation factor 2 complex, nucleus
40	AT5G18660	chloroplast, chloroplast envelope, chloroplast thylakoid, membrane, mitochondrion

*blue colored = 37<x<50 kDa

**red colored = 50<x<75 kDa

*** black colored = 75<x<100 kDa

**** yellow colored = 31<x<37 kDa

Table S2 List of up- and down-regulated genes from transcriptome analysis

357_DOWN_Unique (without uncharacterized gene)			
Gene ID	**Fold Change**	**Q-Value**	**Description**
AT3G63380	10.4	0.0008	Ca2+-transporting ATPase
AT1G78860	9.71	0.0112	putative glycoprotein (EP1)
AT3G22942	9.39	0.0008	G-protein gamma subunit 2
AT3G49620	9.31	0.0014	2-oxoglutarate-Fe(II)-dependent oxygenase domain-containing protein
AT2G35980	8.87	0.0238	late embryogenesis abundant hydroxyproline-rich glycoprotein
AT1G52060	8.04	0.0106	jacalin-like lectin domain-containing protein
AT5G64080	7.08	0.0025	Non-specific lipid-transfer protein-like protein
AT1G53490	7.01	0.0035	RING/U-box domain-containing protein
AT1G56250	6.84	0.0457	F-box protein PP2-B14
AT3G19430	6.74	0.0052	late embryogenesis abundant protein-like protein
AT2G15220	6.5	0.002	basic secretory protein family protein
AT5G54370	5.95	0.0008	late embryogenesis abundant protein-like protein
AT1G78090	5.78	0.0075	trehalose-6-phosphate phosphatase
AT1G51470	5.71	0.0056	myrosinase 5
AT1G17960	5.71	0.0008	threonyl-tRNA synthetase
AT2G43590	5.63	0.0052	chitinase-like protein
AT4G39950	5.54	0.0008	tryptophan N-hydroxylase 1
AT2G04170	5.13	0.002	TRAF-like family protein
AT1G52070	5.03	0.0008	jacalin-like lectin domain-containing protein
AT1G19900	4.93	0.0139	glyoxal oxidase-related protein
AT2G16005	4.82	0.0309	MD-2-related lipid recognition domain-containing protein
AT4G12520	4.61	0.0008	bifunctional inhibitor/lipid-transfer protein/seed storage 2S albumin-like protein
AT3G23250	4.6	0.0008	myb domain protein 15
AT2G41380	4.55	0.0008	S-adenosyl-L-methionine-dependent methyltransferase-like protein
AT5G47980	4.52	0.0154	BAHD acyltransferase
AT1G26820	4.51	0.0304	ribonuclease 3
AT4G12510	4.47	0.0163	bifunctional inhibitor/lipid-transfer protein/seed storage 2S albumin-like protein
AT4G29930	4.31	0.0064	transcription factor bHLH27
AT1G47600	4.22	0.0008	myrosinase 4
AT2G15390	4.12	0.0169	xyloglucan fucosyltransferase
AT4G24340	4.11	0.0353	phosphorylase family protein
AT3G25780	4.09	0.002	allene oxide cyclase 3

357_DOWN_Unique (without uncharacterized gene)			
Gene ID	**Fold Change**	**Q-Value**	**Description**
AT1G36180	4.05	0.0008	acetyl-CoA carboxylase 2
AT5G58940	4	0.0103	calmodulin-binding receptor-like cytoplasmic kinase 1
AT4G22666	3.96	0.003	bifunctional inhibitor/lipid-transfer protein/seed storage 2S albumin-like protein
AT5G60530	3.96	0.0008	late embryogenesis abundant protein-like protein
AT4G19030	3.95	0.0008	aquaporin NIP1-1
AT1G18980	3.94	0.002	germin-like protein subfamily T member 2
AT1G62370	3.86	0.0316	RING/U-box domain-containing protein
AT3G02620	3.81	0.0079	acyl
AT5G04200	3.8	0.0075	metacaspase 9
AT5G22300	3.75	0.0052	bifunctional nitrilase/nitrile hydratase NIT4
AT2G29125	3.7	0.0226	ROTUNDIFOLIA like 2
AT2G21100	3.67	0.0279	disease resistance-responsive
AT1G03700	3.67	0.0406	UPF0497 membrane protein
AT3G22570	3.66	0.0067	bifunctional inhibitor/lipid-transfer protein/seed storage 2S albumin-like protein
AT4G21830	3.66	0.0008	peptide methionine sulfoxide reductase B7
AT1G05620	3.66	0.0008	putative uridine nucleosidase 2
AT5G47990	3.62	0.0008	cytochrome P450 705A5
AT1G54890	3.6	0.0197	Late embryogenesis abundant-related protein
AT2G04050	3.59	0.0025	MATE efflux family protein
AT5G45280	3.57	0.0008	Pectinacetylesterase family protein
AT5G42590	3.53	0.0075	cytochrome P450 71A16
AT5G66280	3.53	0.0128	GDP-mannose 4
AT5G09978	3.49	0.0253	elicitor peptide 7
AT5G48010	3.49	0.0008	thalianol synthase 1
AT1G06820	3.48	0.0008	serine/threonine-protein kinase-like protein CCR2
AT3G48100	3.46	0.0008	two-component response regulator ARR5
AT5G49800	3.45	0.0071	lipid-binding START domain-containing protein
AT1G27920	3.45	0.0169	microtubule-associated protein 65-8
AT4G20240	3.41	0.0082	cytochrome P450
AT1G02360	3.4	0.0008	putative chitinase
AT1G73270	3.36	0.0243	serine carboxypeptidase-like 6
AT4G27070	3.35	0.002	tryptophan synthase beta chain
AT5G42460	3.3	0.0048	F-box and associated interaction domain-containing protein
AT5G15180	3.3	0.0025	peroxidase 56
AT5G23190	3.28	0.0008	cytochrome P450 86B1

357_DOWN_Unique (without uncharacterized gene)			
Gene ID	**Fold Change**	**Q-Value**	**Description**
AT5G60660	3.27	0.002	putative aquaporin PIP2-4
AT1G06090	3.25	0.0347	delta-9 desaturase-like 1 protein
AT2G36010	3.23	0.009	E2F transcription factor 3
AT4G29800	3.23	0.0014	PATATIN-like protein 8
AT3G52790	3.23	0.0008	peptidoglycan-binding LysM domain-containing protein
AT5G45840	3.22	0.0008	leucine-rich repeat protein kinase-like protein
AT2G20980	3.22	0.027	minichromosome maintenance protein 10
AT2G38110	3.21	0.0096	glycerol-3-phosphate acyltransferase 6
AT4G37070	3.21	0.0008	patatin-like protein
AT2G43570	3.19	0.0008	chitinase class 4-like protein
AT5G62480	3.17	0.0035	glutathione S-transferase tau 9
AT1G25220	3.16	0.0035	anthranilate synthase beta subunit 1
AT5G40730	3.16	0.0008	arabinogalactan protein 24
AT2G22500	3.16	0.0008	uncoupling protein 5
AT2G39530	3.16	0.0086	UPF0497 membrane protein
ATHEXP ALPHA 1,5	3.14	0.0093	expansin A14
AT3G48410	3.13	0.0096	alpha/beta-hydrolase domain-containing protein
AT1G23100	3.13	0.0413	GroES-like protein
AT1G48130	3.12	0.0307	1-Cys peroxiredoxin PER1
AT2G14520	3.12	0.002	CBS and transporter associated domain-containing protein
AT1G47480	3.1	0.0039	alpha/beta-hydrolase domain-containing protein
AT1G66270	3.09	0.0008	beta-glucosidase 21
AT3G50930	3.09	0.0048	cytochrome BC1 synthesis
AT3G58270	3.09	0.0121	phospholipase-like protein (PEARLI 4) with TRAF-like domain
AT4G24710	3.06	0.038	P-loop containing nucleoside triphosphate hydrolase-like protein
AT1G71990	3.04	0.0008	alpha-(1
AT4G02270	3.04	0.0008	protein root hair specific 13
AT1G14960	3.03	0.0291	major latex-related protein
AT3G55950	3.02	0.002	putative serine/threonine-protein kinase-like protein CCR3
AT2G24170	2.99	0.0014	endomembrane protein 70-like protein
AT3G47540	2.99	0.0093	putative chitinase
AT5G44610	2.97	0.0008	microtubule-associated protein 18
AT5G13580	2.96	0.0008	ABC transporter G family member 6
AT2G33790	2.96	0.0008	arabinogalactan protein 30
AT2G43610	2.95	0.0008	putative chitinase
AT1G76820	2.94	0.0008	translation initiation factor eIF-5B

357_DOWN_Unique (without uncharacterized gene)			
Gene ID	**Fold Change**	**Q-Value**	**Description**
AT4G34510	2.93	0.0307	3-ketoacyl-CoA synthase 17
AT3G22600	2.91	0.0008	bifunctional inhibitor/lipid-transfer protein/seed storage 2S albumin-like protein
AT4G36430	2.91	0.0397	peroxidase 49
AT2G29750	2.91	0.0008	UDP-glucosyl transferase 71C1
AT1G02335	2.9	0.0417	germin-like protein subfamily 2 member 2
AT1G16550	2.88	0.0052	pseudogene
AT1G66280	2.87	0.0008	beta-glucosidase 22
AT1G08990	2.87	0.0157	plant glycogenin-like starch initiation protein 5
AT3G10710	2.86	0.0115	pectinesterase 24
AT1G60390	2.86	0.0152	polygalacturonase 1
AT3G11430	2.85	0.002	glycerol-3-phosphate acyltransferase 5
AT5G58700	2.83	0.0025	phosphoinositide phospholipase C 4
AT5G07475	2.82	0.0067	plastocyanin-like domain-containing protein
AT3G21230	2.81	0.0056	4-coumarate--CoA ligase 4
AT5G48000	2.81	0.0008	cytochrome P450 708A2
AT4G28940	2.8	0.0179	Phosphorylase-like protein protein
AT5G09530	2.79	0.0008	hydroxyproline-rich glycoprotein family protein
AT3G09220	2.79	0.0008	laccase 7
AT4G22530	2.79	0.0182	S-adenosyl-L-methionine-dependent methyltransferase domain-containing protein
AT1G14370	2.77	0.0312	stress-induced protein KIN1
NTMC2T1,1	2.77	0.0008	synaptotagmin A
AT5G66960	2.76	0.0052	Prolyl oligopeptidase family protein
AT2G37870	2.76	0.0067	protease inhibitor/seed storage/lipid transfer protein (LTP) family protein
AT5G09220	2.75	0.0008	amino acid permease 2
AT1G51860	2.75	0.0052	putative LRR receptor-like serine/threonine-protein kinase
AT3G29100	2.75	0.0067	vesicle transport V-snare 13
AT4G30660	2.74	0.0173	putative low temperature and salt responsive protein
AT5G60020	2.73	0.0118	laccase 17
AT3G01190	2.72	0.0008	peroxidase 27
AT2G42960	2.72	0.0312	putative receptor-like protein kinase
AT1G17170	2.71	0.0184	glutathione S-transferase TAU 24
AT5G19410	2.7	0.0067	ABC transporter G family member 23
AT5G22140	2.7	0.0171	FAD/NAD(P)-binding oxidoreductase family protein
AT4G35350	2.7	0.0008	Xylem cysteine proteinase 1
AT5G43540	2.69	0.0067	C2H2 and C2HC zinc finger-containing protein

357_DOWN_Unique (without uncharacterized gene)			
Gene ID	**Fold Change**	**Q-Value**	**Description**
ATHEXP ALPHA 1,26	2.69	0.0279	expansin A7
AT1G51800	2.69	0.0008	putative leucine-rich repeat protein kinase
AT2G47770	2.68	0.0169	tryptophan-rich sensory protein-like protein
AT3G59370	2.68	0.0187	Vacuolar calcium-binding protein-like protein
AT5G60800	2.67	0.0238	heavy metal transport/detoxification domain-containing protein
AT4G15400	2.67	0.0226	HXXXD-type acyl-transferase-like protein
AT1G19180	2.67	0.0008	protein TIFY 10A
AT3G23470	2.66	0.003	Cyclopropane-fatty-acyl-phospholipid synthase
AT4G38080	2.66	0.0008	hydroxyproline-rich glycoprotein family protein
AT1G76790	2.66	0.0008	O-methyltransferase-like protein
AT4G21850	2.66	0.0008	peptide methionine sulfoxide reductase B9
AT1G68850	2.66	0.0008	peroxidase 11
AT3G22620	2.65	0.0008	bifunctional inhibitor/lipid-transfer protein/seed storage 2S albumin-like protein
AT2G16980	2.65	0.0103	major facilitator protein
AT4G08300	2.64	0.0399	nodulin MtN21 /EamA-like transporter family protein
AT2G03090	2.63	0.0318	expansin A15
AT5G07460	2.62	0.0008	peptide methionine sulfoxide reductase A2
AT2G22510	2.61	0.0008	hydroxyproline-rich glycoprotein family protein
AT1G23720	2.61	0.0008	Proline-rich extensin-like family protein
AT2G40320	2.61	0.0067	protein trichome birefringence-like 33
AT1G14070	2.6	0.0035	fucosyltransferase 7
AT5G61000	2.6	0.0039	Replication factor-A protein 1-like protein
AT3G10660	2.59	0.002	calmodulin-domain protein kinase cdpk isoform 2
AT5G27420	2.59	0.0008	E3 ubiquitin-protein ligase ATL31
AT3G10340	2.59	0.0008	phenylalanine ammonia-lyase 4
AT4G26220	2.56	0.0128	putative caffeoyl-CoA O-methyltransferase
AT4G39940	2.55	0.0008	Adenylyl-sulfate kinase 2
AT3G01420	2.55	0.0008	alpha-dioxygenase
AT2G47140	2.55	0.045	Rossmann-fold NAD(P)-binding domain-containing protein
AT1G66620	2.54	0.0307	E3 ubiquitin-protein ligase SINA-like 2
AT5G63590	2.54	0.0008	flavonol synthase 3
AT4G13310	2.53	0.0441	cytochrome P450 71A20
AT1G66350	2.53	0.0079	DELLA protein RGL1
AT1G11450	2.51	0.0329	nodulin MtN21 /EamA-like transporter protein
AT1G78340	2.5	0.0176	glutathione S-transferase TAU 22

357_DOWN_Unique (without uncharacterized gene)			
Gene ID	**Fold Change**	**Q-Value**	**Description**
AT2G25980	2.5	0.0014	myrosinase-binding protein-like protein
AT5G23830	2.49	0.0134	MD-2-related lipid recognition domain-containing protein
AT3G25290	2.49	0.0134	putative auxin-responsive protein
AT2G39110	2.48	0.0014	protein kinase domain-containing protein
AT4G20780	2.47	0.0056	calcium-binding protein CML42
AT5G40510	2.47	0.0229	Sucrase/ferredoxin-like family protein
AT1G75780	2.47	0.0008	tubulin beta
AT1G29025	2.46	0.0025	Calcium-binding EF-hand family protein
AT2G34500	2.46	0.0008	cytochrome P450
AT3G43960	2.46	0.0035	putative cysteine proteinase
AT2G46140	2.45	0.0048	Late embryogenesis abundant protein
AT3G22800	2.45	0.0025	leucine-rich repeat extensin-like protein 6
AT4G05020	2.45	0.0008	NAD(P)H dehydrogenase B2
AT5G25440	2.45	0.0008	protein kinase family protein
AT3G52370	2.44	0.0014	fasciclin-like arabinogalactan protein 15
AT1G09200	2.44	0.0008	histone H3
AT1G67980	2.43	0.0411	caffeoyl-CoA 3-O-methyltransferase
AT4G05200	2.43	0.0082	cysteine-rich receptor-like protein kinase 25
AT1G78820	2.43	0.0008	D-mannose binding lectin protein with Apple-like carbohydrate-binding domain
AT2G37460	2.43	0.0059	nodulin MtN21 /EamA-like transporter-like protein
AT4G30170	2.43	0.0008	peroxidase 45
AT2G47000	2.42	0.0008	ABC transporter B family member 4
AT4G13620	2.42	0.0452	ethylene-responsive transcription factor ERF062
AT2G33880	2.41	0.0059	homeobox-leucine zipper protein HAT7
AT1G25510	2.4	0.0128	aspartyl protease-like protein
AT2G31020	2.4	0.002	oxysterol binding protein-related protein 1A
AT3G49320	2.39	0.0194	Metal-dependent protein hydrolase
AT3G06680	2.38	0.002	60S ribosomal protein L29-2
AT1G51850	2.38	0.002	Leucine-rich repeat protein kinase family protein
AT1G03840	2.38	0.049	zinc finger protein MAGPIE
AT1G65060	2.37	0.0008	4-coumarate--CoA ligase 3
AT4G21390	2.37	0.0106	S-locus lectin protein kinase-like protein
AT2G45290	2.37	0.0008	Transketolase
AT4G36010	2.36	0.01	pathogenesis-related thaumatin family protein
AT1G61360	2.36	0.0014	S-like receptor protein kinase
AT3G16920	2.35	0.0048	chitinase-like protein 2

357_DOWN_Unique (without uncharacterized gene)

Gene ID	Fold Change	Q-Value	Description
AT4G31500	2.35	0.0008	cytochrome P450 83B1
AT3G18170	2.35	0.0008	Glycosyltransferase family 61 protein
AT1G62800	2.34	0.0365	aspartate aminotransferase
AT5G15290	2.34	0.0008	UPF0497 membrane protein
AT2G17500	2.33	0.0008	auxin efflux carrier-like protein
AT1G06360	2.33	0.0008	delta-9 desaturase-like 5 protein
AT3G09540	2.33	0.0246	pectate lyase
AT2G22330	2.33	0.0008	tryptophan N-hydroxylase 2
AT4G17215	2.32	0.0071	Pollen Ole e 1 allergen and extensin family protein
AT1G02300	2.31	0.0008	putative cathepsin B-like cysteine protease
AT4G00680	2.3	0.0371	actin depolymerizing factor 8
AT4G33550	2.3	0.0008	bifunctional inhibitor/lipid-transfer protein/seed storage 2S albumin-like protein
AT4G13580	2.3	0.003	disease resistance-responsive
AT1G61560	2.3	0.0014	MLO-like protein 6
AT2G38810	2.29	0.0093	histone H2A 8
AT5G50760	2.29	0.0115	SAUR-like auxin-responsive protein
AT5G26260	2.29	0.0008	TRAF-like family protein
AT3G46900	2.28	0.016	copper transporter 2
AT1G30960	2.28	0.0477	GTP-binding protein ERG
AT1G07790	2.28	0.0008	histone H2B
AT5G03630	2.28	0.0008	monodehydroascorbate reductase (NADH)
AT1G08190	2.27	0.0008	zinc transporter 2
AT3G05890	2.26	0.0008	Hydrophobic protein RCI2B
AT3G20860	2.26	0.0314	NIMA-related kinase 5
AT5G60100	2.26	0.0059	two-component response regulator-like APRR3
AT4G29700	2.25	0.0093	alkaline-phosphatase-like protein
AT1G76500	2.25	0.0321	AT-hook motif nuclear localized protein 29
AT2G01520	2.25	0.0008	MLP-like protein 328
AT5G41040	2.25	0.0008	omega-hydroxypalmitate O-feruloyl transferase
AT1G02810	2.25	0.0121	pectinesterase 7
ATWRKY17	2.25	0.0008	putative WRKY transcription factor 17
AT1G30620	2.25	0.0149	UDP-arabinose 4-epimerase
AT4G12910	2.24	0.0103	carboxypeptidase C
AT5G10400	2.24	0.0008	histone H3
AT5G67400	2.24	0.0106	peroxidase 73
AT2G16760	2.23	0.0391	calcium-dependent phosphotriesterase-like protein

357_DOWN_Unique (without uncharacterized gene)			
Gene ID	**Fold Change**	**Q-Value**	**Description**
AT3G02820	2.23	0.0179	CCHC-type zinc knuckle protein
AT5G58860	2.23	0.0008	cytochrome P450 86A1
AT4G33120	2.23	0.0056	S-adenosyl-L-methionine-dependent methyltransferase-like protein
AT1G79450	2.22	0.0365	ALA-interacting subunit 5
AT3G50260	2.22	0.0353	ethylene-responsive transcription factor ERF011
AT3G12965	2.21	0.0035	other RNA
AT3G57010	2.21	0.0025	strictosidine synthase family protein
AT3G04230	2.2	0.0064	40S ribosomal protein S16-2
AT1G44800	2.2	0.0008	nodulin MtN21 /EamA-like protein
AT5G66080	2.2	0.0401	putative protein phosphatase 2C 79
AT1G69040	2.19	0.0008	ACT domain-containing protein
AT4G23690	2.19	0.0008	disease resistance-responsive
AT2G44450	2.17	0.0446	beta glucosidase 15
AT1G24150	2.17	0.0008	formin homologue 4
AT2G32380	2.17	0.0075	putative transmembrane protein 97
AT2G39420	2.16	0.0025	alpha/beta-hydrolase domain-containing protein
AT2G19670	2.16	0.0096	protein arginine N-methyltransferase 1
AT5G18820	2.16	0.01	TCP-1/cpn60 chaperonin family protein
AT2G23540	2.15	0.0008	GDSL esterase/lipase
AT3G09270	2.15	0.0008	glutathione S-transferase TAU 8
AT5G12940	2.15	0.0035	leucine-rich repeat-containing protein
AT3G58710	2.15	0.0128	putative WRKY transcription factor 69
AT3G59760	2.14	0.0008	cysteine synthase
AT3G23570	2.14	0.0103	dienelactone hydrolase family protein
AT1G10780	2.14	0.0318	F-box/RNI-like protein
AT5G15230	2.14	0.0008	gibberellin-regulated protein 4
AT3G08040	2.14	0.0297	MATE efflux family protein
AT5G08260	2.14	0.0048	serine carboxypeptidase-like 35
4CL,1	2.13	0.0008	4-coumarate--CoA ligase 1
AT4G16745	2.13	0.0025	Exostosin family protein
AT5G19520	2.13	0.0014	mechanosensitive channel of small conductance-like 9
AT2G37040	2.13	0.0008	phenylalanine ammonia-lyase 1
AT1G26250	2.13	0.0216	Proline-rich extensin-like family protein
AT1G51830	2.13	0.0079	putative leucine-rich repeat protein kinase
AT4G00110	2.13	0.0205	UDP-D-glucuronate 4-epimerase 3
AT1G77690	2.12	0.0008	auxin transporter-like protein 3

357_DOWN_Unique (without uncharacterized gene)

Gene ID	Fold Change	Q-Value	Description
AT1G24280	2.12	0.0079	glucose-6-phosphate dehydrogenase 3
AT4G30850	2.12	0.0044	heptahelical transmembrane protein2
AT2G15300	2.12	0.0441	leucine-rich repeat protein kinase-like protein
AT5G12420	2.12	0.0008	O-acyltransferase (WSD1-like) family protein
AT4G11290	2.12	0.0008	peroxidase 39
AT4G01750	2.12	0.0056	rhamnogalacturonan xylosyltransferase 2
AT4G12330	2.11	0.0136	cytochrome P450
AT3G04720	2.11	0.0008	hevein-like protein
AT2G31585	2.11	0.0131	other RNA
AT2G38320	2.11	0.0446	trichome birefringence-like 34 protein
AT2G24600	2.1	0.0236	ankyrin repeat-containing protein
AT1G62790	2.1	0.0008	bifunctional inhibitor/lipid-transfer protein/seed storage 2S albumin-like protein
AT3G59890	2.1	0.0284	dihydrodipicolinate reductase 2
AT1G55210	2.1	0.0008	Disease resistance-responsive (dirigent-like protein) family protein
AT4G35160	2.1	0.0039	O-methyltransferase family 2 protein
AT1G72140	2.1	0.0025	putative peptide/nitrate transporter
AT2G37540	2.1	0.0353	Rossmann-fold NAD(P)-binding domain-containing protein
AT1G10370	2.09	0.0008	glutathione S-transferase
AT1G16300	2.09	0.0214	glyceraldehyde 3-phosphate dehydrogenase
AT2G35380	2.09	0.002	peroxidase 20
AT3G18000	2.09	0.0008	phosphoethanolamine N-methyltransferase 1
AT4G11320	2.09	0.0008	putative cysteine proteinase
AT3G03640	2.09	0.0008	putative inactive beta-glucosidase 25
AT2G45750	2.09	0.0106	putative methyltransferase PMT16
AT1G74100	2.09	0.0008	sulfotransferase 16
AT1G65310	2.09	0.0008	xyloglucan:xyloglucosyl transferase
AT4G16260	2.08	0.0008	catalytic/ cation binding / hydrolase
AT1G74680	2.08	0.0044	exostosin-like protein
AT3G06035	2.08	0.0484	glycoprotein membrane precursor GPI-anchored protein
AT1G72230	2.08	0.002	plastocyanin-like domain-containing protein
AT4G29030	2.08	0.0125	Putative membrane lipoprotein
AT5G22630	2.07	0.0014	arogenate dehydratase 5
AT3G54580	2.07	0.0008	Proline-rich extensin-like family protein
AT3G26460	2.07	0.0224	SRPBCC ligand-binding domain-containing protein
AT2G28760	2.07	0.0413	UDP-XYL synthase 6

357_DOWN_Unique (without uncharacterized gene)			
Gene ID	**Fold Change**	**Q-Value**	**Description**
AT2G48130	2.06	0.0008	protease inhibitor/seed storage/lipid transfer protein (LTP) family protein
AT4G17280	2.06	0.0496	putative auxin-responsive protein
AT2G42650	2.06	0.0176	Ribosomal protein ,1/L10e family
AT1G45145	2.06	0.0008	thioredoxin H5
AT5G52990	2.06	0.0145	vesicle-associated membrane protein-like protein
AT1G08280	2.05	0.0194	glycosyl transferase-like 29 protein
AT5G34940	2.05	0.0008	Heparanase-like protein 3
AT5G60890	2.05	0.002	myb domain protein 34
AT1G13740	2.05	0.0366	Ninja-family protein AFP2
AT4G22470	2.05	0.0419	protease inhibitor/seed storage/lipid transfer protein (LTP) family protein
AT4G30670	2.05	0.0008	Putative membrane lipoprotein
AT2G28190	2.05	0.0008	Superoxide dismutase
AT4G29430	2.04	0.0492	40S ribosomal protein S15a-5
AT4G15230	2.04	0.0039	ABC transporter G family member 30
AT1G64640	2.04	0.0025	early nodulin-like protein 8
AT1G06000	2.04	0.0261	UDP-glycosyltransferase-like protein
AT1G74460	2.03	0.0008	GDSL esterase/lipase
AT2G38080	2.03	0.0115	laccase-4
AT1G12040	2.03	0.0452	leucine-rich repeat extensin-like protein 1
AT1G13300	2.03	0.0052	myb-like transcription factor family protein
AT1G13950	2.03	0.0345	translation initiation factor eIF-5A
AT5G64660	2.03	0.0025	U-box domain-containing protein 27
AT5G57480	2.02	0.0265	AAA-type ATPase family protein
AT3G50360	2.02	0.002	calcium-binding protein CML19
AT4G36610	2.02	0.0179	hydrolase
AT5G17700	2.02	0.0136	mate efflux domain-containing protein
AT5G44635	2.02	0.0008	minichromosome maintenance protein 6
AT5G23220	2.02	0.0106	nicotinamidase 3
AT1G04020	2.01	0.0109	BRCA1-associated RING domain protein 1
AT4G29240	2.01	0.0281	leucine-rich repeat-containing protein
AT5G66390	2.01	0.0008	peroxidase 72
AT2G03450	2.01	0.0182	putative inactive purple acid phosphatase 9
AT1G11545	2.01	0.0008	xyloglucan:xyloglucosyl transferase
AT3G12500	2	0.0035	chitinase
AT1G64390	2	0.0008	endoglucanase 6

357_DOWN_Unique (without uncharacterized gene)			
Gene ID	**Fold Change**	**Q-Value**	**Description**
AT3G57630	2	0.0079	exostosin family protein
AT3G48350	2	0.0008	putative cysteine proteinase

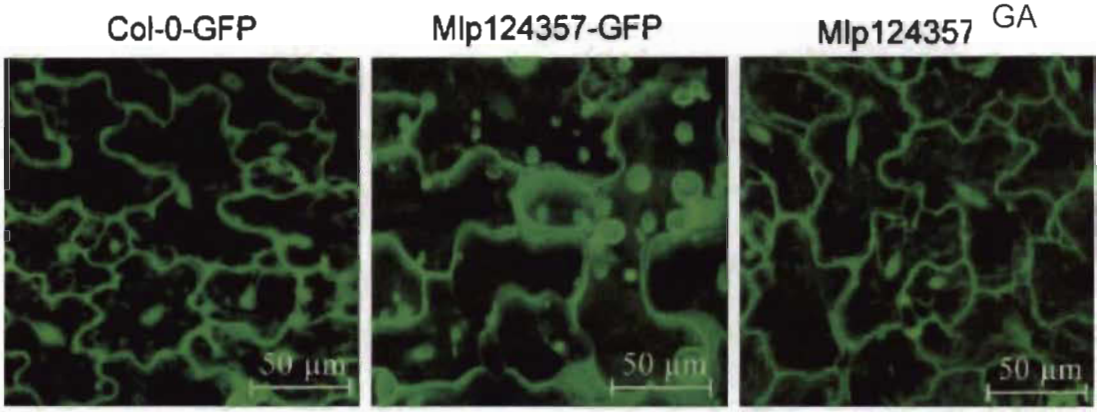

Fig. S1 Mlp124357^{GA} loose tonoplast localization in stable *Arabidopsis* transgenic line. Live -cell imaging of leaf epidermal cells of seven-days old stable *Arabidopsis* Mlp124357 ^{GA} transgenic line. These images are three-dimensional renderings stacks of 50 1-µm-thick slices that overlap by 0.5 µm.

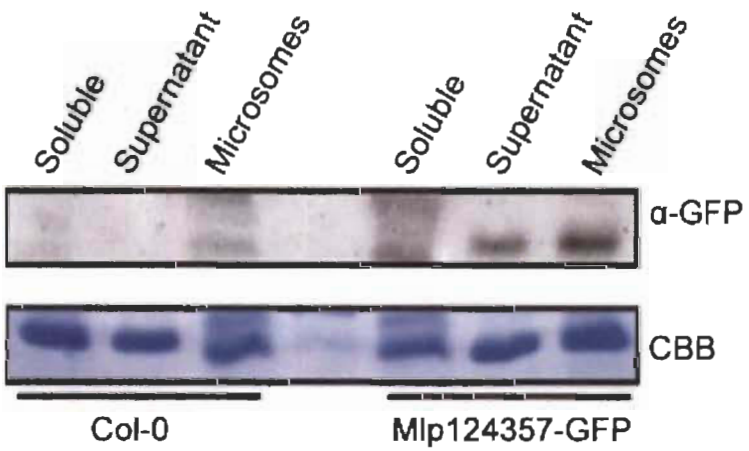

Fig. S2 Distribution of Mlp124357-GFP proteins in subcellular fractions. Cellular membrane fractions were separated from fresh leaves of 3-weeks old Col-0-GFP and Mlp124357-GFP plants by differential centrifugation and Mlp124357 was detected by Western hybridization with an antibody recognizing GFP (anti-GFP).

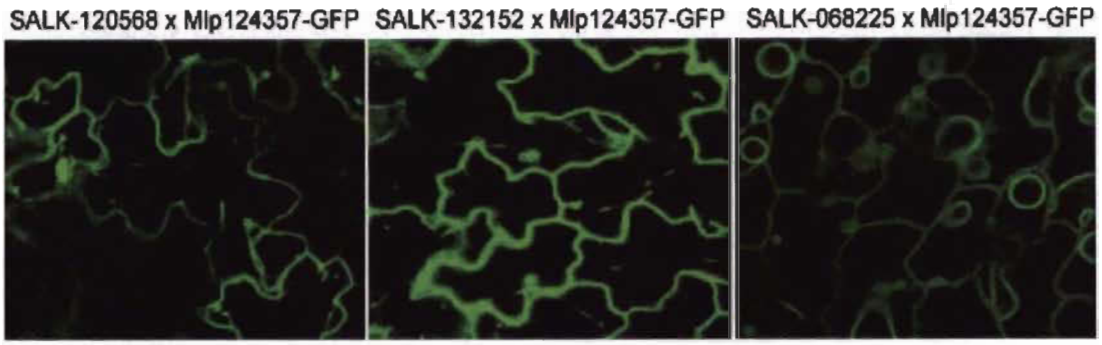

Fig. S3 Mlp124357 does not change the tonoplast, bulbs, and TVSs localization in the absence of AT2G33210, AT5G15650, and AT1G04040 genes in *Arabidopsis*. Live-cell imaging of leaf epidermal cells of the crossing lines where Mlp124357-GFP were crossed with indicated genes knock-out lines; SALK-120568 or SALK-132152 or SALK-068225 x Mlp124357-GFP). N.B. We could not screen the SALK-200520 homozygous line.

```
MlpPDI   ---MKSILVTLITILLFITTTNAGIFNSKGDVKAIDIDRLKKHLKTSSKGTFVAFYAPWC   57
AtPDI11  -MAKSQIWFGFALLALLLV------SAVADDVVVLTDDSFEK-EVGKDKGALVEFYAPWC   52
PopPDI   MERCNQIWYAFGTMALLAV------SALADDVVVLTEDNFEK-EVGQDKGALVEFYAPWC   53
              ..*   :  : *: .          .** .:  * ::*    ..**::* ******

MlpPDI   GHCKSLQPEFEKAATNVKNL--VVFAAVDCDADQNKASCGRDYGVKGFPTIKYFPGTPVA   115
AtPDI11  GHCKKLAPEYEKLGASFKKAKSVLIAKVDCDEQ--KSVC-TKYGVSGYPTIQWFPKGSLE   109
PopPDI   GHCKKLAPEYEKLGSSFKKAKAVLIGKVDCDEH--KGVC-SKYGVSGYPTLQWFPKGSLE   110
         ****.* **:** .:..*:   *::. **** .  *. *  .***.*:**::**    :

MlpPDI   -MDYDQERKAKSMVDYSLRFMPTFAKK-------IKSKKDLQEKISKSSNDRPLVVLFT-   166
AtPDI11  PQKYEGPRNAEALAEYVNKEGGTNVKLAAVPQNVVVLTPDNFDEIVLDQNKDVLVEFYAP   169
PopPDI   PKKYEGPRTAEALAEFVNNEGGSNVKIAAVTSSVVVLTADNFMDIVLDENKDVLVEFYAP   170
           .*:  *.*:::.::  .   : .*        :  . *  :.*  ..*,  ** :::

MlpPDI   ---TATATTPTFKSLSSVFHKKMEVVTATPKAIGEETAKELFSMESIPGLIVFK-GNTDY   222
AtPDI11  WCGHCKSLAPTYEKVATVFKQEEGVVIANLDADAHKALGEKYGVSGFPTLKFFPKDNKAG   229
PopPDI   WCGHCKNLAPIYEKVATAFKSEEDVVVANLEADKYRDLAEKYGVSGFPTLKFFPKGNKAG   230
            ..  :* ::.:::.*:.:  *  *. .*   .  * :.:..:* * .*  .*.

MlpPDI   EKFKGKMNYNTLYEFIKKELQLAEKSKSENQKA------KDEL-----------------   259
AtPDI11  HDYDGGRDLDDFVSFINEKSGTSRDSKGQLTSKAGIVESLDALVKELVAASEDEKKAVLS   289
PopPDI   EEYEGGRDLDDFVAFINEKAGTSRDGKGQLTSKAGIVESLDALVKEFVAAGDDEKKAVFS   290
         ..:.*  : : :  **:::   :...*.:  .        * *

MlpPDI   ------------------------------------------------------------   259
AtPDI11  RIEEEASTLKGSTTRYGKLYLKLAKSYIEKGSDYASKETERLGRVLGKSISPVKADELTL   349
PopPDI   RIEEEVEKLKGSTARHGKIYLKAAKTCMVKGAGYAKNEIERLQRMLEKSISPAKADEFTL   350

MlpPDI   ------------   259
AtPDI11  KRNILTTFVASS   361
PopPDI   KKNILSTFA---   351
```

Fig. S4 Multiple sequence alignment of PDIs. The amino acid sequence of *At*PDI-11, PopPDI, and *Mlp*PDI was compared. Identical/highly conserved residues (*); semi conserved residues (:) and conserved residues (.) are marked. The AtPDI-11 shows 87% and 30% of sequence identity with PopPDI and MlpPDI, respectively.

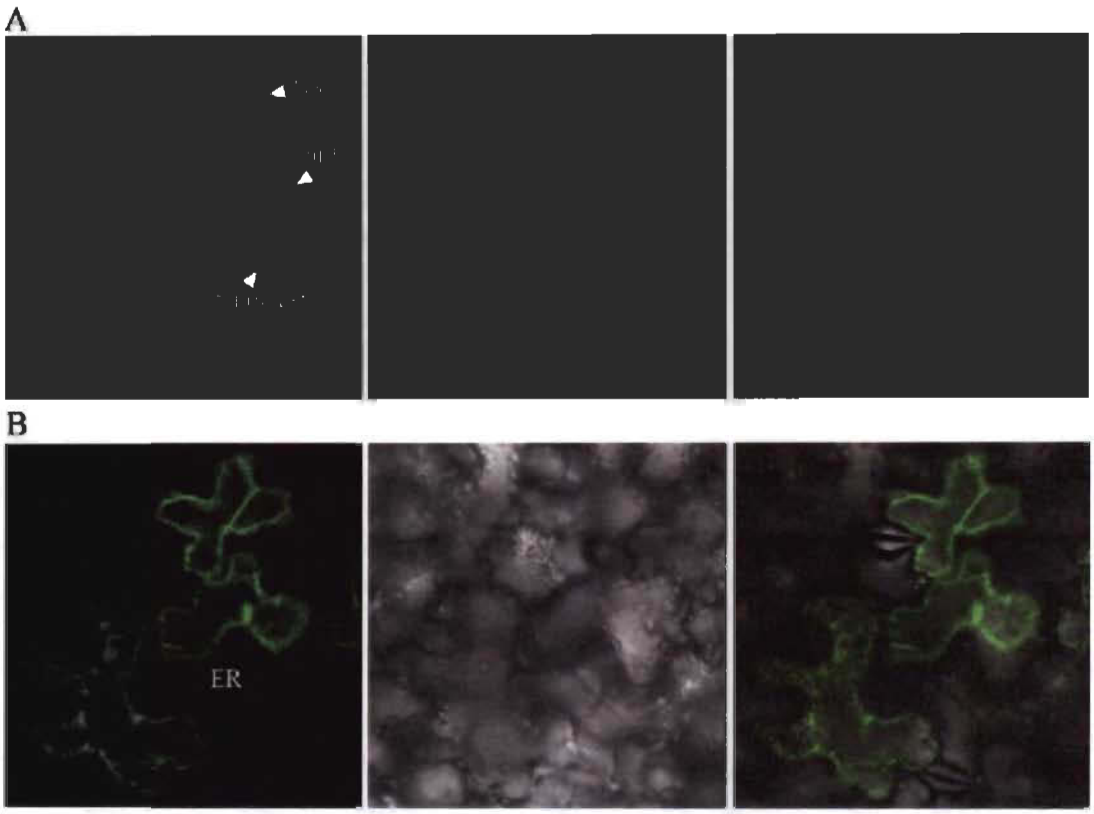

Fig. S5 Sub-cellular localization of AtPDI-11 in *N. benthamiana* epidermal cells. Laser-scanning confocal microscopy shows AtPDI-11-GFP accumulates both in (A) tonoplast (B) endoplasmic reticulum (ER).

Chapter V contains a discussion of the results achieved in Chapters III and IV. Additionally, in this chapter, new directions and perspectives of the studies are described.

CHAPTER V

CONCLUSIONS

5.1 Conclusion

To achieve a successful infection and colonization in plants, pathogens secrete effector proteins into their hosts to modulate the host physiology and immunity. Effectors target a variety of subcellular compartments and molecules in the host, such as proteins and DNA, and modulate their location, stability, or function to the advantage of the pathogen (Chaudhari et al. 2014; Lewis et al. 2009; Win et al. 2012). However, how these effector proteins function inside of the host cells is poorly unknown. Therefore, the identification and functional characterization of effectors will increase our knowledge of the concepts of biotrophy, thus allowing a better understanding of the plant-microbe interaction. In addition, new issues are also raised. This study aimed to obtain molecular insights into the role of Mlp124357, an effector candidate of rust fungi *M. larici-populina*. With the following conclusions, this research provides a better understanding of plant-pathogen interactions.

5.1.1 Mlp124357 localize in the tonoplast, TVS, and bulbs of *Arabidopsis* epidermal cells

Genome sequencing of *M. larici-populina* provided access to DNA sequences encoding 1,184 small secreted proteins and allowed us to functionally characterize the potential candidate secretory effector proteins (CSEPs) among them. *Mlp124357*, the effector investigated in this study, belongs to the CPG4890 gene family of *M. larici-populina*, which has 10 members in the genome of *M. larici-populina* isolate 98AG31. The transgenic lines developed in the *A. thaliana* Col-0 background manifested altered leaf morphology-characterized by narrower leaves, darker green leaves, and chlorosis and drying of the leave tips. In the study in chapter III and IV, we examined the

subcellular localization of Mlp124357 in plant cells using confocal laser scanning microscopy of leaves from *Arabidopsis* seedlings that stably expressing Mlp124357-GFP fusion. We detected the accumulation of Mlp124357 in the vacuolar structures; tonoplast, TVS, and bulb.

5.1.2 Why might Mlp124357 target vacuolar structures?

The fact that Mlp124357 targets vacuolar structures is particularly interesting because it leads to many questions pertaining as to what roles it might play in these cellular (sub-) organelles. The vacuole and vacuolar membrane structures play a vital role in plant programmed cell death and defense response against invading pathogens. Therefore, it is no surprise that fungi target these compartments during infection. Pathogen effectors may target tonoplast to modulate the host tonoplast to suppress the vacuole-mediated defense response. However, how would the *Mlp* pathogen benefit from manipulating host tonoplast and vacuolar sub-structures is only speculative at the moment. On the other hand, no single effector has been demonstrated to cause the bulbs structures in the presence of growing pathogens. Even though the physiological role of these bulbs remains blurred (Saito et al. 2002), it has been suggested that bulb-like structures appear sometimes and then disappear within the vacuole as an initial response of vacuole-mediated programmed cell death (Higaki et al. 2006). However, this study does not provide any other information about the bulb's fate. Therefore, a detail investigation is required to know whether these bulbs affect plant defense response or not.

5.1.3 Marker proteins are not evenly distributed on the bulb membrane

We investigated the distribution of our fusion proteins both in the tonoplast and bulb with the help of high-resolution 3-D imaging from the Z-stack series of leaf epidermal cells of *Arabidopsis* expressing Mlp124357-eGFP or γ-TIP-YFP. We found that two different distribution patterns on the bulb membranes for both Mlp124357-eGFP and the well-known tonoplast marker γ-TIP-YFP. This result suggests the

existence of two distinct bulb types in these cells, some with a regular marker protein distribution and some with exclusion spots.

5.1.4 Protein movement does not occur between bulb and tonoplast

We studied whether tonoplast-associated proteins move freely between the tonoplast and bulb membrane using fluorescence recovery after photobleaching (FRAP) of young epidermal cells of *Arabidopsis* leaf expressing Mlp124357-eGFP or γ-TIP-YFP. We observed the fluorescence of the bleached region of tonoplast recovered completely within one minute, whereas the bleached area of the bulb membrane fluorescence did not recover, despite being tethered to the tonoplast. This result is indicating that neither γ-TIP-YFP nor Mlp124357-eGFP can be expatriated from the tonoplast to the bulbs once they are formed. To be precise, our findings demonstrate that protein exchange from the tonoplast to bulb, or from bulb to bulb, does not occur, at least for these two marker proteins.

5.1.5 Mlp124357 enhance plant susceptibility

We conducted pathogenicity assays using bacterial (*P. syringae* pv. tomato) and oomycete (*H. arabidopsidis* Noco2) pathosystems and we observed that Mlp124357 enhances the growth of both pathogen *H. arabidopsidis* and *P. syringae* indicates the Mlp124357 has virulence activity to enhance the plant susceptibility.

5.1.6 GxxxG motif of Mlp124357 is required to localize in the tonoplast and plant susceptibility

The fact that no transmembrane domain is present in the effector protein sequence, made us investigate how does Mlp124357 interact with membranes. After a careful search, we discovered a GxxxG motif present in Mlp124357. Many reports have shown that the GxxxG motifs are responsible for membrane protein interaction (Cymer et al. 2012; Fink et al. 2012; Li et al. 2012). Through mutagenesis, we revealed that the

GxxxG motif within Mlp124357 sequence is required for the tonoplast localization. The GxxxG motif is not only important for localization but also for the virulence activity of the effector to enhance plant susceptibility.

5.1.7 Mlp124357 interact with protein disulfide isomerase

To identify plant interactors of Mlp124357, an immunoprecipitation and mass-spectrometry were performed. We identified five different proteins as potentially interacting with Mlp124357 and crossed their T-DNA insertion lines with the Mlp124357 transgenic line and confirmed *Arabidopsis* protein disulfide isomerase-11 as positive interactor of Mlp124357. We also confirmed that not only the *Arabidopsis* but also the host poplar protein disulfide isomerase interacts with the Mlp124357 using a complementation test. Further confirmation of the association between protein disulfide isomerase and Mlp124357 was done using yeast-two hybrid and molecular modeling.

5.1.8 Protein disulfide isomerase is a helper but not a virulence target of Mlp124357

Protein disulfide isomerase was investigated as a potential virulence target of Mlp124357 through a series of infection assays in the model plant *Arabidopsis* where PDI was either knocked out or overexpressed. This has shown that it is unlikely to be a virulence target, as overexpression does not reduce the ability of pathogens and increase the plant susceptibility.

Studies to determine whether or not it can function as a helper protein to Mlp124357 remain inconclusive, although pathogenicity tests suggest that it may be. The discovery of a new helper of a *M. larici-populina* effector protein would be of particular interest because it has not been reported before. The importance of helper proteins in plant-microbe interactions for virulence-or avirulence-outcomes is becoming increasingly well-understood and serves to highlight both the sophistication of microbial infection strategies as well as the internal surveillance mechanisms of plants.

Since many effectors have conserved cysteine, we also assessed whether PDI was also an generic interactor of effectors, the interaction between Mlp124357 and PDI appears to be specific since no other effector yielded a positive interaction with the PDI.

5.1.9 The Mlp124357 effector affect plant transcriptome

The altered phenotype leaf phenotype of Mlp124357-expressing plants prompted us to investigate the effect of Mlp124478 expression on the plant transcriptome. We performed transcriptome profiling of 4-days-old *A. thaliana* Mlp124357 stable transgenic line and Col-0 expressing GFP only. A gene ontology (GO) analysis in terms of biological function, revealed that changes in Mlp124357-GFP *A. thaliana* transgenic line transcriptomes occur mostly by a down-regulation of the expression of genes involved in diverse functions, mostly related to defense response regulation.

5.2 Perspectives/ Outlook

The future of genetic manipulation of crops in order to generate higher disease resistance looks promising. With a better understanding of the interactions at the molecular level between microbes and their hosts and greater control over the genome of organisms, we have never been so well placed to maintain the food security of a fast-expanding population. Indeed, the present work demonstrates the first instance of simultaneous importance of the protein disulfide isomerase for virulence activity of fungal effector. Thus, in and of itself, should prove beneficial to the community of the preliminary results in the present thesis that may confer some resistance to *M. larici-populina.*

5.2.1 Assessment and confirmation of virulent target of Mlp124357

Since the Mlp124357 effector interacts with protein disulfide isomerase in vacuolar structures (tonoplast, TVS, and bulbs) of *Arabidopsis* cell, we sought to confirm whether protein disulfide isomerase act as helper or target. We found that the

protein disulfide isomerase may act as a helper of *M. larici-populina* secreted effector protein. Although Mlp124357 interacts with *At*PDI-11 in vacuolar structures (tonoplast, TVS, and bulbs), however, it can change the *Arabidopsis* transcriptome. Whilst this remains very much an open question, the present thesis has opened up several avenues for study. Efforts should be made into ascertaining, for certain, whether or not the Mlp124357 might target and interact with another protein. It is possible that Mlp124357 strongly accumulates in the tonoplast, where it interacts with its true target. We have a list of putative proteins from the IP; these putative proteins can be considered to start from to identify the true target of the effector.

5.2.2 Structural studies

Further structural studies of Mlp124357 can be considered based on the production of effector proteins in *Escherichia coli* and successful purification and will have resolved the three-dimensional structure of Mlp124357, using NMR spectroscopy. A solved structure will show us that sequence-unrelated effectors can adopt folds similar to known proteins and encourage the use of biochemical and structural approaches to functionally characterized rust effectors.

5.2.3 Host-induced gene silencing (HIGS) of Mlp124357

Since Mlp124357 was found to enhance plant susceptibility in the present study, suggesting it has a virulence activity. Therefore, it would be interesting to use one of the RNA interference (RNAi) approaches to downregulate or silence Mlp124357 transcript level to control *M. larici-populina*. Host-Induced Gene Inhibition (HIGS) is one of the novel RNA-based approaches that has been successfully used to control fungal pathogens that infect various crops which are agronomically importance, for example powdery mildew (*Blumeria graminis*, (Nowara et al. 2010). members of the genus Puccinia (Yin et al. 2011). Similarly, this approach has proven effective against oomycetes (Niblett and Bailey 2012). The siRNA molecules generated by the host are translocated within the fungus via extrahaustorial membranes; this can occur either by

nutrient transport or by vesicle trafficking mechanisms, or by pathways to be discovered (Panwar et al. 2013).

Unfortunately, to date, no mutant populations of rust fungi exist, and genetic transformation of rust fungi has not been achieved. However, the availability of a genome sequence for the *M. larici-populina* has made this species a good candidate for rust effector studies and also provided a valuable resource to investigate rust biology at the genome level for other rust species. Therefore, it would be interesting to explore the role of HIGS of Mlp124357 in a susceptible host background. We could exploit the RNAi concept to silence the Mlp124357 gene in poplar cultivars, thus generating transgenic lines resistance to *M. larici-populina*.

5.3 Final Conclusions

Taken together, the present thesis introduces Mlp124357 as an important effector protein of *M. larici-populina* for pathogenesis. To summarize, we propose the model showed in Fig. 5.1. After being secreted from *M. larici-populina*, Mlp124357 localizes to the tonoplast, TVS, and bulbs with the help of GxxxG motif where it binds with protein disulfide isomerase and enhances plant susceptibility. Our results are also applicable to the development of pathogen model for studying another similar type of pathogens. We hope that sharing these observations will contribute to future efforts to prevent rust diseases.

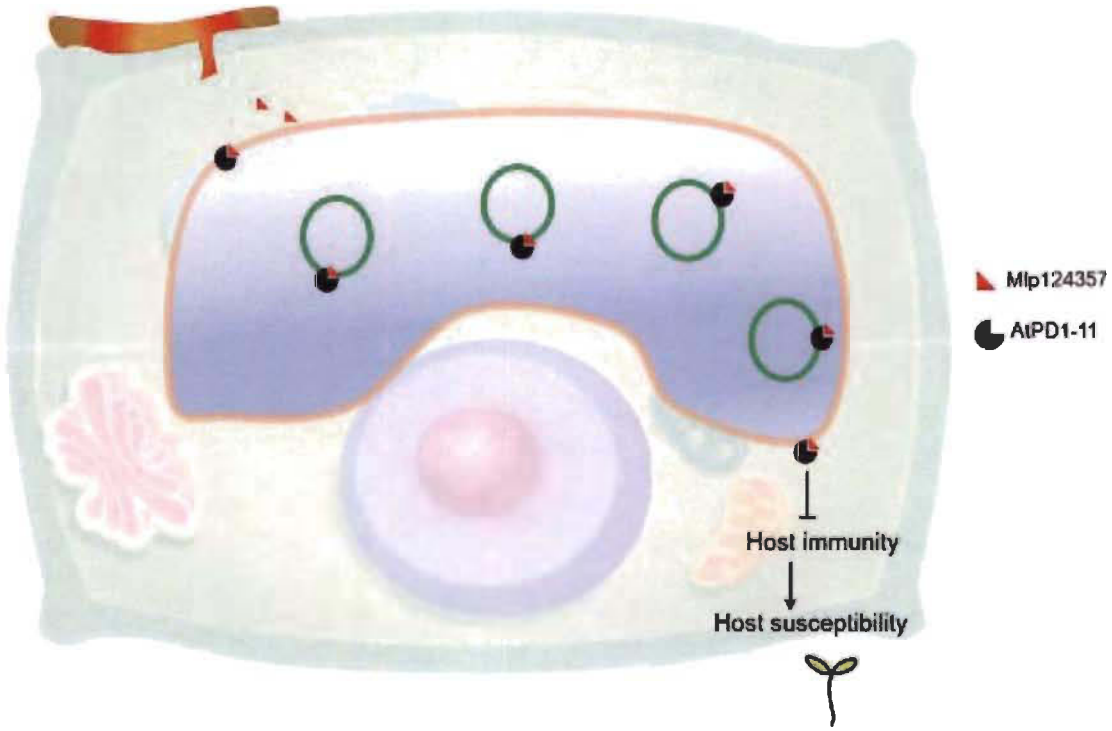

Figure 5.1 Proposed functional model for Mlp124357.
The Mlp124357 localized in vacuolar membrane and membranous structures and proposed to bind to protein disulfide isomerase and enhance plant susceptibility.

REFERENCES

Abramovitch RB, Anderson JC, Martin GB (2006) Bacterial elicitation and evasion of plant innate immunity. Nature Reviews Molecular Cell Biology 7(8):601

Aime MC, Toome M, McLaughlin DJ (2014) 10 Pucciniomycotina Systematics and Evolution. Springer, p. 271-294

Allen RL, Bittner-Eddy PD, Grenville-Briggs LJ, et al. (2004) Host-parasite coevolutionary conflict between *Arabidopsis* and downy mildew. Science 306(5703):1957-1960

Amselem J, Cuomo CA, Van Kan JA, et al. (2011) Genomic analysis of the necrotrophic fungal pathogens Sclerotinia sclerotiorum and Botrytis cinerea. PLoS genetics 7(8):e1002230

Anderson JC, Pascuzzi PE, Xiao F, Sessa G, Martin GB (2006) Host-mediated phosphorylation of type III effector AvrPto promotes Pseudomonas virulence and avirulence in tomato. The Plant Cell 18(2):502-514

Arias SL, Theumer MG, Mary VS, Rubinstein HR (2012) Fumonisins: probable role as effectors in the complex interaction of susceptible and resistant maize hybrids and Fusarium verticillioides. Journal of agricultural and food chemistry 60(22):5667-5675

Armstrong MR, Whisson SC, Pritchard L, et al. (2005) An ancestral oomycete locus contains late blight avirulence gene Avr3a, encoding a protein that is recognized in the host cytoplasm. Proceedings of the National Academy of Sciences 102(21):7766-7771

Bai X, Correa VR, Toruño TY, Ammar E-D, Kamoun S, Hogenhout SA (2009) AY-WB phytoplasma secretes a protein that targets plant cell nuclei. Molecular plant-microbe interactions 22(1):18-30

Block A, Li G, Fu ZQ, Alfano JR (2008) Phytopathogen type III effector weaponry and their plant targets. Current opinion in plant biology 11(4):396-403

Boch J, Scholze H, Schornack S, et al. (2009) Breaking the code of DNA binding specificity of TAL-type III effectors. Science 326(5959):1509-1512

Boller T, He SY (2009) Innate immunity in plants: an arms race between pattern recognition receptors in plants and effectors in microbial pathogens. Science 324(5928):742-744

Bolton AS, Burles S, Koopmans LV, et al. (2008) The sloan lens ACS survey. V. The full ACS strong-lens sample. The Astrophysical Journal 682(2):964

Borrás-Hidalgo O (2004) Basic insight in plant-pathogen interaction. Biotecnologia Aplicada 21(1):1-4

Bos JI, Armstrong MR, Gilroy EM, et al. (2010) Phytophthora infestans effector AVR3a is essential for virulence and manipulates plant immunity by stabilizing host E3 ligase CMPG1. Proceedings of the National Academy of Sciences 107(21):9909-9914

Caillaud M-C, Wirthmueller L, Fabro G, et al. Mechanisms of nuclear suppression of host immunity by effectors from the *Arabidopsis* downy mildew pathogen *Hyaloperonospora arabidopsidis* (*Hpa*). In: Cold Spring Harbor symposia on quantitative biology, 2012a. vol 77. Cold Spring Harbor Laboratory Press, p. 285-293

Caillaud MC, Piquerez SJ, Fabro G, et al. (2012b) Subcellular localization of the Hpa RxLR effector repertoire identifies a tonoplast-associated protein HaRxL17 that confers enhanced plant susceptibility. The Plant Journal 69(2):252-265

Catanzariti A-M, Dodds PN, Lawrence GJ, Ayliffe MA, Ellis JG (2006) Haustorially expressed secreted proteins from flax rust are highly enriched for avirulence elicitors. The Plant Cell 18(1):243-256

Chapman S, Kavanagh T, Baulcombe D (1992) Potato virus X as a vector for gene expression in plants. The Plant Journal 2(4):549-557

Chaudhari P, Ahmed B, Joly DL, Germain H (2014) Effector biology during biotrophic invasion of plant cells. Virulence 5(7):703-709

Chester KS (1933) The problem of acquired physiological immunity in plants. The Quarterly Review of Biology 8(3):275-324

Chisholm ST, Coaker G, Day B, Staskawicz BJ (2006) Host-microbe interactions: shaping the evolution of the plant immune response. Cell 124(4):803-814

Coaker G, Falick A, Staskawicz B (2005) Activation of a phytopathogenic bacterial effector protein by a eukaryotic cyclophilin. Science 308(5721):548-550

Collemare J, Lebrun MH (2011) Fungal secondary metabolites: ancient toxins and novel effectors in plant–microbe interactions. Effectors in Plant-Microbe Interactions: 379-402

Cooke JE, Rood SB (2007) Trees of the people: the growing science of poplars in Canada and worldwide. Botany 85(12):1103-1110

Cunnac S, Lindeberg M, Collmer A (2009) Pseudomonas syringae type III secretion system effectors: repertoires in search of functions. Current opinion in microbiology 12(1):53-60

Cymer F, Veerappan A, Schneider D (2012) Transmembrane helix–helix interactions are modulated by the sequence context and by lipid bilayer properties. Biochimica et Biophysica Acta (BBA)-Biomembranes 1818(4):963-973

De Wit PJ (2016) Apoplastic fungal effectors in historic perspective; a personal view. New Phytologist 212(4):805-813

Deslandes L, Rivas S (2012) Catch me if you can: bacterial effectors and plant targets. Trends in plant science 17(11):644-655

Djamei A, Schipper K, Rabe F, et al. (2011) Metabolic priming by a secreted fungal effector. Nature 478(7369):395

Dodds PN, Lawrence GJ, Catanzariti A-M, Ayliffe MA, Ellis JG (2004) The Melampsora lini AvrL567 avirulence genes are expressed in haustoria and their products are recognized inside plant cells. The Plant Cell 16(3):755-768

Dodds PN, Rathjen JP (2010) Plant immunity: towards an integrated view of plant–pathogen interactions. Nature Reviews Genetics 11(8):539

Dong S, Stam R, Cano LM, et al. (2014) Effector specialization in a lineage of the Irish potato famine pathogen. Science 343(6170):552-555

Dowkiw A, Husson C, Frey P, Pinon J, Bastien C (2003) Partial resistance to *Melampsora larici-populina* leaf rust in hybrid poplars: genetic variability in inoculated excised leaf disk bioassay and relationship with complete resistance. Phytopathology 93(4):421-427

Du Y, Berg J, Govers F, Bouwmeester K (2015) Immune activation mediated by the late blight resistance protein R1 requires nuclear localization of R1 and the effector AVR 1. New Phytologist 207(3):735-747

Duplessis S, Bakkeren G, Hamelin R (2014) Advancing knowledge on biology of rust fungi through genomics Advances in botanical research. vol 70. Elsevier, p. 173-209

Duplessis S, Cuomo CA, Lin Y-C, et al. (2011a) Obligate biotrophy features unraveled by the genomic analysis of rust fungi. Proceedings of the National Academy of Sciences 108(22):9166-9171

Duplessis S, Hacquard S, Delaruelle C, et al. (2011b) *Melampsora larici-populina* transcript profiling during germination and timecourse infection of poplar leaves reveals dynamic expression patterns associated with virulence and biotrophy. Molecular Plant-Microbe Interactions 24(7):808-818

Escobar NM, Haupt S, Thow G, Boevink P, Chapman S, Oparka K (2003) High-throughput viral expression of cDNA–green fluorescent protein fusions reveals novel subcellular addresses and identifies unique proteins that interact with plasmodesmata. The Plant Cell 15(7):1507-1523

Fink A, Sal-Man N, Gerber D, Shai Y (2012) Transmembrane domains interactions within the membrane milieu: principles, advances and challenges. Biochimica et Biophysica Acta (BBA)-Biomembranes 1818(4):974-983

Flor HH (1971) Current status of the gene-for-gene concept. Annual review of phytopathology 9(1):275-296

Frey P, Gérard P, Feau N, Husson C, Pinon J (2005) Variability and population biology of *Melampsora* rusts on poplars. Rust diseases of Willow and Poplar: 63-72

Gaouar O, Morency M-J, Letanneur C, Séguin A, Germain H (2016) The 124202 candidate effector of *Melampsora larici-populina* interacts with membranes in Nicotiana and *Arabidopsis*. Canadian Journal of Plant Pathology 38(2):197-208

Gaulin E (2017) Effector-mediated communication of filamentous plant pathogens with their hosts Advances in Botanical Research. vol 82. Elsevier, p. 161-185

Germain H, Joly DL, Mireault C, et al. (2018) Infection assays in *Arabidopsis* reveal candidate effectors from the poplar rust fungus that promote susceptibility to bacteria and oomycete pathogens. Molecular plant pathology 19(1):191-200

Gimenez-Ibanez S, Hann DR, Ntoukakis V, Petutschnig E, Lipka V, Rathjen JP (2009) AvrPtoB targets the LysM receptor kinase CERK1 to promote bacterial virulence on plants. Current biology 19(5):423-429

Glazebrook J (2005) Contrasting mechanisms of defense against biotrophic and necrotrophic pathogens. Annu Rev Phytopathol 43:205-227

Goodin M, Yelton S, Ghosh D, Mathews S, Lesnaw J (2005) Live-cell imaging of rhabdovirus-induced morphological changes in plant nuclear membranes. Molecular plant-microbe interactions 18(7):703-709

Goodin MM, Chakrabarty R, Banerjee R, Yelton S, DeBolt S (2007) New gateways to discovery. Plant Physiology 145(4):1100-1109

Goodin MM, Dietzgen RG, Schichnes D, Ruzin S, Jackson AO (2002) pGD vectors: versatile tools for the expression of green and red fluorescent protein fusions in agroinfiltrated plant leaves. The Plant Journal 31(3):375-383

Goodin MM, Zaitlin D, Naidu RA, Lommel SA (2008) Nicotiana benthamiana: its history and future as a model for plant–pathogen interactions. Molecular plant-microbe interactions 21(8):1015-1026

Goswami RS, Kistler HC (2004) Heading for disaster: Fusarium graminearum on cereal crops. Molecular plant pathology 5(6):515-525

Gu K, Yang B, Tian D, et al. (2005) R gene expression induced by a type-III effector triggers disease resistance in rice. Nature 435(7045):1122

Guo A, Salamo G, Duchesne D, et al. (2009) Observation of P T-symmetry breaking in complex optical potentials. Physical Review Letters 103(9):093902

Haas BJ, Kamoun S, Zody MC, et al. (2009) Genome sequence and analysis of the Irish potato famine pathogen Phytophthora infestans. Nature 461(7262):393

Hacquard S, Delaruelle C, Frey P, Tisserant E, Kohler A, Duplessis S (2013) Transcriptome analysis of poplar rust telia reveals overwintering adaptation and tightly coordinated karyogamy and meiosis processes. Frontiers in plant science 4:456

Hacquard S, Delaruelle C, Legué V, et al. (2010) Laser capture microdissection of uredinia formed by *Melampsora larici-populina* revealed a transcriptional switch between biotrophy and sporulation. Molecular plant-microbe interactions 23(10):1275-1286

Hacquard S, Joly DL, Lin Y-C, et al. (2012) A comprehensive analysis of genes encoding small secreted proteins identifies candidate effectors in *Melampsora larici-populina* (poplar leaf rust). Molecular plant-microbe interactions 25(3):279-293

Hacquard S, Petre B, Frey P, Hecker A, Rouhier N, Duplessis S (2011) The poplar-poplar rust interaction: insights from genomics and transcriptomics. Journal of pathogens 2011

Higaki T, Kutsuna N, Okubo E, Sano T, Hasezawa S (2006) Actin microfilaments regulate vacuolar structures and dynamics: dual observation of actin microfilaments and vacuolar membrane in living tobacco BY-2 cells. Plant and Cell Physiology 47(7):839-852

Hogenhout SA, Van der Hoorn RA, Terauchi R, Kamoun S (2009) Emerging concepts in effector biology of plant-associated organisms. Molecular plant-microbe interactions 22(2):115-122

Horbach R, Navarro-Quesada AR, Knogge W, Deising HB (2011) When and how to kill a plant cell: infection strategies of plant pathogenic fungi. Journal of plant physiology 168(1):51-62

Huitema E, Bos JI, Tian M, Win J, Waugh ME, Kamoun S (2004) Linking sequence to phenotype in Phytophthora–plant interactions. Trends in microbiology 12(4):193-200

Joly DL, Feau N, Tanguay P, Hamelin RC (2010) Comparative analysis of secreted protein evolution using expressed sequence tags from four poplar leaf rusts (*Melampsora* spp.). BMC genomics 11(1):422

Jones JD, Dangl JL (2006) The plant immune system. nature 444(7117):323

Jorge V, Dowkiw A, Faivre-Rampant P, Bastien C (2005) Genetic architecture of qualitative and quantitative *Melampsora larici-populina* leaf rust resistance in hybrid poplar: genetic mapping and QTL detection. New Phytologist 167(1):113-127

Kawamura A, Mizuno Y, Minamidani T, et al. (2009a) The second survey of the molecular clouds in the Large Magellanic Cloud by NANTEN. II. Star formation. The Astrophysical Journal Supplement Series 184(1):1

Kawamura Y, Hase S, Takenaka S, et al. (2009b) INF1 elicitin activates jasmonic acid-and ethylene-mediated signalling pathways and induces resistance to bacterial wilt disease in tomato. Journal of Phytopathology 157(5):287-297

Kay S, Hahn S, Marois E, Hause G, Bonas U (2007) A bacterial effector acts as a plant transcription factor and induces a cell size regulator. Science 318(5850):648-651

Kemen E, Jones JD (2012) Obligate biotroph parasitism: can we link genomes to lifestyles? Trends in plant science 17(8):448-457

Khang CH, Berruyer R, Giraldo MC, et al. (2010) Translocation of Magnaporthe oryzae effectors into rice cells and their subsequent cell-to-cell movement. The Plant Cell 22(4):1388-1403

Koornneef M, Meinke D (2010) The development of *Arabidopsis* as a model plant. The Plant Journal 61(6):909-921

Kunjeti SG, Iyer G, Johnson E, et al. (2016) Identification of Phakopsora pachyrhizi candidate effectors with virulence activity in a distantly related pathosystem. Frontiers in plant science 7:269

Lee AH-Y, Hurley B, Felsensteiner C, et al. (2012) A bacterial acetyltransferase destroys plant microtubule networks and blocks secretion. PLoS pathogens 8(2):e1002523

Lee S-J, Rose JK (2010) Mediation of the transition from biotrophy to necrotrophy in hemibiotrophic plant pathogens by secreted effector proteins. Plant signaling & behavior 5(6):769-772

Lewis JD, Guttman DS, Desveaux D The targeting of plant cellular systems by injected type III effector proteins. In: Seminars in cell & developmental biology, 2009. vol 20. Elsevier, p. 1055-1063

Li E, Wimley WC, Hristova K (2012) Transmembrane helix dimerization: beyond the search for sequence motifs. Biochimica et Biophysica Acta (BBA)-Biomembranes 1818(2):183-193

Li T, Huang S, Zhou J, Yang B (2013) Designer TAL effectors induce disease susceptibility and resistance to Xanthomonas oryzae pv. oryzae in rice. Molecular plant 6(3):781-789

Lorrain C, Hecker A, Duplessis S (2015) Effector-mining in the poplar rust fungus *Melampsora larici-populina* secretome. Frontiers in plant science 6:1051

Ma W, Guttman DS (2008) Evolution of prokaryotic and eukaryotic virulence effectors. Current opinion in plant biology 11(4):412-419

Martin FM, Uroz S, Barker DG (2017) Ancestral alliances: plant mutualistic symbioses with fungi and bacteria. Science 356(6340):eaad4501

McCann HC, Guttman DS (2008) Evolution of the type III secretion system and its effectors in plant–microbe interactions. New Phytologist 177(1):33-47

Meyerowitz EM (1989) *Arabidopsis*, a useful weed. Cell 56(2):263-269

Meyerowitz EM (2001) Prehistory and history of *Arabidopsis* research. Plant physiology 125(1):15-19

Miot BS, Frey P, Pinon J (1999) Varietal mixture of poplar clones: Effects on infection by *Melampsora larici-populina* and on plant growth. European journal of forest pathology 29(6):411-423

Mur LA, Laarhoven LJ, Harren FJ, Hall MA, Smith AR (2008) Nitric oxide interacts with salicylate to regulate biphasic ethylene production during the hypersensitive response. Plant Physiology 148(3):1537-1546

Nimchuk Z, Marois E, Kjemtrup S, Leister RT, Katagiri F, Dangl JL (2000) Eukaryotic fatty acylation drives plasma membrane targeting and enhances function of several type III effector proteins from Pseudomonas syringae. Cell 101(4):353-363

Niblett C, Bailey A (2012) Potential applications of gene silencing or RNA interference (RNAi) tocontrol disease and insect pests of date palm. Emirates Journal of Food and Agriculture:462-469

Nowara D, Gay A, Lacomme C, et al. (2010) HIGS: host-induced gene silencing in the obligate biotrophic fungal pathogen Blumeria graminis. The Plant Cell 22(9):3130-3141

Nürnberger T, Brunner F (2002) Innate immunity in plants and animals: emerging parallels between the recognition of general elicitors and pathogen-associated molecular patterns. Current opinion in plant biology 5(4):318-324

Nürnberger T, Brunner F, Kemmerling B, Piater L (2004) Innate immunity in plants and animals: striking similarities and obvious differences. Immunological reviews 198(1):249-266

Ossowski S, Schneeberger K, Clark RM, Lanz C, Warthmann N, Weigel D (2008) Sequencing of natural strains of *Arabidopsis thaliana* with short reads. Genome research 18(12):2024-2033

Panwar V, McCallum B, Bakkeren G (2013) Host-induced gene silencing of wheat leaf rust fungus Puccinia triticina pathogenicity genes mediated by the Barley stripe mosaic virus. Plant molecular biology 81(6):595-608

Pernaci M, De Mita S, Andrieux A, et al. (2014) Genome-wide patterns of segregation and linkage disequilibrium: the construction of a linkage genetic map of the poplar rust fungus *Melampsora larici-populina*. Frontiers in plant science 5:454

Persoons A, Hayden KJ, Fabre B, et al. (2017) The escalatory Red Queen: Population extinction and replacement following arms race dynamics in poplar rust. Molecular ecology 26(7):1902-1918

Petre B, Kamoun S (2014) How do filamentous pathogens deliver effector proteins into plant cells? PLoS biology 12(2):e1001801

Petre B, Lorrain C, Saunders DG, et al. (2016) Rust fungal effectors mimic host transit peptides to translocate into chloroplasts. Cellular microbiology 18(4):453-465

Petre B, Saunders DG, Sklenar J, et al. (2015) Candidate effector proteins of the rust pathogen *Melampsora larici-populina* target diverse plant cell compartments. Molecular Plant-Microbe Interactions 28(6):689-700

Pinon J, Frey P (1997) Structure of *Melampsora larici-populina* populations on wild and cultivated poplar. European Journal of Plant Pathology 103(2):159-173

Pinon J, Frey P (2005) Interactions between poplar clones and *Melampsora* populations and their implications for breeding for durable resistance. Rust diseases of willow and poplar:139-154

Rédei GP (1975) *Arabidopsis* as a genetic tool. Annual review of genetics 9(1):111-127

Rehmany AP, Gordon A, Rose LE, et al. (2005) Differential recognition of highly divergent downy mildew avirulence gene alleles by RPP1 resistance genes from two *Arabidopsis* lines. The Plant Cell 17(6):1839-1850

Rep M, Van Der Does HC, Meijer M, et al. (2004) A small, cysteine-rich protein secreted by Fusarium oxysporum during colonization of xylem vessels is required for I-3-mediated resistance in tomato. Molecular microbiology 53(5):1373-1383

Rooney HC, van't Klooster JW, van der Hoorn RA, Joosten MH, Jones JD, de Wit PJ (2005) Cladosporium Avr2 inhibits tomato Rcr3 protease required for Cf-2-dependent disease resistance. Science 308(5729):1783-1786

Rovenich H, Boshoven JC, Thomma BP (2014) Filamentous pathogen effector functions: of pathogens, hosts and microbiomes. Current opinion in plant biology 20:96-103

Saito C, Ueda T, Abe H, et al. (2002) A complex and mobile structure forms a distinct subregion within the continuous vacuolar membrane in young cotyledons of *Arabidopsis*. The Plant Journal 29(3):245-255

Saunders DG, Win J, Cano LM, Szabo LJ, Kamoun S, Raffaele S (2012) Using hierarchical clustering of secreted protein families to classify and rank candidate effectors of rust fungi. PloS one 7(1):e29847

Schornack S, van Damme M, Bozkurt TO, et al. (2010) Ancient class of translocated oomycete effectors targets the host nucleus. Proceedings of the National Academy of Sciences 107(40):17421-17426

Schwessinger B, Zipfel C (2008) News from the frontline: recent insights into PAMP-triggered immunity in plants. Current opinion in plant biology 11(4):389-395

Selosse M-A (2000) La symbiose : structures et fonctions, rôle écologique et évolutif. Vuibert

Shan L, He P, Li J, et al. (2008) Bacterial effectors target the common signaling partner BAK1 to disrupt multiple MAMP receptor-signaling complexes and impede plant immunity. Cell host & microbe 4(1):17-27

Sijmons PC, Grundler FM, von Mende N, Burrows PR, Wyss U (1991) *Arabidopsis thaliana* as a new model host for plant-parasitic nematodes. The Plant Journal 1(2):245-254

Sohn KH, Lei R, Nemri A, Jones JD (2007) The downy mildew effector proteins ATR1 and ATR13 promote disease susceptibility in *Arabidopsis thaliana*. The Plant Cell 19(12):4077-4090

Song J, Win J, Tian M, et al. (2009) Apoplastic effectors secreted by two unrelated eukaryotic plant pathogens target the tomato defense protease Rcr3. Proceedings of the National Academy of Sciences 106(5):1654-1659

Stergiopoulos I, de Wit PJ (2009) Fungal effector proteins. Annual review of phytopathology 47:233-263

Strange RN, Scott PR (2005) Plant disease: a threat to global food security. Annu Rev Phytopathol 43:83-116

Sugio A, MacLean AM, Grieve VM, Hogenhout SA (2011) Phytoplasma protein effector SAP11 enhances insect vector reproduction by manipulating plant development and defense hormone biosynthesis. Proceedings of the National Academy of Sciences 108(48):E1254-E1263

Szurek B, Marois E, Bonas U, Van den Ackerveken G (2001) Eukaryotic features of the Xanthomonas type III effector AvrBs3: protein domains involved in transcriptional activation and the interaction with nuclear import receptors from pepper. The Plant Journal 26(5):523-534

Tanaka S, Brefort T, Neidig N, et al. (2014) A secreted Ustilago maydis effector promotes virulence by targeting anthocyanin biosynthesis in maize. elife 3:e01355

Teixeira PJPL, de Toledo Thomazella DP, Reis O, et al. (2014) High-resolution transcript profiling of the atypical biotrophic interaction between Theobroma cacao and the fungal pathogen Moniliophthora perniciosa. The Plant Cell 26(11):4245-4269

Thomma BP, Van Esse HP, Crous PW, de Wit PJ (2005) Cladosporium fulvum (syn. Passalora fulva), a highly specialized plant pathogen as a model for functional studies on plant pathogenic Mycosphaerellaceae. Molecular plant pathology 6(4):379-393

Tian M, Huitema E, da Cunha L, Torto-Alalibo T, Kamoun S (2004) A Kazal-like extracellular serine protease inhibitor from Phytophthora infestans targets the tomato pathogenesis-related protease P69B. Journal of Biological Chemistry 279(25):26370-26377

Tian M, Win J, Song J, van der Hoorn R, van der Knaap E, Kamoun S (2007) A Phytophthora infestans cystatin-like protein targets a novel tomato papain-like apoplastic protease. Plant physiology 143(1):364-377

Tuskan GA, Difazio S, Jansson S, et al. (2006) The genome of black cottonwood, Populus trichocarpa (Torr. & Gray). science 313(5793):1596-1604

Van den Burg HA, Harrison SJ, Joosten MH, Vervoort J, de Wit PJ (2006) Cladosporium fulvum Avr4 protects fungal cell walls against hydrolysis by plant chitinases accumulating during infection. Molecular Plant-Microbe Interactions 19(12):1420-1430

Vialle A, Frey P, Hambleton S, Bernier L, Hamelin RC (2011) Poplar rust systematics and refinement of *Melampsora* species delineation. Fungal Diversity 50(1):227

Vleeshouwers VG, Oliver RP (2014) Effectors as tools in disease resistance breeding against biotrophic, hemibiotrophic, and necrotrophic plant pathogens. Molecular plant-microbe interactions 27(3):196-206

Weiberg A, Wang M, Lin F-M, et al. (2013) Fungal small RNAs suppress plant immunity by hijacking host RNA interference pathways. Science 342(6154):118-123

Win J, Chaparro-Garcia A, Belhaj K, et al. Effector biology of plant-associated organisms: concepts and perspectives. In: Cold Spring Harbor symposia on quantitative biology, 2012. vol 77. Cold spring harbor laboratory press, p. 235-247

Xiang T, Zong N, Zou Y, et al. (2008) Pseudomonas syringae effector AvrPto blocks innate immunity by targeting receptor kinases. Current biology 18(1):74-80

Yang B, Sugio A, White FF (2006) Os8N3 is a host disease-susceptibility gene for bacterial blight of rice. Proceedings of the National Academy of Sciences 103(27):10503-10508

Yesilirmak F, Sayers Z (2009) Heterelogous expression of plant genes. International journal of plant genomics 2009

Zheng X-y, Spivey NW, Zeng W, et al. (2012) Coronatine promotes Pseudomonas syringae virulence in plants by activating a signaling cascade that inhibits salicylic acid accumulation. Cell host & microbe 11(6):587-596

Zhou J-M, Chai J (2008) Plant pathogenic bacterial type III effectors subdue host responses. Current opinion in microbiology 11(2):179-185

Yin C, Jurgenson JE, Hulbert SH (2011) Development of a host-induced RNAi system in the wheat stripe rust fungus Puccinia striiformis f. sp. tritici. Molecular Plant-Microbe Interactions 24(5):554-561

Zipfel C, Felix G (2005) Plants and animals: a different taste for microbes? Current opinion in plant biology 8(4):353-360

Zipfel PF, Hallström T, Hammerschmidt S, Skerka C (2008) The complement fitness factor H: role in human diseases and for immune escape of pathogens, like pneumococci. Vaccine 26:I67-I74